The role of CX3CR1 in pancreatic cancer

Eleonora Li Causi

This thesis submitted in partial fulfillment of the requirement of the degree of

Doctor of Philosophy (PhD)

at Queen Mary University of London

July 2017

Center for Cancer and Inflammation

Barts Cancer Institute

Queen Mary University of London

Charterhouse Square,

London EC1M 6BQ

I, Eleonora Li Causi, confirm that the research included within this thesis is my own work or that where it has been carried out in collaboration with, or supported by others, that this is duly acknowledged below and my contribution indicated. Previously published material is also acknowledged below.

I attest that I have exercised reasonable care to ensure that the work is original, and does not to the best of my knowledge break any UK law, infringe any third party's copyright or other Intellectual Property Right, or contain any confidential material.

I accept that the College has the right to use plagiarism detection software to check the electronic version of the thesis.

I confirm that this thesis has not been previously submitted for the award of a degree by this or any other university.

Signature:

Date:

Details of collaboration and publications:

1. Survival data collected with the help of Dr Juliana Candido, Centre for Cancer & Inflammation, Barts Cancer Institute, Queen Mary University of London, London

2. RNA of KPC tumours for RNA-sequencing was extracted by Dr Juliana Candido, Centre for Cancer & Inflammation, Barts Cancer Institute, Queen Mary University of London, London

3. RNA-Sequencing was performed by the Wellcome Trust Centre for Human Genetics (University of Oxford, UK)

4. RNA-sequencing analysis was performed by Dr Eleni Maniati, Centre for Cancer & Inflammation, and Dr Ai Nagano, Bioinformatics Core, Barts Cancer Institute, Queen Mary University of London, London

5. The MEK1/2 Inhibitor Pimasertib Enhances Gemcitabine Efficacy in Pancreatic Cancer Models by Altering Ribonucleotide Reductase Subunit-1 (RRM1). Vena F, Li Causi E, Rodriguez-Justo M, Goodstal S, Hagemann T, Hartley JA, Hochhauser D. Clin Cancer Res. 2015 Dec 15;21(24):5563-77. doi: 10.1158/1078-0432.CCR-15-0485. Epub 2015 Jul 30.

Abstract

Pancreatic adenocarcinoma (PDAC) is the fourth leading cause of cancer death in Western countries. The PDAC tumour microenvironment (TME) is characterized by a dense stromal reaction, consisting of many cell types including fibroblasts and immune cells.

The chemokine receptor, CX3CR1 forms a high-affinity axis with its unique ligand CX3CL1 and is expressed on monocytes, macrophages and T cells. CX3CR1 is also present on pancreatic malignant cells, where it has been associated with metastasis formation.

The aim of my project is to investigate the role of CX3CR1 in the progression and development of pancreatic cancer in a genetically engineered mouse model of PDAC, the CX3CR1$^{GFP/GFP}$LSL-KRAS$^{G12D/+}$LSL-Trp53$^{R172H/+}$Pdx1-Cre (CKPC) mouse. In these mice, the CX3CR1 protein is not functional but they express GFP.

I have found that the absence of CX3CR1 in KPC mice has no effect in their lifespan and response to chemotherapy. Comparison of the immune infiltrate of the tumours revealed that the lack of CX3CR1 causes a significant decrease in T cells and a possible increase in myeloid cells in CKPC mice compared to KPC mice.

Expression analysis of several inflammatory cytokines in the TME showed a significant difference in IL-10 between KPC and CKPC mice. There was also a significant increase in levels of, CX3CL1, both locally and in the plasma.

Finally, we performed RNA-seq on KPC and CKPC tumours. My analysis revealed 607 differentially-expressed genes, some of which encoded other chemokines or protein regulating the immune system. In particular, I observed the upregulation of *Cxcl10* and *Cxcl12*, and the downregulation of *Gata3* and *S100a4,* which could explain the decrease in T cells in the TME of CKPC mice.

In conclusion, although the lack of CX3CR1 modifies the TME in this genetic model of PDAC, these changes do not affect the lifespan or the response to chemotherapy.

Acknowledgements

It is my pleasure to acknowledge the roles of several individuals who were instrumental for completion of my PhD research.

First of all, I would like to express my gratitude to my supervisor Frances Balkwill for the support for her patience and advice. Her guidance helped me in all the time of PhD, especially during the writing of this thesis.

I would also like to acknowledge Dr Juliana Candido, who introduced me to the world of myeloid cells and assisted me in the first steps with animal work, and Dr Eleni Maniati, who was always available for advice and help.

I thank also my colleagues for the ideas, the stimulating discussion and for the breaks and chats during the most difficult times.

Last but not least, I would like to thank my family with their presence even at a distance: my parents who have always believed in me and always supported any decision I made, and my sister, who always listened to whatever I have to say and helps when I have to put things in perspective.

Table of Contents

List of Figures

List of Tables

Abbreviations

°C	Degree Celsius
α-SMA	Alpha smooth muscle actin
ACKR	Atypical chemokine receptor
ADEX	Aberrantly differentiated endocrine exocrine
Arg1	Arginase1
B2m	β2 microglobulin
BSA	Bovine Serum Albumin
CCL	Chemokine (C-C motif) ligand 2
CCR	Chemokine (C-C motif) receptor
CD	Cluster of differentiation
cDNA	Complementary DNA
Cdh1	E-cadherin
CDK	Cyclin Dependent kinase
CDK2A	Cyclin Dependent kinase 2A
CEBP	Ccaat-enhance binding protein
CKPC	$CX3CR1^{GFP/GFP}$LSL-$KRAS^{G12D/+}$LSL$Trp53^{R172H/+}$Pdx1-Cre
CNS	Central nervous system
CPM	Count per million
cqn	Conditional quantile normalization
CSF1	Colony stimulating Factor 1
CSF1R	Colony stimulating Factor 1 receptor
Cox-2	Cyclooxygenase-2
CREB	cAMP-responsive element-binding protein
CTL	Cytotoxic T cell
CXCL	Chemokine (C-X-C motif) ligand
CXCR	Chemokine (C-X-C motif) receptor
CX3CL1	Chemokine (C-X3-C motif) ligand 1
CX3CR1	Chemokine (C-X3-C motif) receptor 1

DAPI	4',6-diamidino-2-phenylindole
DC	Dendritic cell
DE	Differentially expressed
DMEM	Dulbecco's Modified Eagle's Medium
DNA	Data not available
ECM	Extra-cellular matrix
EDTA	Ethylenediaminetetraacetic acid
ELISA	Enzyme-linked immunosorbent assay
EpCAM	Epithelial Cell Adhesion Molecule
ERK	E26 transformation-specific
FACS	Fluorescence Assisted cell sorting
FBS	Fetal bovine serum
Fc	Fragment, crystallizable
FGF-2	Fibroblast growth factor 2
FOLFIRINOX	Fluorouracil, leucovorin, irinotecan and oxaliplatin
FVD	Fixed Viability Dye
GEMM	Genetically engineered mouse models
GFP	Green fluorescent protein
GLM	Generalised linear model
GM-CSF	Granulocyte-macrophage colony-stimulating factor
GO	Gene ontology
GPCR	G protein coupled receptors
GTP	Guanosine triphosphate
HIF-1	Hypoxia inducible factor 1
HIV	Human immunodeficiency virus
HRP	Horseradish peroxidase
IFN	Interferon
IG	Immunoglobulin
IGF2	Insulin like growth factor 2
IL	Interleukin
iNOS	Inducible nitric oxide synthase
IPMN	Intra-ductal papillary mucinous neoplasms

KO	Knock-out
KPC	LSL-KRAS$^{G12D/+}$LSLTrp53$^{R172H/+}$Pdx1-Cre
KRAS	Kirsten rat sarcoma viral oncogene homolog
LincRNA	Long intergenic non-coding RNA
lncRNAs	Long non-coding RNAs
M1	Classically activated macrophage 1
M2	Alternatively activated macrophage 2
MDSC	Myeloid-derived suppressor cell
MCN	Mucinous cystic neoplasms
MEK	Mitogen-activated protein kinase kinase
Mest	Mesoderm-specific transcript
MLN	Mesenteric lymph nodes
mRNA	Messenger RNA
Mrc1	Mannose Receptor C-Type 1
MS	Multiple sclerosis
NA	Not available
ND	No difference
NF-kB	Nuclear Factor kappa-light-chain-enhancer of activated B cells
NK	Natural killer cell
NLR	NOD-like receptor
ns	Not significant
ORF	Open reading frame
PanIN	Pancreatic Intraepithelial neoplasia
PBS	Phosphate buffered saline
PBS-T	Phosphate buffered saline plus 0.1% Tween-20
PCA	Principal component analysis
PDAC	Pancreatic Ductal Adenocarcinoma
Pdx-1	Pancreatic and duodenal homobox-1
PFA	Paraformaldehyde
pNET	Pancreatic neuroendocrine tumours
PSC	Pancreatic stellate cells
qRT-PCR	Quantitative real-time polymerase chain reaction

RA	Rheumatoid arthritis
rcf	Relative centrifugal field
RIN	RNA integrity number
RNA-Seq	RNA- sequencing
RPKM	Reads per kilobase of transcript per million mapped reads
rRNA	Ribosomal RNA
SDF-1	Stromal-derived factor 1
STAT	Signal transducer and activator of transcription
TAM	Tumour-associated macrophage
TGF	Transforming growth factor
Th	T helper cells
TIL	Tumour infiltrating lymphocytes
TMB	Tetramethylbenzidine
TME	Tumour microenvironment
TNF	Tumour Necrosis Factor
TP53	Tumour protein p53
TR	T cell Receptor
Treg	T regulatory cells
TSP-1	thrombospondin-1
VEGF	Vascular endothelial growth factor
WT	Wild-type

Chapter 1 Introduction

1.1 Pancreatic cancer

1.1.1 The pancreas

The pancreas is an organ of the digestive system and the endocrine system. It is localised in the abdominal cavity behind the stomach. The pancreas performs endocrine and exocrine functions. The endocrine pancreas consists of cell clusters named islets of Langerhans; these islets are essential for the regulation of blood glucose levels and glucose metabolism and are composed by four primary types of cell: α cells secreting glucagon, β cells secreting insulin, δ delta cells secreting somatostatin and PP cells, or γ cells, secreting pancreatic polypeptide (Mastracci and Sussel 2012).

Exocrine functions of the pancreas involve the release of enzymes, such as lipases, amylases and proteases, which help in the digestion of food. These enzymes are contained within the pancreatic fluid, which is released into the duodenum (Cleveland, Sawyer et al. 2012).

1.1.2 Pancreatic tumours

Pancreatic cancer can develop from either the endocrine or exocrine pancreas. Pancreatic neuroendocrine tumours (pNETs) are rare endocrine tumours, representing 1-2% of all pancreatic tumours, but the incidence of these tumours has increased in the past 20 years (Zhou, Zhang et al. 2012, McKenna and Edil 2014). pNETs have different clinical characteristics and are grouped into 'functioning' and 'non-functioning' types, based on the amount of hormones produced (Burns and Edil 2012). The functioning type tumours secrete large quantities of hormones, such as insulin and glucagon into the bloodstream, which induces symptoms including low blood sugar, favouring relatively early detection. The most common functioning pNETs are insulinomas and gastrinomas, named after the hormones they secrete (McKenna and Edil 2014). The non-functioning type of pancreatic cancer lacks the capability to secrete enough hormones to give

rise to overt clinical symptoms. For this reason, non-functioning pNETs are often diagnosed when they have already metastasised (McKenna and Edil 2014).

Pancreatic exocrine tumours represent the majority of all pancreatic cancers, accounting for the 95% of all pancreatic tumours (Pancreatic-Cancer-UK 2016). The most common exocrine tumour is adenocarcinoma, accounting for 85% of all pancreatic tumours. Beside adenocarcinoma, the other exocrine pancreatic tumours are constituted of rare tumour types, such as mucinous tumours which constitute about 2-5% of all pancreatic tumours (H Chen 2015), and acinar cell carcinoma of the pancreas, which consists of 1-2% of all pancreatic tumours (La Rosa, Sessa et al. 2015).

1.1.3 Pancreatic ductal-adenocarcinoma

Pancreatic ductal-adenocarcinoma (PDAC) is the most common pancreatic tumour. PDAC is one of the most malignant types of solid tumours and it is one of the major causes of cancer death in the western world (Ryan, Hong et al. 2014). PDAC is the fourth most common cause of cancer in the USA (Ryan, Hong et al. 2014) and it is the eleventh in the UK (cancer-research-UK 2014). The median survival of patients from diagnosis is about 18-24 months with a 5-year survival rate of approximately 5% (Reznik, Hendifar et al. 2014). It was predicted that in 2014 more than 46000 new patients would have been diagnosed with PDAC (Ryan, Hong et al. 2014).

Pancreatic cancer incidence is linked to a number of risk factors, such as old age, smoking, diabetes and chronic pancreatitis (Kamisawa, Wood et al. 2016). However, among these evidence for a causative association has only been reported for cigarette smoking, which doubles the risk of developing pancreatic cancer (Iodice, Gandini et al. 2008, Kamisawa, Wood et al. 2016). In some studies alcohol consumption, obesity and a western diet have been proposed as additional risk factors (Ryan, Hong et al. 2014). Individuals with family history of PDAC have increased risk of developing the disease; 10% of pancreatic cancer cases have a familial basis (Kamisawa, Wood et al. 2016).

Pancreatic cancer mainly occurs in people aged between 60 and 80 years, with a mean of 71 years (Ryan, Hong et al. 2014, Kamisawa, Wood et al. 2016). Moreover, cancer incidence is different between sexes, men have 50% greater incidence of the disease compared to women (Kamisawa, Wood et al. 2016).
The poor survival of patients diagnosed with PDAC may be due to the fact that at the time of diagnosis approximately 85% of patients have advanced stage disease with local invasion or metastasis and cannot be submitted to surgery with curative intent (Vincent, Herman et al. 2011, Ryan, Hong et al. 2014).

1.1.4 Pathophysiology of PDAC

PDAC tumours are primarily located in the head of the pancreas (65%), then in the body (15%) and tail (10%) of the organ (Corbo, Tortora et al. 2012). On the basis of their degree of differentiation, PDACs are divided into three grades: well, moderately, and poorly differentiated (Kamisawa, Wood et al. 2016).

PDAC arises from non-invasive, histologically distinct precursor lesions known as pancreatic intraepithelial neoplasia (PanIN), which is the most frequent (Figure 1.1), intra-ductal papillary mucinous neoplasms (IPMN) and mucinous cystic neoplasms (MCN) (Corbo, Tortora et al. 2012).

Depending on the grade of cellular and tissue degeneration, PanINs are traditionally sub-classified into PanIN-1, PanIN-2 and PanIN-3 (Figure 1.1). PanINs-1 are characterized by cells with a columnar shape, basally oriented, uniform and with round nuclei. In PanIN-2 lesions the tall columnar cells can exhibit flat or papillary shape. Additionally, they exhibit nuclear abnormality, such as loss of nuclear polarity, change in nuclear size, and nuclear pseudostratification. PanIN-3 lesions display the highest degree of dysplasia. These lesions are formed by papillae and cribriform structures. Moreover, the nuclei in PanIN-3 lesions are enlarged, and poorly oriented (Hruban, Maitra et al. 2008).

IPMNs are constituted by cysts, which are more than 1 cm in size, and are characterised by the production of a mucinous liquid (Kamisawa, Wood et al.

2016). MCNs, instead, occur exclusively in women, and are composed of columnar, mucin-producing epithelium and supported by ovarian-type stroma. Moreover, MCNs do not interact with the pancreatic ductal system (Kamisawa, Wood et al. 2016).

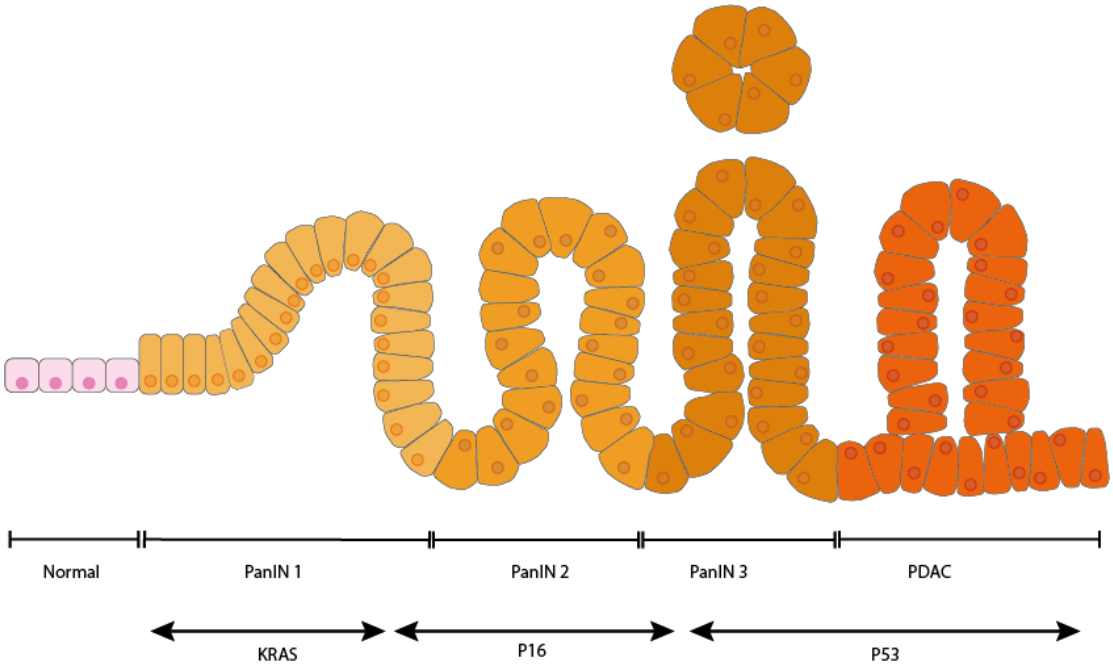

Figure 1.1 Progression model for pancreatic cancer
Progression from histologically normal epithelium to PDAC, through low-grade and high-grade PanIN stages (PanIN1-3). Each step is associated with the accumulation of specific genetic alterations (Hruban, Wilentz et al. 2000).

1.1.5 Genetics of PDAC

PDAC, from the genetic point of view, can be explained by the accumulation of acquired mutations. The mutated genes, found in most of the tumours, belong mostly to one of these two categories: oncogenes (such as *Kras*) or tumour-suppressor genes (such as *p16* and *TP53*) (Table 1.1). The different mutations occurring during pancreatic carcinogenesis correlate with PDAC pathological and physiological characteristics. In fact, molecular analysis of PanINs demonstrated that the majority of genomic alterations appear at a specific PanIN stage (Figure 1.1) (Bardeesy and DePinho 2002).

KRAS (Kirsten rat sarcoma viral oncogene homolog) is the most mutated gene in PDAC, with KRAS mutations found in more than 90% of cases. The *KRAS* gene

encodes for a small GTPase that mediates cellular signalling downstream of growth factor receptors. In PDAC, *KRAS* is mutated at codon 12 and this constitutively activates gene expression. *KRAS* mutations are typically found in the earliest PanIN-1 lesions (Hezel, Kimmelman et al. 2006, Kamisawa, Wood et al. 2016).

CDKN2A is the most frequently mutated tumour suppressor gene, with loss of function present in more than 90% of all PDAC. *CDKN2A* encodes for the p16 protein, member of the INK4 family of cyclin Dependent kinase (CDK) inhibitors. p16 is an essential cell-cycle regulator, controlling the cell cycle progression at the G1/S checkpoint: the loss of p16 activity results in uncontrolled cell growth. Mutations in *CDKN2A* gene are found in late stages of tumour progression (Bardeesy and DePinho 2002, Reznik, Hendifar et al. 2014, Kamisawa, Wood et al. 2016).

TP53 (tumour protein p53) is the second most commonly mutated suppressor gene in PDAC. *TP53* encodes for a 53 kDa transcription factor, responsible for regulating the expression of several genes involved in cell cycle regulation/arrest, apoptosis, differentiation, DNA surveillance and repair. *TP53* loss of function is due to missense alterations in the DNA-binding domain. *TP53* is mutated in more than 75% of pancreatic tumours and is detected in late-stage PanINs and invasive carcinomas (Hezel, Kimmelman et al. 2006, Kamisawa, Wood et al. 2016).

Another common mutation in PDAC is in the *SMAD4* gene. *SMAD4* encodes for a transcriptional regulator, which plays a major role in the transforming growth factor beta (TGF-β) signalling cascade. *SMAD4* mutations are found in about 50% of tumours, and they arise in PanIN-3 and invasive carcinoma (Hezel, Kimmelman et al. 2006, Wood and Hruban 2012).

Gene	Type	Cellular function	Mutated in PDAC
KRAS	Oncogene	ERK-MAP kinase signalling	>90%
CDKN2A	Tumour suppressor gene	G1-S phase cell cycle inhibition	>90%
TP53	Tumour suppressor gene	Cell-cycle arrest	75%
CyclinD	Oncogene	Cell-cycle progression	65%
SMAD4	Tumour suppressor gene	TGF-β	55%
BRCA2	Genome maintenance gene	DNA damage repair	7-10%
BRAF	Oncogene	ERK-MAP kinase signalling	5%
MLH1/MLH2	Genome maintenance gene	DNA damage (mismatch) repair	4%

Table 1.1 Most commonly mutated genes in PDAC
List of the most mutated gene in PDAC. For each mutated gene it is illustrated the type of gene, its cellular function and the percentages affected in PDAC. Table modified from (Ottenhof, de Wilde et al. 2011, Wood and Hruban 2015).

In 2015, a whole genome analysis on 100 pancreatic tumour samples gave the most complete description of the genomic events of PDAC (Waddell, Pajic et al. 2015). This study confirmed the importance of *KRAS*, *TP53*, *SMAD4* and *CDKN2A* mutations.

This study also classified PDAC tumours in four subtypes by patterns in the variation of chromosomal structure. These identified subtypes were named stable, locally rearranged, scattered and unstable. The stable subtype accounted for 20% of all samples and it is characterised by less than 50 structural variation events and aneuploidy. The locally rearranged subtype, 30% of all samples, presented a significant focal event in up to two chromosomes. The scattered subtype, presented in 36% of all samples, exhibited a moderate range of non-random chromosomal damage and less than 200 structural variation events. Finally, the remaining 14% of all samples constituted the unstable subtype, which showed more than 200 structural variation events (Waddell, Pajic et al. 2015).

Pancreatic tumours have been also classified according to their gene expression profile. Analysis of the transcriptional profiles of primary PDAC samples from several studies allowed Collisson et al. to define three PDAC subtypes: classical, quasi-mesenchymal and exocrine-like. The classical subtype is characterised by high levels of adhesion-associated and epithelial genes, the quasi-mesenchymal subtype showed high expression of mesenchyme-associated genes, while the exocrine-like subtype exhibited relatively high expression of tumour cell–derived digestive enzyme genes (Collisson, Sadanandam et al. 2011).

In 2016, Bailey et al. integrated genomic and transcriptomic analysis of PDAC samples (Bailey, Chang et al. 2016). The genomic analysis identified 32 recurrently mutated genes that aggregate into 10 pathways and confirmed *KRAS*, *TP53*, *SMAD4* and *CDKN2A* as the four most mutated genes in PDAC. The transcriptomic analysis allowed them to identify 4 PDAC subtypes: squamous, pancreatic progenitor, immunogenic and aberrantly differentiated endocrine exocrine (ADEX). Each of the four subtypes correlated with specific histopathological features. The squamous subtype correlated with adenosquamous carcinomas; the pancreatic progenitor and the immunogenic subtypes correlated with mucinous non-cystic adenocarcinomas and carcinomas arising from IPMN (mucinous); and the ADEX subtype correlated with rare acinar cell carcinomas (Bailey, Chang et al. 2016). Moreover, the immunogenic subtype is associated with evidence of a significant immune infiltrate. When they compared their classification with the one published by Collisson (Collisson, Sadanandam et al. 2011) they found that 3 of their subtypes (squamous, pancreatic progenitor and ADEX) correspond with the one identified in this study (Bailey, Chang et al. 2016).

1.1.6 Symptoms and treatments

PDAC patients, in almost all cases, are diagnosed in with advanced disease. This is caused by the lack of, or non-specific, symptoms in the early stage of cancer. In fact, most common symptoms of pancreatic cancer are weight loss, abdominal pain, nausea and vomiting, bloating, changes in bowel habit, dyspepsia, new-onset diabetes, pruritus, lethargy, back pain, shoulder pain, and jaundice (Keane, Horsfall

et al. 2014, Kamisawa, Wood et al. 2016). Therefore, in the majority of the cases PDAC is diagnosed when the tumour has already spread into the surrounding tissue and metastasised. At diagnosis less than 20% of patients are suitable for surgery (Ryan, Hong et al. 2014, Cid-Arregui and Juarez 2015).

Due to the presence of micrometastases at diagnosis, 60-90% of patients who undergo surgical removal of their tumour developed tumour recurrence (Cid-Arregui and Juarez 2015). The administration of either chemotherapy or radiotherapy after surgery (adjuvant therapy) improves survival rates significantly. In some cases, in order to shrink the tumour and to eliminate micrometastases chemotherapy or radiotherapy therapies can be applied before surgery (neoadjuvant therapy) (Cid-Arregui and Juarez 2015). .

In the treatment of PDAC, gemcitabine and 5-Fluorouracil (5-FU) are the two drugs that have been shown to increase the survival in patients, as single agents. 5-FU is a uracil analogue, characterised by an extra fluorine in position five; it acts as an inhibitor of thymidylate synthase, an enzyme responsible for the conversion of deoxyuridine monophosphate (dUMP) into deoxythymidine monophosphate (dTMP), causing DNA damage (Longley, Harkin et al. 2003, Teague, Lim et al. 2015).

Gemcitabine (2',2'-difluorodeoxycytidine) is a pyrimidine analogue in which the hydrogen atoms on the 2' carbon of deoxycytidine are replaced by fluorine atoms. Gemcitabine, when converted in the triphosphate active form (dFdCTP), is incorporated into DNA, instead of cytidine (de Sousa Cavalcante and Monteiro 2014, Teague, Lim et al. 2015). Gemcitabine has increased patient overall survival compared to 5-FU, with a median survival rate of 5.7–6.3 months. For this reason, gemcitabine is considered to be the single agent of choice in advanced pancreatic cancer (Snady, Bruckner et al. 2000, Cid-Arregui and Juarez 2015).

Many clinical trials tried to improve the gemcitabine overall survival by adding different drugs, such as oxiplatinum, cetuximab and bevacizumab. Unfortunately, none of these combination therapies showed any beneficial effect on patient survival (Cid-Arregui and Juarez 2015, Teague, Lim et al. 2015). An exception is

FOLFIRINOX, a combination of 4 different agents: leucovorin (folinic acid), 5-FU, irinotecan and oxaliplatin. Several studies showed that patients with metastatic pancreatic cancer treated with FOLFIRINOX have better median overall survival, progression-free survival, and objective responses compared to gemcitabine (Conroy, Desseigne et al. 2011, Marsh Rde, Talamonti et al. 2015). However, despite encouraging results, this regiment is associated with significant toxicities and the outlook for patients with pancreatic cancer remains poor. Subsequently gemcitabine combined with abraxane was also shown to significantly improve survival rates compared to gemcitabine (Von Hoff, Ervin et al. 2013).

1.1.7 Mouse models of pancreatic cancer

Genetically engineered mouse models (GEMMs) represent an invaluable tool in the study of cancer as they accurately mimic some of the pathophysiological and molecular features of human pancreatic tumours. They can also be used to test the efficacy of new therapeutic candidates (Herreros-Villanueva, Hijona et al. 2012). Although GEMMs are powerful tools in the study of cancer, they are limited by several factors. They are expensive and time-consuming to generate and maintain, and it is difficult to track tumour development. Most of the GEMM use recombinases, such as the Cre recombinases, to excise a specific DNA sequence, which is identified by short repeats called loxP sites.

The most used mouse model, which recapitulates the critical gene lesions involved in the human pancreatic cancers, is the LoxP-Stop-LoxP-K-ras$^{G12D/+}$; LSL-Trp53$^{R172H/+}$; Pdx-1-Cre mouse model (KPC model) (Hingorani, Wang et al. 2005). In these mice, Cre recombinase, under the control of the transcription factor pancreatic and duodenal homobox-1 (Pdx-1), remove the loxP-flanked sequence from the pancreas epithelium activating K-ras^{G12D} and Trp53^{R172H} mutation. The K-ras^{G12D} mutation causes the constitutive activation of Ras signaling whilst the TP53^{R172H} is functionally equivalent to a null mutation (Hingorani, Wang et al. 2005, Herreros-Villanueva, Hijona et al. 2012).

The KPC mouse recapitulates the pathological, histological, genomic and clinical signatures of human pancreatic cancer (Hingorani, Wang et al. 2005). These mice

present with early PanIN lesions between four and six weeks of age. From 10 weeks old the animals manifest signs of the disease, developing cachexia, abdominal distension, and hemorrhagic ascites. Most of the mice also develop metastasis in the liver, diaphragm and adrenals.

The median survival of these mice is approximately 5-6 months with a maximum survival of 12 months (Herreros-Villanueva, Hijona et al. 2012). However, these mice do not mimic perfectly human PDAC; for instance in the KPC mouse tumorigenesis occurs in multi-focal sites in the pancreas while in human tumours usually emerge as a single neoplastic focus (Guerra and Barbacid 2013).

1.2 The tumour microenvironment

Tumours do not only contain malignant cells. In fact, tumours also comprise of a variety of other cell types, regulatory proteins and other soluble factors as well as features such as hypoxia and acidosis: together these form the tumour microenvironment (TME) (Feig, Gopinathan et al. 2012, Turley, Cremasco et al. 2015). Cancer cells interact with the other components of the TME, which influence tumour progression, metastasis formation and response to therapy (Turley, Cremasco et al. 2015).

1.2.1 Pancreatic tumour microenvironment

The PDAC TME is characterized by an abundant fibrotic tissue reaction referred to as the desmoplastic reaction. Approximately 80% of the tumour mass is made up of stroma, which is composed of extra-cellular matrix (ECM) proteins, new blood vessels, cancer associated fibroblast (CAF), mesenchymal cells (MSC), activated pancreatic stellate cells (PSC) and immune cells (Figure 1.1) (Lunardi, Muschel et al. 2014, Ryan, Hong et al. 2014).

The TME is not a static entity but it is constantly changing in their composition especially during the progression from PanIN-1 to invasive PDAC. Early PanIN

lesions may be associated with small amounts of stroma surrounding the normal pancreatic ducts. On the other hand, in PanIN-3 lesions there is already an enhanced stroma formation, and the progression to invasive carcinoma is associated with a further increase in this component (Vincent, Herman et al. 2011, Feig, Gopinathan et al. 2012).

Another characteristic of desmoplasia in pancreatic cancer is the poor and disorganized vascularization, which results in hypoxic conditions that contribute to tumour progression and metastasis (Quail and Joyce 2013). This lack of adequate vasculature, together with the abundant stroma, can prevent the effective delivery of chemotherapy to the tumour cells (Neesse, Michl et al. 2011).

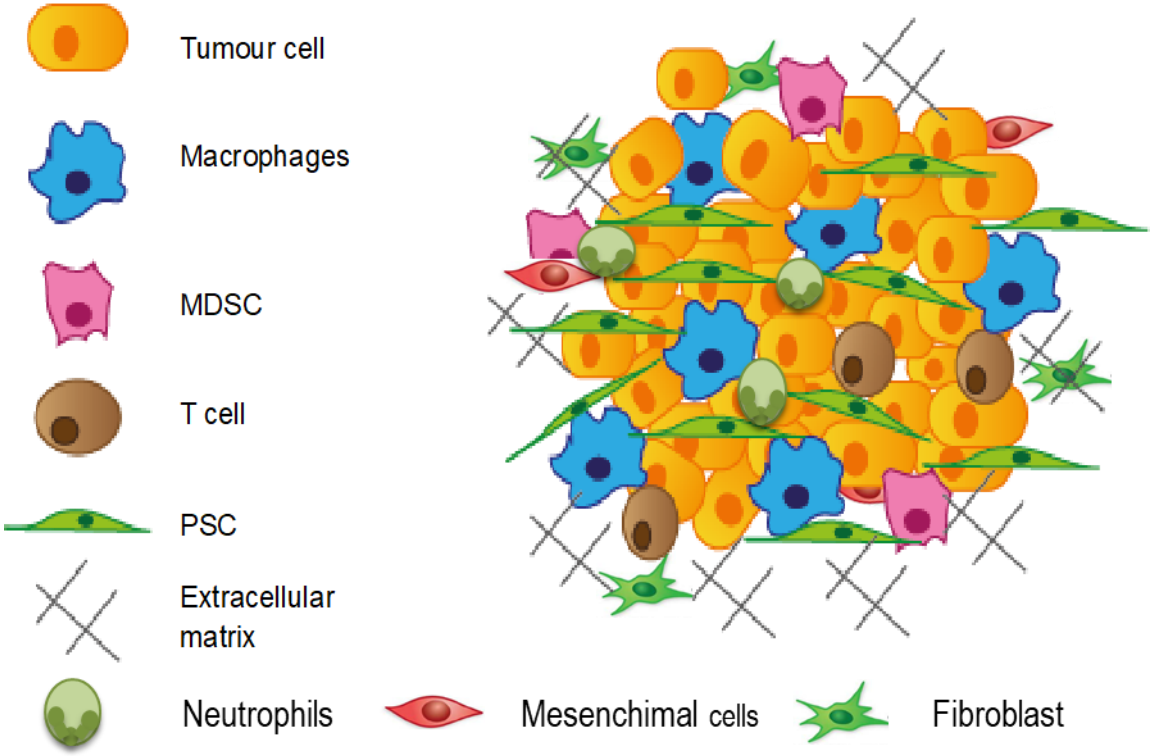

Figure 1.2 Schematic representation of the tumour microenvironment in pancreatic tumours
Cancer cells in primary tumours are surrounded by a complex microenvironment rich in extracellular matrix that also includes pancreatic stellate cells (PSC), fibroblasts, mesenchymal cells and several types of immune cells including macrophages, myeloid-derived suppressor cells (MDSCs) T cells and neutrophils Adapted from (Evans and Costello 2012)

1.2.2 Acidosis and hypoxia

Areas of acidosis, an increase in the acidity of the tissue, and hypoxia, an inadequate supply of oxygen within a tissue, can be found in almost every solid tumour (Bailey, Wojtkowiak et al. 2012, Feig, Gopinathan et al. 2012). The levels of acidosis and hypoxia fluctuate within the tumour and during tumour progression.

The hypoxic environments in tumours are caused by an increase in oxygen consumption by tumour cells, and by an impaired vasculature, limiting the amount of available oxygen into the tumor tissue (Feig, Gopinathan et al. 2012). Consequences of the hypoxic environment include: alteration of cancer cell metabolism, remodeling of ECM, increasing the migratory and metastatic behavior of malignant cells, reducing the responsiveness to chemotherapy and radiotherapy treatments and inducing resistance (Yuen and Diaz 2014, Eales, Hollinshead et al. 2016).

Acidosis is the result of an increased excretion of lactic acid and the inability of the tumor vasculature to remove lactic acid waste from the TME. The presence of acidosis reduces the efficacy of chemotherapy and increases the metastatic potential of cancer cells (Bailey, Wojtkowiak et al. 2012).

1.2.3 The extracellular matrix

PDAC is characterized by the presence of an abundant ECM, which comprises collagens, hyaluronic acid, and other extracellular matrix component (Ryan, Hong et al. 2014). Type I and III collagen and fibronectin are the most abundant components present in the ECM of pancreatic cancer and are secreted predominantly by PSCs (Rasheed, Matsui et al. 2012, Lunardi, Muschel et al. 2014). ECM components, accumulated during carcinogenesis, alter the architecture of normal pancreatic tissue, causing the alteration of blood and lymphatic vessels distributions (Feig, Gopinathan et al. 2012).

The ECM provides a supporting structure for tumour growth (Mahadevan and Von Hoff 2007, Carr and Fernandez-Zapico 2016). For example, ECM proteins, such as laminin and fibronectin, promote survival and prevent death of pancreatic tumour cells (Pandol, Edderkaoui et al. 2009). In fact, the interaction between laminin and fibronectin with cancer cell integrin receptors leads to intracellular events that promote cancer cell survival and growth (Pandol, Edderkaoui et al. 2009). Moreover, the ECM can become a protective barrier against chemotherapy and radiotherapy (Whatcott, Posner et al. 2012, Schober, Jesenofsky et al. 2014). In particular, the tumour collagen content showed an inverse correlation with macromolecule penetration (Whatcott, Posner et al. 2012).

1.2.4 Tumour vasculature

Angiogenesis is essential for the growth of solid tumours and metastasis formation (Quail and Joyce 2013). As mentioned in the previous paragraph, the vasculature in PDAC is profoundly impaired by the massive presence of ECM (Ryan, Hong et al. 2014). PDAC tissues have a low micro-vessel density compared to other solid malignancies (Feig, Gopinathan et al. 2012). Functional analysis of PDAC vasculature showed that vessels have variable diameters, abnormal multiple branching and disrupted inter-endothelial junctions. Additionally, the vessels are collapsed. This phenomenon is caused by high interstitial pressure and leads to a reduced delivery of small molecule drugs (Longo, Brunetti et al. 2016). Indeed, a consequence of PDAC poor vascularisation and high interstitial pressure is the decreased penetration of chemotherapy inside the tumours. Interestingly, it has been shown that the normalization of high interstitial pressure, by targeting hyaluronic acid, re-expands the microvasculature allowing chemotherapy to reach the tumour area (Provenzano, Cuevas et al. 2012).

To promote angiogenesis cancer cells and other cells in the TME including macrophages and stellate cells, secrete angiogenic factors such as vascular endothelial growth factor (VEGF), fibroblast growth factor 2 (FGF-2), interleukin 6 (IL-6), IL-8 and angiopoietins (Longo, Brunetti et al. 2016). VEGF is overexpressed in the majority of PDAC and correlates with a high microvessel density, disease

progression, increased risk of metastatic spread, and a poor prognosis (Whipple and Korc 2008). Since angiogenesis plays a major role in tumour growth and metastasis formation, it has been chosen as a possible therapeutic target in PDAC using VEGFR inhibitors or anti-VEGF-A antibodies (Whipple and Korc 2008). Therefore, several preclinical and clinical trials are taking place in PDAC using anti-angiogenic therapies. Unfortunately, in a phase III clinical trial pancreatic tumour patients who received gemcitabine in combination with bevacizumab, an anti-VEGF-A monoclonal antibody, did not show improvement in the overall survival (Longo, Brunetti et al. 2016).

1.2.5 Cancer associated fibroblasts, CAFs, and mesenchymal stromal cells, MSCs

CAFs are activated fibroblasts found in the tumour stroma. CAF morphology is similar to myofibroblasts, large spindle-shaped cells that are activated during the wound healing process (Tao, Huang et al. 2017) . Markers used to identify CAFs are α-smooth muscle actin (α-SMA), fibroblast activation protein (FAP) and platelet derived growth factor receptor-α and β (PDGFR α and β). CAFs promote tumour growth by the secretion of autocrine and/or paracrine cytokines, growth factors, such as EGF. Moreover, the soluble factors secreted by CAFs are involved in the recruitment of immune cells into the tumour, angiogenesis and metastasis (Tao, Huang et al. 2017).

In transgenic mice the depletion of α-SMA+ myofibroblasts leads to undifferentiated tumors with enhanced hypoxia, epithelial-to-mesenchymal transition, cancer stem cells and ability to metastasize and with reduced animal survival (Bolm, Cigolla et al. 2017). In mice and PDAC patients, low CAFs in the TME correlate with reduced survival (Ozdemir, Pentcheva-Hoang et al. 2014). Moreover, clinical trials targeting stromal myofibroblasts resulted in accelerated disease progression and immunotherapy combined with loss of myofibroblasts prolongs survival in mice (Ozdemir, Pentcheva-Hoang et al. 2014).

MSCs constitute a population of multipotent and undifferentiated adult cells with extensive self-renewal properties and the ability to differentiate into a variety of mesenchymal lineage cells. MSCs have both an anti-inflammatory and an immunomodulatory activity on the immune system (Klimczak and Kozlowska 2016). MSCs can be recruited by cancer cells and support tumour growth and progression. In particular, MSCs can induce cancer cells to evade the immune system, promote tumour angiogenesis, invasion and metastasis, epithelial-mesenchymal transition (EMT) and induction of stem-like properties that allow cancer stem cells to increase their survivability through the circulation (Chang, Schwertschkow et al. 2015).

1.2.6 Pancreatic stellate cells

PCSs are found in the exocrine portion of the healthy pancreas, near the acinar cells and represent about 4% of the total cells (Vonlaufen, Joshi et al. 2008, Apte, Pirola et al. 2012). In the quiescent state they are characterised by a star-like morphology and have lipid droplets, containing vitamin A within their cytoplasm (Vonlaufen, Joshi et al. 2008). The quiescent PCSs have a low proliferative capacity and produce low amounts of ECM (Vonlaufen, Joshi et al. 2008).

PSCs switch to an activate state after pancreatic injury, with morphological and functional changes (Apte, Pirola et al. 2012). Activated PSCs acquire a 'myofibroblast-like' phenotype, and lipid droplets disappear from the cytoplasm (Bachem, Zhou et al. 2008). PSCs start to express cytoskeletal protein named alpha smooth muscle actin (α-SMA) and secrete large amounts of ECM proteins including collagens, fibronectin and laminin (Vonlaufen, Phillips et al. 2008, Apte, Pirola et al. 2012). The activation of PSCs during pancreatic injury is caused by the presence of inflammatory cytokines such as IL-1, IL-6, and tumour necrosis factor alfa (TNF-α), growth factors like transforming growth factor β1 (TGF-β1), ethanol and its metabolites, and oxidative stress (Bachem, Zhou et al. 2008).

PSCs are capable of sustaining their activated state through autocrine signalling. For instance, they secrete growth factors such as platelet-derived growth factor,

connective tissue growth factor and endothelin 1 this generate an autocrine loop that maintain PSCs activation and increased production of fibrous ECM (Phillips 2012). PSCs also secrete inflammatory cytokines like TGF-β1, IL-1, IL-8 and IL-15 (Apte, Pirola et al. 2012).

In vitro studies of co-cultures of PCSs with pancreatic cancer cells showed that PSCs induced the proliferation of malignant cells, increased their migratory and invasion ability and reduced cancer cell apoptosis (Vonlaufen, Joshi et al. 2008, Apte, Pirola et al. 2012). Moreover, *in vivo* studies using an orthotopic mouse model, found that mice injected with cancer cells and PSCs developed larger tumours compared to mice injected only with cancer cells. Mice injected with both PSCs and cancer cells also developed distant metastases unlike mice injected with cancer cells alone (Vonlaufen, Joshi et al. 2008). PSCs are also able to stimulate angiogenesis by the secretion of VEGF and periostin (Erkan, Reiser-Erkan et al. 2009).

1.2.7 Soluble factors

There are many soluble mediators in the TME secreted by the malignant cells and other cell types. These soluble factors released in the TME include cytokines, chemokines, enzymes, such as cyclooxygenase-2 (COX-2) and metalloproteases (Farrow and Evers 2002). Cytokines such as TNF-α, interleukin IL-1α IL-1β, IL-6 and IL-10, found in the pancreatic TME create an inflammatory environment (Farrow and Evers 2002, Colotta, Allavena et al. 2009, Steele, Jamieson et al. 2013). These cytokines initiate inflammatory responses and are secreted by infiltrating leukocytes and malignant cells (Smyth, Cretney et al. 2004, Colotta, Allavena et al. 2009).

The IL-1 family cytokines IL-1α, IL-1β interact with membrane-bound IL-1 receptor type (IL-1R) I or II. IL-1α and IL-1β are produced by cancer cells and also by cells of the TME. IL-1β is expressed in several different malignant cell types, including breast, gastric, pancreatic, prostate, head and neck, liver, lung, cervix, and biliary duct (Lewis, Varghese et al. 2006). IL-1α levels are increased in tumour tissue and correlated with the survival of PDAC patients (Wormann, Diakopoulos

et al. 2014). Multiple *in vitro* studies have demonstrated that IL-1 promotes tumour progression, invasion, migration, sustaining angiogenesis and inducing an immunosuppressive environment (Smyth, Cretney et al. 2004, Wormann, Diakopoulos et al. 2014).

IL-6 is produced by tumour cells, fibroblasts and myeloid cells in the TME and after binding with its receptor, it activates signal transducer and activator of transcription 3 (STAT3) in both inflammatory cells and epithelial cells. IL-6 and STAT3 are constitutively active in tumours, leading to the up-regulation of genes involved in proliferation, survival, angiogenesis, migration, and inflammation, promoting tumour progression (Kumari, Dwarakanath et al. 2016). In PDAC patients, increased IL- 6 serum levels positively correlated with tumour stage and decreased survival (Wormann, Diakopoulos et al. 2014). Studies have suggested that IL-6 promotes PDAC development by enhancing the pro-tumorigenic STAT3 signalling (Wormann, Diakopoulos et al. 2014). For example, in a mouse model of PDAC IL-6, and STAT3 have been shown to be involved in pancreatic cancer initiation (Lesina, Kurkowski et al. 2011). In this study, the inactivation of IL-6 or STAT3 inhibited PanIN progression and reduced the progression of PDAC. Moreover, the aberrant activation of STAT3 accelerated tumour progression through PanIN stages and PDAC (Lesina, Kurkowski et al. 2011).

IL-10 is produced by cancer cells and cells of the TME, such as macrophages. The role of IL-10 in tumour progression is extremely controversial. Indeed, some studies showed that IL-10 positively promotes tumour growth, whereas others suggested that IL-10 is involved in the suppression of angiogenesis and metastasis (Mannino, Zhu et al. 2015). In pancreatic cancer patients, tissue and serum levels of IL-10 are increased. The presence of IL-10 promotes an anti-inflammatory microenvironment, which reduces the function of effector cells, such as natural killer cells and dendritic cells, and induces a shift toward Th2 cytokines (Wormann, Diakopoulos et al. 2014).

TNF-α is produced by cancer cells or by cells of the TME (Balkwill 2009). Several studies reported the increase of serum TNF-α concentration in different cancer

types, such as chronic lymphocytic leukaemia, Barrett's adenocarcinoma, prostate cancer, breast cancer, and cervical carcinoma. During carcinogenesis TNF-α is involved in tumour cell proliferation, angiogenesis, and metastasis (Wang and Lin 2008). In PDAC, high expression of TNF-α is an independent prognostic marker of poor survival. Zhao et al 2016 found that *in vivo* treatments with an anti-TNF-α antibody reduced desmoplasia and the inflammatory TME in PDAC. Moreover, the combination of anti-TNF-α treatments with chemotherapy, partly overcome chemoresistance, increasing the survival of PDAC mouse model (Zhao, Fan et al. 2016).

1.2.8 The immune infiltrate in pancreatic cancer

The cancer microenvironment has a diverse leukocyte population consisting of neutrophils, dendritic cells (DCs), macrophages, myeloid derived suppressor cells (MDSCs), monocytes, mast cells, natural killers (NK), eosinophils, B and T cells, (Figure 1.2 and Table 1.2) (Heinemann, Reni et al. 2014, Lunardi, Muschel et al. 2014). Infiltrating immune cells in the tumour microenvironment supports tumour progression by releasing growth and survival factors, matrix remodelling factors, immunosuppressive molecules and inflammatory mediators. (Wachsmann, Pop et al. 2012, Lunardi, Muschel et al. 2014).

Tumour cells have the ability to produce numerous chemotactic cytokines and chemokines that attract leukocytes. In addition, tumour cells influence components of the immune system in order to create an environment that promotes tumour growth and progression (Wormann, Diakopoulos et al. 2014). This may explain why most of the immune-infiltrated leukocytes have an immunosuppressive phenotype. This immunosuppressive population includes tumour-associated macrophages (TAMs), MDSCs and regulatory T cells (T_{regs}) (Cox and Olive 2012, Wormann, Diakopoulos et al. 2014). On the contrary, lymphocytes are mostly responsible for the anti-tumour immune response (Wachsmann, Pop et al. 2012).

Macrophages

The most abundant leukocyte subset in PDAC is TAMs, which can be identified by the expression of F4/80 in mouse or CD68 in humans. TAMs cluster around neoplastic ducts from very early stages (Mielgo and Schmid 2013) and are recruited to tumour sites by chemoattractants, including chemokines CCL2, CCL3, CCL4, CCL5, and CCL8. In addition, TAMs can be recruited via stromal-derived factor 1 (SDF-1), also known as CXCL12, and thrombospondin-1 (TSP-1) (Mielgo and Schmid 2013). Once in the tumour and activated, macrophages secrete various growth factors and cytokines into the immediate microenvironment, indirectly contributing to an altered stromal environment and to an enhanced desmoplasia.

TAMs can be broadly divided into two different population ns, the classical/M1-activated macrophages, which in humans are $CD68^{+}$, and the alternative/M2-activated macrophages, $CD163^{+}$. The M1-activated macrophages act against intracellular pathogens as well as tumour cells, providing an anti-tumorigenic response by secreting TNF-α (Ruffell, Affara et al. 2012, Mielgo and Schmid 2013). The M2-activated macrophages initiate a pro-tumorigenic response by promoting tumour growth, angiogenesis and invasion and suppressing the adaptive immunity (Ruffell, Affara et al. 2012) (Sica and Mantovani 2012). It is thought that the polarisation of TAMs from a tumour-suppressive M1 phenotype to a M2 phenotype is initiated by cytokines, including IL-10 and TGF-β received from T regulatory and tumour cells (Sica and Mantovani 2012). However, macrophages *in vivo* do not strictly adhere to the M1/M2 classification but instead they show a broad spectrum of phenotypes, in which M1 and M2 represent the two extremes of polarization. Moreover, in the TME, macrophages exhibit extraordinary plasticity, adapting their phenotype and effector functions in response to local stimuli (Sica and Mantovani 2012).

In PDAC macrophages are significantly increased compared to normal pancreatic tissue; TAMs with a M2 phenotype have been associated with a poor prognosis (Wachsmann, Pop et al. 2012).

MDSCs

MDSCs represent a prominent population in many tumour types as well as in the spleens of cancer patients and in mouse models of cancer (Cox and Olive 2012, Wormann, Diakopoulos et al. 2014). MDSCs are characterized by the expression of Gr-1 on their surface and they are recruited into tumours by granulocyte-macrophage colony-stimulating factor (GM-CSF), which is secreted by tumour cells (Bayne, Beatty et al. 2012). Within the tumour microenvironment the presence of MDSCs inversely correlates with that of cytotoxic T cells (CTL) (Clark, Hingorani et al. 2007). *In vivo* mouse model studies of PDAC have shown increased numbers of MDSCs in the TME. In particular, in a spontaneous mouse pancreatic carcinoma model, the increase of MDSCs was associated with their ability to suppress T-cell response (Wachsmann, Pop et al. 2012). In PDAC patients the levels of MDSCs in the circulation are increased when compared to healthy controls; and this is a poor prognostic factor (Sideras, Braat et al. 2014).

Neutrophils

The role of neutrophils in cancer is not fully understood although they have been implicated in several aspects of tumourigenesis such as tumour initiation, growth, proliferation, angiogenesis and metastatic spreading (Ocana, Nieto-Jimenez et al. 2017). Neutrophils are attracted into the TME by CXCR2 ligands, CXCL1, CXCL2 and CXCL5. Neutrophils mediate pro-tumour mechanisms by the secretion of several soluble factors, such as reactive oxygen species (ROS), proteases, cytokines and chemokines (Sionov, Fridlender et al. 2015).

Neutrophils are rarely found in PDAC biopsies although analysis of blood samples from PDAC patients revealed that elevated pre-operative neutrophil-lymphocyte ratio correlated with poorer prognosis (Evans and Costello 2012) .

T Cells

Few studies have addressed the role of tumour infiltrating lymphocytes, TILs in PDAC. The presence of $CD3^+$ T cells has been reported both in human and mice tumours (Evans and Costello 2012). $CD3^+$ T cells are mostly localized as aggregates

in the stroma while very few cells are reaching the tumour area (Wachsmann, Pop et al. 2012). The stroma has a large population of $CD4^+$ T lymphocytes and macrophages with a small population of $CD8^+$ T cells and B cells (Evans and Costello 2012). The role of both $CD4^+$ T and $CD8^+$ T lymphocytes and B cells in PDAC immunity is poorly understood (Wachsmann, Pop et al. 2012).

Amongst TILs, the role of T_{regs} cells is better understood. Both circulating and tumour resident T_{regs} are significantly increased in patients with PDAC compared to healthy controls. Moreover, the presence of T_{regs} within the tumour correlates with the stage and progression of disease. T_{regs} display an immunosuppressive phenotype and mediate the immune evasion of cancer cells in PDAC, by the suppression of $CD4^+$ T lymphocytes (Evans and Costello 2012). Interestingly, *in vivo* studies suggest that decreasing or depleting T_{regs} cells, in a mouse model of PDAC, results in the inhibition of tumour growth and the promotion of a tumour-specific immune response (Viehl, Moore et al. 2006, Tan, Goedegebuure et al. 2009).

Cell type	Activation stage in pancreatic cancer	Roles in tumour progression
NK	Deactivated	Unable to Induce tumour cytotoxicity
CD8+ T cells	Deactivated	Unable to kill tumour cells
TAM (M1)	Decreased	Anti-tumorigenic
TAM (M2)	Increased	Decrease survival, promote angiogenesis ad enhance metastasis
MDSCs	Increased	Decrease survival, suppress T cell response
T_{regs}	Increased	Decrease survival, mediate immune evasion and suppress T cell response

Table 1.2 Cells of the immune system in PDAC
List of major immune cells present in PADC, their activation state and their effect during tumour progression. NK: natural killer cell; TAM: tumour associated macrophage; MDSC: myeloid derived suppressor cell; T_{regs}: regulatory T cells.

The study of the TME is becoming fundamental to better understand how tumours are formed, progress and metastasise (Feig, Gopinathan et al. 2012). Additionally, understanding the roles of TME components has revealed new possible therapeutic targets, such as anti-angiogenic drugs and immunotherapy (Cid-Arregui and Juarez 2015). However, the study of the TME has revealed that there is huge variability in its composition. The dissimilarities in the TME are observed not only between tumours of different organs, but also within the same tumour type.

In pancreatic cancer the TME represent the biggest part of the tumour mass. Several studies revealed that the reciprocal interactions between tumour cells and components of TME have an important role in tumour initiation, progression, metastasis and chemioresistance (Carr and Fernandez-Zapico 2016). Large-scale genomic and transcriptomic analysis can help to identify new pathways and molecular components with potential therapeutic relevance. For example, the Bailey's study correlate the enrichment of expression patterns, that characterize specific immune cell populations, to better identify the molecular mechanisms that are active in the TME (Bailey, Chang et al. 2016). In the last years, several pre-clinical and clinical trials targeting different molecules, pathways or cells of the TME have been conducted. In early phase clinical trials, promising results have been obtained using immunotherapy (Cid-Arregui and Juarez 2015).

1.3 The chemokine superfamily

Chemokines are chemotactic cytokines mainly known for their ability to direct migration of immune cells. The chemokine superfamily includes approximately 50 chemotactic cytokines in humans and mice (Griffith, Sokol et al. 2014). Chemokines are involved in several biological processes, such as immune cell chemotaxis, embryogenesis, haematopoiesis, angiogenesis, wound healing, development and maintenance of immune tissues, and response to infection (Zlotnik and Yoshie 2012, Anders, Romagnani et al. 2014). Chemokines have been classified into four subgroups: CXC, CC, CX3C, and XC, according to the number and the spacing between the first two conserved cysteine residues in the amino terminal part of the

protein. The sequence homology among the chemokines is variable, between 20-90% (Anders, Romagnani et al. 2014).

Chemokines are small proteins, approximately 8-12 kDa, with conserved sequence. The majority of chemokines are soluble proteins, with the exception of CX3CL1 and CXCL16 which have a membrane-bound form. Most human chemokines have orthologs in mice and vice versa. However, some chemokines, such as CCL13, CXCL8, CCL14 and CCL18, are expressed only in humans, while CCL12 and CXCL15 are found only in mice (Zlotnik and Yoshie 2000).

Chemokines can be broadly divided into two functional groups: homeostatic or inflammatory chemokines (Table 1.3 and Figure 1.3) (Zlotnik and Yoshie 2000, Griffith, Sokol et al. 2014). Homeostatic chemokines are constitutively expressed and produced, while inflammatory chemokines are induced by the presence of stimuli, such as during times of infection or injury (Griffith, Sokol et al. 2014). Homeostatic chemokines are constitutively expressed in the body and play a pivotal role in hematopoiesis and in the development and maintenance of the immune system (Zlotnik and Yoshie 2012). In particular, they regulate the development of primary and secondary lymphoid organs during embryogenesis, stem cell homing, leukocyte maturation, homing of leukocyte precursors during haematopoiesis, immune surveillance and maintaining homeostatic leukocyte traffic, (Anders, Romagnani et al. 2014, Griffith, Sokol et al. 2014). Furthermore, over the past decade it has become clear that the expression of chemokines and their respective receptors is not restricted to hematopoietic cells (Balkwill 2012).

Inflammatory chemokines are induced by pro-inflammatory stimuli, such as TNF-α and IL-1, in order to recruit effector leukocytes to sites of infection, inflammation, tissue injury and tumours. Most inflammatory chemokines display a wide range of functions, acting on cells of both the innate and the adaptive immune system (Turner, Nedjai et al. 2014).

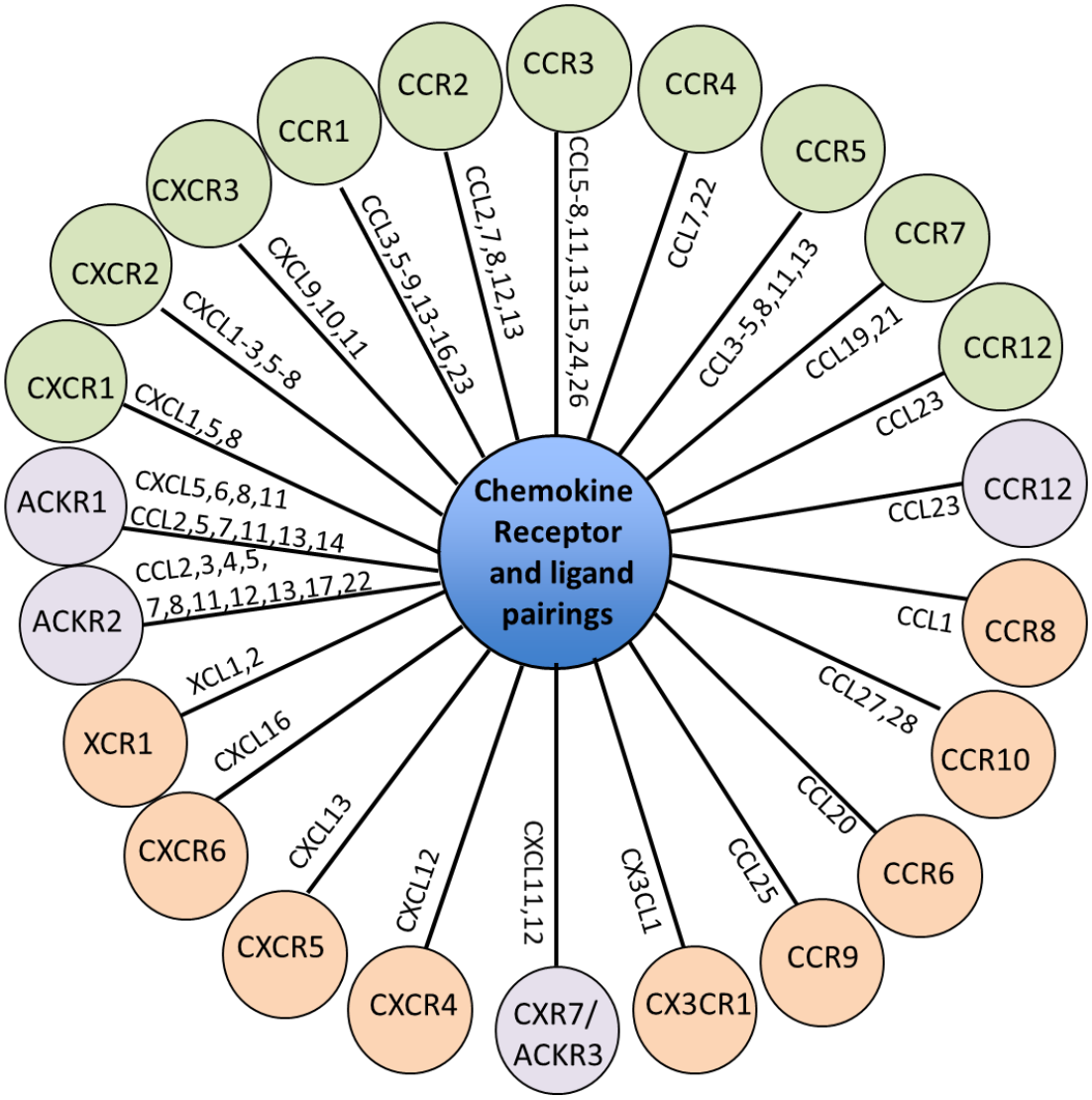

Figure 1.3 Chemokines and chemokine receptors pairing
The chemokine receptors belonging to XC, CC, CXC, and CX3C subfamilies are represented around the outer ring of the wheel, with their chemokine ligands shown along the wheel spokes. In green are shown the inflammatory chemokine in orange are shown the homeostatic chemokines and in purple are shown the atypical chemokines. Adapted from (White, Iqbal et al. 2013).

1.3.1 Chemokine receptors

Chemokines signal through seven transmembrane G protein coupled receptors (GPCR), referred to chemokine receptors. Approximately 20 different chemokine receptors have been characterized to date in humans and mice, and these are divided into four families depending on the type of chemokine they bind. They have been named according the chemokine subgroups, XC, CC, CXC, and CX3C followed

by “R” (for receptor) and a number indicating the order of their discovery (Zlotnik and Yoshie 2000).

Some chemokine receptors bind multiple chemokines, and vice versa, while others have exclusive chemokine receptor/ligand interactions (Table 1.3, Figure 1.3) (Lazennec and Richmond 2010, Roy, Evans et al. 2014). Most receptors generally bind to ligands that are restricted to one class of chemokines, i.e. CC or CXC ligands bind to CCR or CXCR respectively. Overall this suggests a high level of redundancy and compensatory mechanisms between chemokines. However, it has been proposed that the interaction between different chemokines with the same receptor may activate different signalling pathways (Murphy, Baggiolini et al. 2000). In particular, studies on CXCR3 have shown that there is no redundancy of ligand/receptor responses at a molecular level, suggesting a range of interactions that confers considerable flexibility to the response (O'Boyle 2012).

1.3.3 Structure and Signalling

The chemokine receptors share many structural features:

- Similar in size (about 350 amino acids)
- Short acidic N-terminal end
- Seven helical transmembrane domains with three intracellular and three extracellular hydrophilic loops
- Presence of the canonical sequence DRYLAIV within their second intracellular loop, important for G-protein coupling and signalling
- Intracellular C-terminus containing serine and threonine residues important for receptor regulation

The N-terminal domain of the chemokine receptor is extracellular and determines ligand binding specificity, while the C-terminal of the chemokine receptor interacts with the G proteins to allow intracellular signalling after receptor activation. (Patel, Channon et al. 2013)

The binding between a chemokine and its receptor induces a conformational change to the receptor leading to the activation of the coupled G proteins (Zweemer, Toraskar et al. 2014). Upon activation the Gβγ heterodimers disconnect

from the Gα subunit, allowing both subunits to propagate downstream signal transduction pathways. Both the α and the βγ subunits complex mediate chemokine-induced signals; however, it is the Gβγ subunits, which are required for chemotaxis (Figure 1.4).

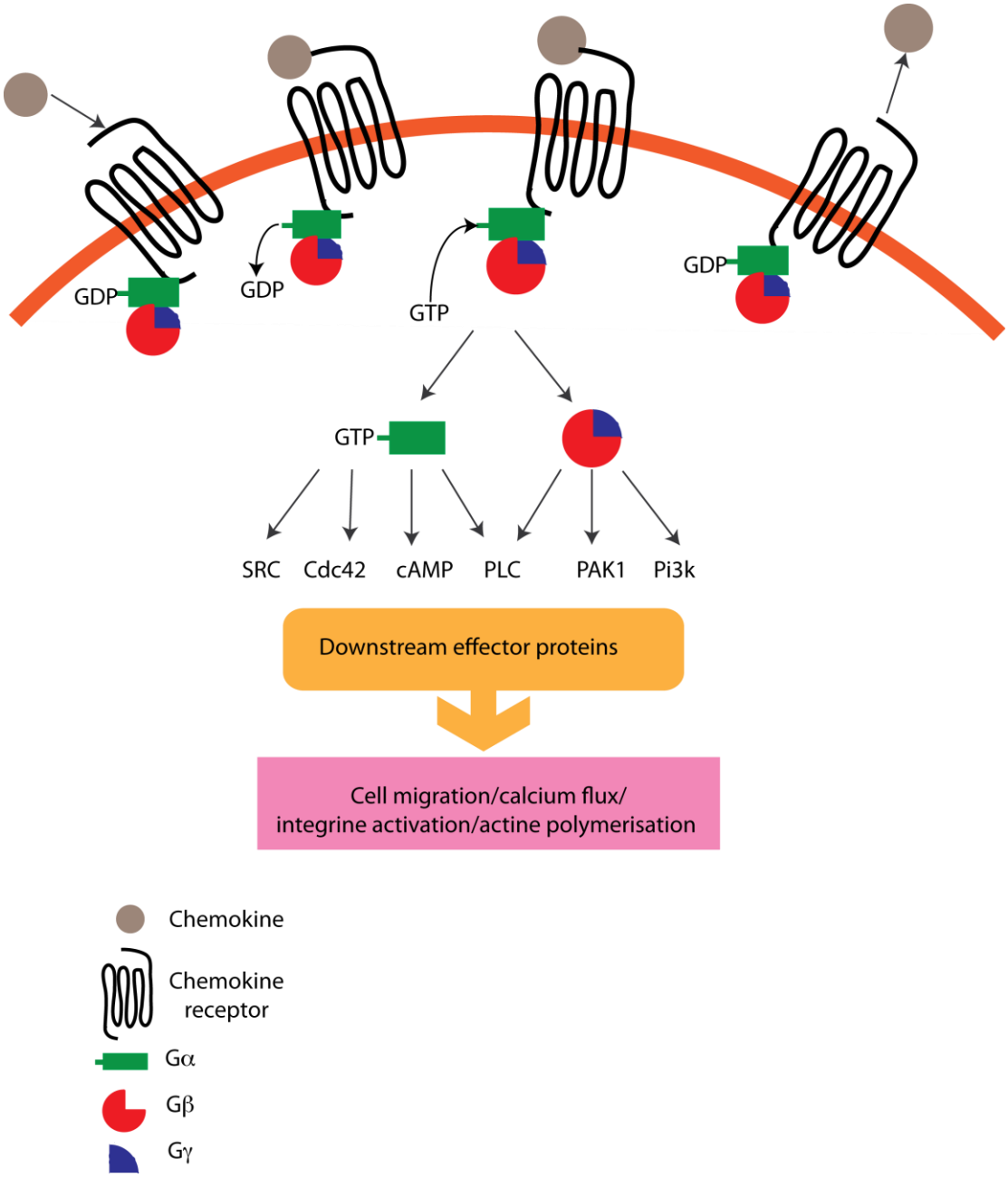

Figure 1.4 Chemokine-chemokine receptor signalling
Schematic representation of Chemokines of chemokine-chemokine receptors signalling pathways. Chemokines binding to its receptors activates G proteins. The Gα and Gβγ subunits dissociate and regulate downstream effector functions such as activation of SRC, Cdc42, cAMP, PLC, PAK1 and Pi3K (O'Hayre, Salanga et al. 2008).

1.3.4 Atypical chemokine receptors

Atypical (decoy or silent) chemokine receptors (ACKRs) are a subfamily of chemokine receptors that upon chemokine binding are unable to mediate the GPCR signalling events of "classical" chemokine receptors which lead to chemotaxis (Bachelerie, Graham et al. 2014). Four atypical chemokine receptors have been identified ACKR1/DARC, ACKR2/D6, ACKR3/CXCR7, and ACKR4/CCX-CKR/CCRL1 (Bachelerie, Graham et al. 2014).

The atypical receptors present, like the "classical chemokine", seven transmembrane domain but in most of them the highly conserved "DRYLAIV" motif is missing, preventing the activation of the coupled G protein (Nibbs and Graham 2013). The main function of the atypical chemokine receptors is to act as scavengers in order to remove an excess of chemokines, regulating the innate and adaptive immune response (Nomiyama, Osada et al. 2011). Atypical receptors can also generate signals through the downstream biochemical cascades of G-protein-independent signalling of GPCRs for example β-arrestins (Ulvmar, Hub et al. 2011).

1.3.5 Chemokines and chemokine receptors in disease

Several diseases have been associated with inappropriate activation of the chemokine network. In fact, abnormal regulation of both chemokines and their receptors has been shown to play a role in autoimmune disorders (inflammatory bowel disease, multiple sclerosis, psoriasis, atherosclerosis and rheumatoid arthritis), vascular and viral diseases and cancers (Table 1.3) (Gerard and Rollins 2001, Cheng and Chen 2014).

Atherosclerosis is a chronic inflammatory disease in which the arterial wall thickens, forming a plaque, through the damage of endothelial cells, the recruitment of leukocytes and the proliferation of vascular smooth muscle cells. Chemokines, in particular CCL2 and CX3CL1, have been implicated in the recruitment of monocytes inside the arterial lesion where they differentiate into macrophages, causing plaque formation and progression (Saederup, Chan et al.

2008, Weber 2008).

Rheumatoid arthritis (RA) is a chronic inflammatory autoimmune disease of the synovia of the joints. It is characterised by the infiltration of inflammatory cells. Some chemokines and chemokine receptors have been implicated in leukocyte ingress into the inflamed synovium and in synovial angiogenesis. CXCL8, CXCL5 and CXCL1, secreted by both synovial-lining cells and infiltrating leukocytes, are the most abundant chemokines present in the sera and synovial fluids in RA patients (Szekanecz, Vegvari et al. 2010, Raman, Sobolik-Delmaire et al. 2011).

Multiple sclerosis (MS) is a chronic neuroinflammatory disease characterised by the demyelination of neurons, neurodegeneration and by the recruitment of T lymphocytes and macrophages into the central nervous system. High levels of CXCL10, CCL3, and CCL5 have been found into MS lesions, which mediate the migration of T cells into the central nervous system (Gerard and Rollins 2001, Cheng and Chen 2014).

An example of the involvement of chemokine and their receptor in viral diseases can be observed during human immunodeficiency virus 1 (HIV-1) infection. The chemokine receptors involved during HIV-1 pathogenesis are principally CXCR4 and CCR5. Several studies have demonstrated that CXCR4 and CCR5 are required by the virus to entry into host cells. Moreover, it has been shown that people with a polymorphism in the CCR5 gene are resistant to viral infection (Gerard and Rollins 2001, Suresh and Wanchu 2006).

Chemokine receptors	Disease
CCR1	MS, psoriasis, RA and cancer
CCR2	MS, RA, atherosclerosis and cancer
CCR4	Asthma
CCR5	HIV and Cancer
CCR7	Cancer
CXCR3	MS, RA and cancer
CXCR4	HIV and cancer
CX3CR1	Atherosclerosis and cancer

Table 1.3 Chemokine receptors implicated in disease processes
Some chemokine receptors and the diseases in which they are involved. Adaptation from (Allen, Crown et al. 2007).

1.4 Chemokines and chemokine receptors in cancer

Chemokines and their receptors, which play an essential role in cellular migration and cell-cell interactions, are also involved in the movement of cells in and out of a tumour. In addition to their primary role as chemoattractants, chemokines and their receptors are also involved in other aspect of tumour development, such as tumour cell growth, metastasis formation and angiogenesis (Lazennec and Richmond 2010).

In the TME, the chemokines network it is really complex. In fact, both tumour and non-tumour cells not only can secrete several types of chemokines; but, at the same time, these cells can also express on their membrane a wide range of chemokine receptors. This results in the recruitment, activation and/or regulations of different cell types mediating the balance between anti- and pro-tumour responses (Lazennec and Richmond 2010). Chemokines and their receptors have been found expressed in several cancer types (Table 1.4). Interestingly, chemokine receptors which have been found on tumour cells, are generally not expressed on their normal tissues.

CXCR4 is one of the most commonly reported chemokine receptor expressed in cancers, present on at least 23 different tumours (Table 1.4) (Lazennec and Richmond 2010). This receptor is involved in metastasis formation and invasion (Mehrad, Keane et al. 2007, Sarvaiya, Guo et al. 2013).

Chemokine receptor	Chemokines	Tumour expression
CXCR4	CXCL12	23 different cancers including breast, prostate and melanoma
CXCR2	CXCL1, CXCL2, CXCL3, CXCL5, CXCL6, CXCL7 and CXCL8	Melanoma, pancreas, ovarian, prostate and lung
CCR2	CCL2, CCL7, CCL8 and CCL13	Multiple myeloma, prostate and breast
CCR4	CC17 and CCL22	Breast and T-cell lymphoma
CCR7	CCL19 and CCL21	Breast, melanoma, gastric, cervical, stomach, colorectal, T cell lymphoma and CCL
CCR10	CCL26, CCL27 and CCL28	Melanoma
CX3CR1	CX3CL1	Pancreas, prostate, breast and neuroblastoma

Table 1.4 Chemokine receptors in cancer
List of chemokine receptors which are upregulated in cancer. The table also shows the ligands for each chemokine receptors, and the tumours in which they are found. Adaptation from (Balkwill 2012).

1.4.1 Regulation of chemokines and chemokine receptors in cancer

Many different mechanisms can be involved in the altered expression of chemokines and chemokine receptors in cancer. The expression of chemokines and their receptors expression is regulated both by genetic and epigenetic mechanisms and environmental signals originated from the TME (Nagarsheth, Wicha et al. 2017). For example, mutations in the *RAS* gene, one of the most frequently mutated oncogene in human cancer, induce the production of tumour-promoting

inflammatory cytokines and chemokines, including CXCL1 and CXCL8. NF-kB (nuclear factor kappa-light-chain-enhancer of activated B cells), a key signalling factor often activated in cancer cells, can contribute to the transcription of chemokines and chemokines receptors (Richmond 2002, Maxwell, Gallagher et al. 2007). In breast cancer, the abnormal translocation of β-catenin induces the activation of several transcription factors and leads to the transcription and expression of CCL2, which has been implicated in the development of metastasis and invasion (Mestdagt, Polette et al. 2006).

Genetic mutations in chemokines and their receptors can also induce a pro-tumour effect. A study reported that a cancer cell line with a point mutation in the CXCR4 gene showed a delayed *in vivo* growth compared to non-mutated CXCR4. Importantly, the mutant receptor responds to CXCL12 signals (Ierano, Giuliano et al. 2009, Nagarsheth, Wicha et al. 2017).

Conditions present within the tumour, such as hypoxia and a rich cytokine environment can induce the transcription of certain chemokine or their receptors. For example, hypoxia triggers CXCL12 expression in primary human ovarian tumour cells, mechanism mediated by the transcription factor hypoxia-inducible factor 1 (HIF-1) (Kryczek, Lange et al. 2005, Nagarsheth, Wicha et al. 2017). HIF-1 it is also responsible of the expression of CXCR4 in renal cell carcinoma and of CXCR7 expression in rhabdomyosarcoma cells (Nagarsheth, Wicha et al. 2017).

1.4.2 The role of chemokines and chemokine receptors in malignant cells

Chemokines and their receptors play several roles during tumour progression, such as tumour cell growth, survival, and metastasis formation. The expression of chemokine receptors on cancer cells has been associated with their proliferation. For example, CXCR4 is involved in the tumour growth of many tumours and its inhibition induces apoptosis in ovarian cancer, hepatic cancer and chronic lymphocytic leukaemia cells (Sarvaiya, Guo et al. 2013). CXCL12 also plays an

important role in promoting the tumour growth of several cancer types, including leukaemia, glioma, non- Hodgkin's lymphoma, breast cancer, ovarian cancer, small cell lung cancer, and colon cancer (Sarvaiya, Guo et al. 2013). CXCR2 and its ligands have been shown to play a role in the growth of pancreatic, head and neck, and non-small cell lung carcinomas (Table 1.4) (Mukaida, Sasaki et al. 2014).

Moreover, the chemokine network can induce the tumour growth by generation of an autocrine loop induced by the secretion of chemokines by tumour cells itself. For example, the secretion of CXCL1, CXCL2, CXCL3 and CXCL8 by melanoma cells induce an autocrine loop which promotes tumour growth and proliferation. Indeed, blocking the corresponding chemokine receptor, CXCR2, to these ligands was found to attenuate melanoma cell proliferation (Payne and Cornelius 2002). Additionally, CXCL1, CXCL2 and CXCL3 have been associated with the tumour growth of pancreatic, cancer and gastric cancer.

The binding of chemokine to their receptors on tumour cells promote the proliferation and survival of tumour cells in several ways: inducing the activation of the MAPK/Erk signalling pathway, upregulating the expression of Mdm2, downregulating Bcl-2 expression or inhibiting the activation of caspase-3 and caspase-9.

Several lines of evidence support a role for the chemokine network in the invasion and metastasis of cancer (Sarvaiya, Guo et al. 2013). In breast cancer, CXCR4 and CCR7 are highly expressed and direct metastases to organs that are rich in their respective ligands (Muller, Homey et al. 2001, Sarvaiya, Guo et al. 2013). Moreover, CXCR4 promotes metastasis formation also in ovarian, prostate, and lung cancers (Raman, Sobolik-Delmaire et al. 2011); while CCR7 play a role in squamous cell, colorectal and gastric carcinomas metastatization. Breast cancer cells expressing CXCR4 are able to metastasize towards sites where CXCL12 is produced, such as the lymph nodes, lungs, liver and bone marrow (Mukherjee and Zhao 2013). The expression of CCR7 on tumour cells is associated with metastasis to the lymph nodes where its ligands, CCL19 and CCL21, are constitutively produced (Sarvaiya, Guo et al. 2013).

CXCR3 is another chemokines which induce cancer metastasis. In fact, the expression of CXCR3 has been associated with the pulmonary metastases of murine breast cancers, as well as the lymph node metastases of murine melanoma and colon cancer (Ma, Norsworthy et al. 2009). CCR9 and CCR10 expression on melanoma cells are associated with metastasis; CCR9 promote metastasization into the intestine while CCR10 into the lymph nodes (Raman, Sobolik-Delmaire et al. 2011)

1.4.3 Chemokines and chemokine receptors in leukocyte recruitment in the TME

The chemokines secreted into the TME are important in leukocyte trafficking in and out of the tumour. Notably, the type and the amount of chemokines and chemokines receptors are both important to determine which cell types are recruited into the tumour. Indeed, the alterations in the immune infiltration that is observed during tumour progression are caused by changing in the amount and the composition of chemokines ad their receptors present in the TME (Nagarsheth, Wicha et al. 2017). Each chemokine can recruit certain cell populations (Table 1.5). For this reason, the subset of immune cells present into the TME is, at least in part, determined by the network of chemokines secreted by malignant cells and stromal cells. For example, the presence of CC chemokines in the TME has been associated with the infiltration of macrophage and lymphocyte in human carcinomas of the breast, cervix, pancreas, sarcomas and glioma (Balkwill 2004).

CCL2 and CCL5 are the main attractants of monocytes into the TME (Nagarsheth, Wicha et al. 2017). CCL2 and CCL5 are secreted in breast cancer, melanoma, esophageal cancer, colon cancer, prostate cancer and pancreatic cancer (Mantovani, Savino et al. 2010). The CCL2–CCR2 signalling it is responsible for the recruitment of macrophages into the TME of many cancers. CCL2 levels correlate with the amount of TAMs in many tumours and are associated with poor patient prognosis in some cancers, such as breast cancer (Pollard 2004). The presence of macrophages affects tumour progression, angiogenesis, metastasis and chemotherapy response (Nagarsheth, Wicha et al. 2017). Moreover, the presence

of TAMs in the TME promotes an immune-suppressive environment by the production of immunosuppressive molecules, like TGF-β and IL-10, which will lead to the suppression of adaptive immunity (Pollard 2004).

The CXCL5/CXCR2 and CXCL12/CXCR4 axes are involved in the recruitment of MDSCs into the TME of many cancers, such as breast cancer (Nagarsheth, Wicha et al. 2017).

The presence of CXCL9 and CXCL10 in the TME recruit TILs that express CXCR3. High levels of CXCL9 and CXCL10 are associated with the infiltration of $CD8^+$ T cells, and in patients with ovarian cancer and colon cancer this correlates with a decrease in metastasis formation and improved survival (Nagarsheth, Wicha et al. 2017). The recruitment of TILs can be mediated also by CXCL16, which is found over-expressed in neuroblastoma, pancreatic and breast carcinoma (Mantovani, Savino et al. 2010). Tregs cells are recruited into the TME by the CCL22-CCR4 signalling pathway, CCL22 is secreted mainly by tumour cells and macrophages (Nagarsheth, Wicha et al. 2017).

Chemokines	Immune cells recruited	Effects on the TME
CCL2	Monocytes and MDSCs	Promotes tumour cell proliferation, vascularization and metastasis
CCL3	Monocytes and macrophages	Promotes cancer extravasation
CCL5	Monocytes and macrophages	Induces metastasis
CCL22	Tregs	Induces antitumour immunity
CXCL8	Neutrophils and MDSCs	Promotes invasion, migration, apoptosis and angiogenesis Increase the immunogenecity of the tumour
CXCL12	B cells, pDCs, monocytes and T cells	Promotes proliferation, survival metastasis and angiogenesis
CXCL14	DCs	Promotes invasions Inhibits proliferation, metastasis and increase apoptosis
CXCL17	MDSCs	Promotes angiogenesis
CXCL9 and CXCL10	T cells and NK cells	Inhibits angiogenesis

Table 1.5 Chemokine functions and immune cells recruitment
List of chemokines associated with the immune populations that they recruit into the TME and their function during tumour progression. DC, dendritic cell; MDSC: myeloid-derived suppressor cell; NK: natural killer; pDC: plasmacytoid dendritic cells; Treg cell: regulatory T cell. Modified from (Nagarsheth, Wicha et al. 2017).

1.4.4 Chemokines and chemokine receptors and angiogenesis

Chemokines have an important role in tumour angiogenesis. Chemokines perform their role in angiogenesis by either directly binding their receptors on endothelial cells and regulating their functions, or by inducing the expression of pro-angiogenic factors and promote the recruitment of pro-angiogenic immune cells and endothelial progenitors to the TME (Sarvaiya, Guo et al. 2013).

The CXC chemokine family plays a critical role in angiogenesis. The presence or absence of a three amino acid sequence, glutamic acid-leucine-argenine (referred as the 'ELR' motif), further subdivided the CXC chemokine family into two groups. Studies have established that angiogenic activity of CXC chemokines depends on the presence of the ELR motif in the CXC sequence. In fact, CXC chemokines that are ELR^+ display potent angiogenic activities and stimulate endothelial cell chemotaxis, whereas ELR^- chemokines are angiostatic (Santoni, Bracarda et al. 2014). ELR^+ chemokines mediate their pro-angiogenic functions both as autocrine growth factors and as potent paracrine mediators of angiogenesis, which required the activation of NF-κB pathway (Santoni, Bracarda et al. 2014). CXCL1, CXCL2, CXCL3, CXCL5, CXCL6, CXCL8, CXCL12, CCL2, CCL11 and CCL16 belong to the angiogenic type of chemokines whereas CXCL4, CXCL9, CXCL10, CXCL11 and CXCL14 are angiostatic. Moreover, studies have shown that ELR^+ chemokines bind to CXCR1 and CXCR2, while the ELR^- chemokines bind to CXCR3, CXCR4 and CXCR5 (Mehrad, Keane et al. 2007, Santoni, Bracarda et al. 2014).

Some of CC chemokines also play a role in angiogenesis, such as CCL2, CCL11, CCL16, and CCL21. The first three chemokines have been shown to promote angiogenesis while CCL21 has an anti-angiogenic effect on tumours (Santoni, Bracarda et al. 2014).

Chemokines and their receptors are involved in several steps of tumour progression, and metastasis, therefore they have been considered as a therapeutic target (Mukaida, Sasaki et al. 2014, Vela, Aris et al. 2015). Pre-clinical studies showed that CXCR4 antagonists significantly reduced the size of primary tumours and had anti-metastatic effects in mouse models of melanoma, osteosarcoma, breast and prostate tumours (Allavena, Germano et al. 2011, Nagarsheth, Wicha et al. 2017).

1.5 CX3CL1 and its receptor

CX3CL1, also known as fractalkine or neurotactin, is the only member of the CX3C chemokine group (Bazan, Bacon et al. 1997). In steady-state conditions, CX3CL1 is

expressed in the brain, lungs, kidney, intestines, pancreas, adipose tissue and liver. Its expression is upregulated in inflammatory conditions. At cellular level, CX3CL1 it is expressed by neurons, adypocytes, epithelial, endothelial and smooth muscle cells (Jung, Aliberti et al. 2000, Kim, Vallon-Eberhard et al. 2011).

CX3CL1 exists both as a soluble and as a cell membrane protein. Mature membrane bound fractalkine is a 371 (mouse) or 373 (human) amino acid peptide. It contains four domains: a chemokine domain joined by a mucin-like stalk to a transmembrane domain, that is proposed to act as an adhesion molecule, and a cytoplasmic domain (Figure 1.5) (Kim, Vallon-Eberhard et al. 2011). The extracellular domain is shed from the cell surface by the ADAM10 and ADAM17 metalloproteases (Figure 1.5) (Hundhausen, Misztela et al. 2003, Kim, Vallon-Eberhard et al. 2011). The shedding of membrane bound CX3CL1 into a soluble form represents a key regulatory mechanism for CX3CL1 signalling. The release of soluble CX3CL1 from endothelial and epithelial cells occurs both constitutively and in an inducible manner (Hundhausen, Misztela et al. 2003, Kim, Vallon-Eberhard et al. 2011). The constitutive cleavage of CX3CL1 occurs manly by ADAM10. Appropriate stimuli, such as lipopolysaccharide (LPS) and interleukin IL-1β, accelerate the CX3CL1 shedding by ADAM17 (Liu, Jiang et al. 2016). The shedding of CX3CL1 by ADAM17 is increased in several pathological condition such as cancer, diabetes, atherosclerosis, ischemia, arthritis, neurological and immune diseases (Menghini, Fiorentino et al. 2013).

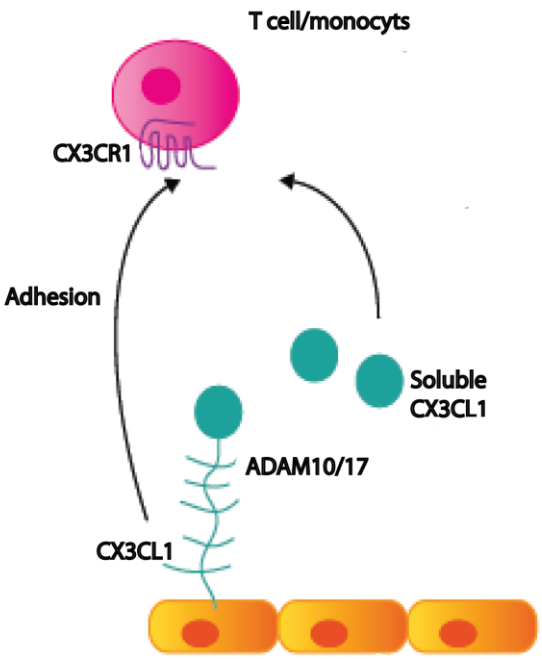

Figure 1.5 Structure of CX3CL1 and its receptor
Membrane-bound CX3CL1 enables the integrin-independent capture and firm adhesion of leukocytes via the G-coupled receptor CX3CR1. Cleavage of cell-surface CX3CL1 by metalloproteinases (ADAM 10/17) generates a soluble chemokine, which binds CX3CR1 on nearby cells, via signalling intermediates, can induce cell chemotaxis and survival. Modified from (Kasama, Odai et al. 2008).

CX3CR1 is the sole receptor for CX3CL1 (Imai, Hieshima et al. 1997). This receptor is a G-coupled receptor and is expressed on monocytes, macrophages, dendritic cells, T cells, NK cells and microglia (Imai, Hieshima et al. 1997, Jung, Aliberti et al. 2000). Receptor binding by soluble fractalkine induces phosphorylation of Akt and ERK in a time- and dose-dependent manner (Lee, Namkoong et al. 2006). .

Both transmembrane and soluble forms of CX3CL1 bind to CX3CR1, but each form mediates distinct functions. Transmembrane CX3CL1 serves as an adhesion molecule, mediating enhanced leukocyte adhesion to endothelial cells under flow conditions, without the activation of integrins (Fong, Robinson et al. 1998, Schulz, Schafer et al. 2007). This activity is largely independent of CX3CR1-mediated G-protein activation but is predominantly a result of the physical interaction of the

transmembrane chemokine with its receptor. By contrast, soluble CX3CL1 acts as a chemoattractant inducing directional cell migration of monocytes, NK cells, T cells and B cells, via CX3CR1 signalling and activation of G -proteins (Gautier, Jakubzick et al. 2009, Corcione, Ferretti et al. 2012). CX3CL1/CX3CR1 interactions are also vital for many homeostatic processes, including the survival of $CX3CR1^{high}$ blood monocytes (Landsman, Bar-On et al. 2009), wound healing (Ishida, Gao et al. 2008) and trans-endothelial migration for immune surveillance (Auffray, Fogg et al. 2007).

The generation, by Jung et al, of the $CX3CR1^{GFP/GFP}$ mouse model, in which the CX3CR1 locus has been replaced by GFP reporter gene, allowed investigation of the expression and the function of this chemokine receptor. In this model, they substituted the first 390 bp of the second CX3CR1 exon with GFP, encoding the N terminus of the receptor, which is crucial for interacting with CX3CL1 (Jung, Aliberti et al. 2000). The study revealed that the homozygous mutant $CX3CR1^{GFP/GFP}$ mice did not exhibit any developmental defects, were generated in normal Mendelian distribution, and were fertile (Jung, Aliberti et al. 2000). Moreover, they demonstrated that the CX3CL1-CX3CR1 axis did not play essential role in monocyte recruitment in peritonitis, DC differentiation and migration in response to microbial antigens or contact sensitizers, and the microglial response to nerve injury (Jung, Aliberti et al. 2000).

However, other researches have shown that the CX3CL1/CX3CR1 network is known to be involved in various pathological conditions, such as cancer, inflammation, infection, diabetes and autoimmunity diseases (Jung, Aliberti et al. 2000, Kim, Vallon-Eberhard et al. 2011). For instance, CX3CR1 is responsible for recruiting dendritic cells and a subset of monocytes in models of atherosclerosis (Liu, Yu et al. 2008). CX3CR1 deficiency results in impaired microglia migration in a mouse model of age-related macular degeneration (Combadiere, Feumi et al. 2007).

1.5.1 CX3CR1 in cancer

Several studies have reported an upregulation of CX3CR1 in cancers such as prostate (Shulby, Dolloff et al. 2004), breast (Andre, Cabioglu et al. 2006) and pancreatic (Allavena, Germano et al. 2011) (see Figure 1.6). CX3CR1 expression is associated with increased migration and metastasis formation (Marchesi, Piemonti et al. 2008, Marchesi, Locatelli et al. 2010).

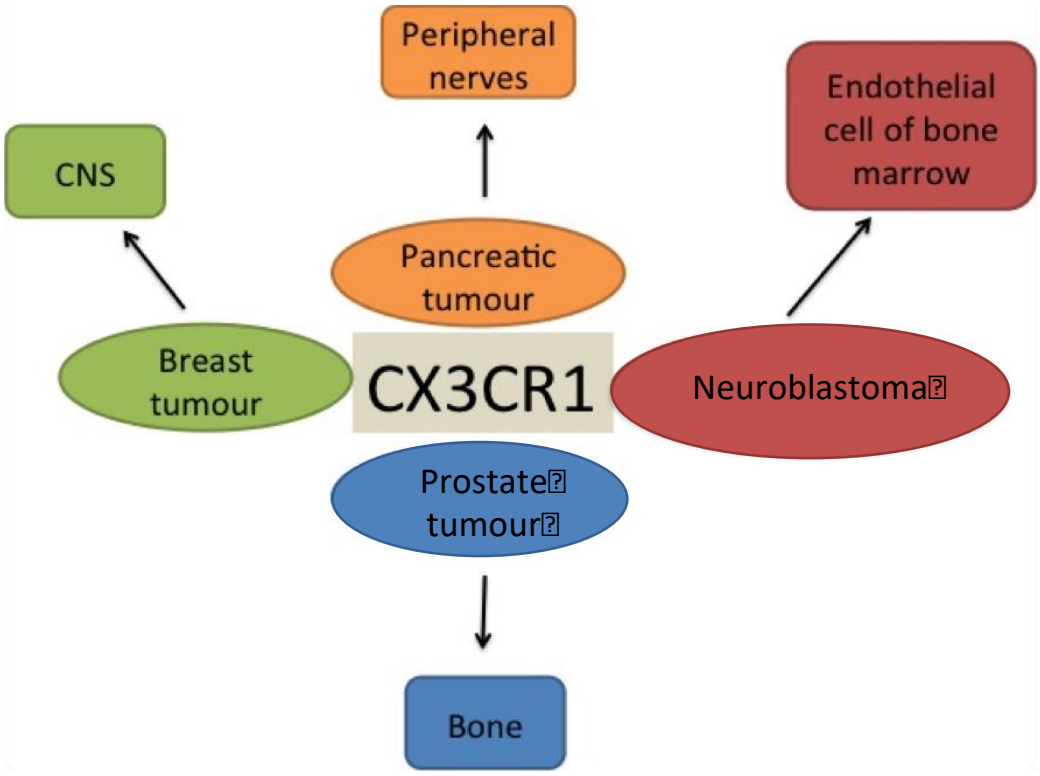

Figure 1.6 CX3CR1 in cancer and metastasis
Scheme showing in which tumours CX3CR1 is upregulated and the organs or tissue to which it mediated the migration and the metastasis formation. CNS: central nervous system. Modified from (Marchesi, Locatelli et al. 2010).

There is evidence that CX3CR1 plays a role in different stages of tumour progression. In lung tumours, malignant cells recruit macrophages by secreting CCL2 and CX3CL1. The CCR2-CCL2 and CX3CR1-CX3CL1 cross talk between cancer cells and the recruited macrophages enhances cancer cell proliferation and migration (Schmall, Al-Tamari et al. 2015).

The CX3CR1/CX3CL1 axis has been also implicated in B cell malignancies, where it might support the communication between CLL cells, which coexpress CX3CR1 and

its ligand, and the TME (Ferretti, Pistoia et al. 2014). In breast cancer CX3CR1 expression by tumour cells was associated with metastasis to the brain. Moreover, CX3CL1 expression showed a positive correlation with increased TILs but it correlated negatively with overall survival (Liu, Jiang et al. 2016). In neuroblastoma, soluble CX3CL1 stimulates $CX3CR1^{+}$ cancer cells to transmigrate through human bone marrow endothelium, implying a prometastatic effect. In human colon carcinoma the expression of CX3CR1 is correlated with poor prognosis. Furthermore, depletion of CX3CR1 resulted in the significant inhibition of liver metastasis formation. Metastatic tumours in CX3CR1 KO mice exhibit also increase in apoptosis and decrease in vasculature, which seemed to be mediated by macrophages. In fact, it has been observed that in hepatic metastases macrophages expressed CX3CR1 (Zheng, Yang et al. 2013).

CX3CR1 is highly expressed in both human pancreatic tumour cell lines and in primary PDAC tumour tissues, whilst a 'benign' epithelial pancreatic duct cell line and 'normal' exocrine pancreas do not express the receptor (Allavena, Germano et al. 2011). Interestingly, CX3CR1 expression is an early feature of pancreatic carcinogenesis, being found already in PanIN-1. In addition, expression is increased from PanIN-1 to PanIN-3 (Celesti, Di Caro et al. 2013).

Marchesi et al. showed that in pancreatic cancer the CX3CL1-CX3CR1 axis is responsible for the neurotropism of tumour cells to peripheral nerves, which is known as perineural invasion (PNI). $CX3CR1^{+}$ tumour cells migrate in response to its ligand CX3CL1 (Allavena, Germano et al. 2011). There is also a positive correlation between CX3CR1 expression and the grade of PNI; high receptor expression was associated with increased neuron invasion by cancer cells (Allavena, Germano et al. 2011) (Marchesi, Locatelli et al. 2010). Their work proposed that CX3CR1 gives PDAC tumour cells an adhesive advantage to bind to neurons.

1.6 Aim of this thesis

The aim of this thesis is to investigate the role of CX3CR1 in a murine model of pancreatic cancer, the KPC model. I will examine if the lack of CX3CR1 in KPC mice has an effect on overall survival of mice, response to chemotherapy and on the tumour microenvironment, focusing on immune cell infiltration and inflammation.

Chapter 2 Methods

2.1 Animal husbandry

The conditional CX3CR1$^{GFP/+}$Lox-Stop-Lox-KRAS$^{G12D/+LSL}$-Trp53$^{R172H/+}$ and the CX3CR1$^{GFP/+}$Pdx1-Cre strains were interbred to obtain CX3CR1$^{GFP/GFP}$LSL-KRAS$^{G12D/+}$LSLTrp53$^{R172H/+}$Pdx1-Cre (CKPC) and LSL-KRAS$^{G12D/+}$ LSLTrp53$^{R172H/+}$Pdx1-Cre (KPC) mutant mice. All mice were genotype at weaning and samples sent to Transnetyx, Inc.

The mice were constantly monitored for the appearance of palpable tumours, ascites, swollen abdomen, weight loss, inability to move, reduced food ingestion and visible symptoms of pain (hunching, piloerection and isolation from other mice). The presence of any of these symptoms was considered an endpoint human criteria. Thus, mice were culled by neck dislocation. Animal procedures were carried out in accordance with the U.K. Home Office Animal and Scientific Procedures Act 1986.

Strain	Mutation	GFP	CX3CR1 WT
KPC	KRAS$^{G12D/+}$ Trp53$^{R172H/+}$	NO	YES
CKPC	KRAS$^{G12D/+}$ Trp53$^{R172H/+}$	YES	NO

Table 2.1 Description of the mice strains
The table summarises the mutations that characterise the mice strains used in the experiments.

2.2 Tissue processing

Blood, pancreatic tumour, spleen, mesenteric lymph nodes and legs were collected from each mouse. The tumour and spleen were cut in half, one half of each organ was transferred into a cryovials and snap frozen in liquid nitrogen and stored at -80°C. The other half as well as the mesenteric lymph nodes and legs, were placed in a bijou tube with phosphate buffered saline (PBS) (SIGMA - D8537) and kept on ice until further processing for flow cytometry staining.

2.2.1 Blood processing

Mice were anaesthetised by 3% isoflurane/1% 0_2 anaesthesia. Cardiac puncture was performed with a 1 ml syringe (Henke Sass Wolf - cat. No 5010-200V0) coupled to a 27G needle (BD Microlance - Cat. No 302200) previously coated with Ethylenediaminetetraacetic acid (EDTA) (Invitrogen - Cat. No 9262) to avoid blood clots. Typically, 0.5 to 1 ml of blood were obtained. Subsequently, blood was centrifuged with three consecutive times to separate the plasma from cells.

1. 200 relative centrifugal force (rcf) for 10 minutes at 4°C
2. 2300 rcf for 5 minutes at 4°C
3. 16100 rcf for 3 minutes at 4°C.

After the process, plasma was collected in an eppendorf tube and stored at -80°C. For blood cell analysis, pellets obtained after centrifugations were transferred into a 50 mL falcon tube and incubated with red blood cell lysis buffer (eBioscence - Cat. No 00-4300-54) for 10 minutes at room temperature. Lysis reaction was stopped by adding 10 ml of FACS buffer [2.0 mM EDTA and 5% of bovine serum albumin (BSA) in PBS] and then centrifuged at 320 rcf for 5 minutes at 4°C. The pellet was resuspended in 5 ml of FACS buffer.

2.2.2 Pancreatic tumours

Each tumour was longitudinally cut in half. Half of the tumour was snap frozen in liquid nitrogen or dry ice and the other half was placed in ice-cold PBS and kept on ice. Using a scalpel the tumour was cut into small pieces and transferred into a 50 ml falcon containing 5 ml of Dulbecco's Modified Eagle's Medium (DMEM) (Sigma – Cat. No P4333) plus 2.0 mg/ml of collagenase IV (sigma – cat. No C9263-1G) and 10 mg/ml of DNase (sigma - cat. No D4513). Tumour digestion was performed in an orbital shaker at 150 rpm for 20 minutes at 37°C. The reaction was stopped by adding 10 ml of FACS buffer. The digested tumour was then passed through a 70 µm cell strainer (Fischer Scientific – Cat. No 11597522) with FACS buffer to obtain a single cell suspension and centrifuged at 320 rcf for 5 minutes at 4°C. Finally, the pellet was resuspended in 10 ml of FACS buffer.

2.2.3 Spleen

Spleen was collected from each mouse in ice-cold PBS and kept on ice until further disruption through a 70 µm cell strainer with FACS buffer. The obtained suspension was centrifuged at 320 rcf for 5 minutes at 4°C. The cell pellet was resuspended in 10 ml of red blood lysis buffer solution (prepared as in 2.2.1) and incubated for 10 minutes at room temperature. Lysis was stopped by adding 10 ml of FACS buffer and then centrifuged at 320 rcf for 5 minutes at 4°C. Finally, the pellet was resuspended in FACS buffer.

2.2.4 Mesenteric lymph nodes

1-3 MLN were collected in ice-cold PBS and kept on ice until they were disrupted through a 70 µm cell straining with FACS buffer and then centrifuged at 320 rcf for 5 minutes at 4°C. The pellet was resuspended in 5 ml of FACS buffer.

2.2.5 Bone marrow

Hind legs of each mouse were collected in ice-cold PBS and kept on ice. The femurs and tibias were flushed with FACS buffer using a 27G needle. The obtained cell suspension was passed through a 70 µm cell strainer with FACS buffer and then centrifuged as explained in 2.2.3. Red blood cell lysis was performed as described in 2.2.1.

2.3 Staining for flow cytometry analysis

For each organ 0.5-3 x 10^6 of cells were plated into a v-bottom 96-well cell plate (Termo Fisher – Cat. No 2605) and centrifuged at 320 rcf for 5 minutes at 4°C. For blocking non-specific binding sites, cells were resuspended and incubated for 15 minutes on ice in 50 µl ice-cold FACS buffer containing anti-mouse CD16/32 (fragment crystallisable) receptors (eBioscience – 14-0161-86) diluted 1:100 in FACS buffer. After, 50 µl of antibody master mix (2X) was added to each sample (Table 2.2) and incubated for 30 minutes on ice in the dark. Samples were washed

twice in FACS buffer, by centrifugation at 320 rcf for 5 minutes at 4°C. In order to visualise dead cells, 50 µl of Fixed Viability Dye (FVD) (eBioscience – Cat. No 65-0863-18), diluted (1:250) in PBS, was added to each sample and incubated for 30 minutes on ice in the dark. After 2 washes, samples were resuspended in 100 µl of FACS buffer and kept at 4°C until analysis by flow cytometry. Flow cytometry was performed using an LSRFortesa cell analyser (BD biosciences). Data were analysed using the FLowJo software (Tree Star, Oregon, USA).

Marker	Fluorochrome	Dilution 1X	Company	Cat. N.
CD45	Brilliant Violet 785	1:100	Biolegend	103149
CD11b	Brilliant Violet 650	1:100	Biolegend	101239
Ly6G	AlexaFlor700	1:100	eBioscence	56-5931
Ly6C	e-Flour650	1:100	eBioscence	48-5932
F4/80	PE	1:100	Biolegend	123110
CD3	Pe-Cy7	1:50	Biolegend	100320
CD4	Brilliant Violet 605	1:200	Biolegend	100548
CD8	APC	1:200	eBioscence	17-0081
CD19	PerCP-Cy5.5	1:200	Biolegend	115534

Table 2.2 List of the antibodies used for flow cytometry analysis
Table describes conjugated antibodies, obtained from eBioscience and Biolegend, used for flow cytometric analysis listing the coupled fluorochrome, dilution, company and catalogue number for each antibody. APC: allophycocyanin, PE: Phycoerythirin, Pe-Cy7: Phycoerythirin-cyanine-7 and PerCP-Cy5.5: Peridinin-chlorophyll proteins- Cyanine-5.5.

2.4 Immunofluorescence staining

Tumour sections, obtained from frozen tumour samples, were air-dried for 30 minutes. Slides were fixed in 4% PFA for 20 minutes at room temperature, washed in PBS and permeabilised with 0.1% Triton-X100 (Sigma-Aldrich T8787) in PBS for 5 minutes at room temperature. Tumour sections were blocked with mouse background blocker (MenaPath MP-961) for 1 hour at room temperature. Sections were incubated with primary antibody, isotype control and/or conjugated antibody diluted in 5% goat serum and 2.5% BSA in PBS for 1 hour at room

temperature (Table 2.3). Sections were washed with PBS with 0.1% Tween-20 (Sigma-Aldrich – P7949) (PBS-T) and, when stained with primary antibody, incubated with a goat anti-rabbit Alexa-546 secondary antibody (Invitrogen A21245) for 1 hour, diluted 1:1000, at room temperature in the absence of light. Sections were rinsed three times with PBS-T and once with water.

The slides were mounted using Prolong Gold antifade reagent with 4'6-Diamidino-2-Phenylindole (DAPI) (Invitrogen P36931).

Antibody	Conjugated	Dilution	Company	Catalogue number
F4/80	NO	1:300	Serotec	MCA497R
CX3CR1	NO	1:50	ABCAM	AB8021
E-cadherin	eFlour660	1:100	eBioscience	50-3249
Goat anti-rabbit	Alexa Fluor 546	1:1000	Invitrogen	A21245

Table 2.3 List of the primary antibodies used for Immunofluorescence staining
Table describes primary antibodies used for immunofluorescence staining, detailing the coupled fluorochrome (when present), dilution used, purchaser and catalogue number for each antibody.

2.5 Tumour protein extraction

For protein extraction, 75 mg of frozen tumour was homogenised in 1 ml of lysis buffer (150 nM NaCl (Sigma-Aldrich – 71380), 20 mM Tris pH 7.5 (Sigma-Aldrich – T1503), 1 mM EDTA, 1 mM EGTA (Invitrogen E4378), 1% Triton X-100 (Sigma-Aldrich – X100) plus complete mini protease inhibitor cocktail tablet (Roche – 11836153001) and phosphatase inhibitors II and III (Sigma-Aldrich - P5726 and P0044, respectively). Samples were homogenised using a gentleMACS homogeniser. The homogenised tissue was centrifuged at 200 rcf for 5 minutes, transferred into an eppendorf tube and sonicated using probe solicitor at 40% amplitude for 5-15 seconds on ice. After rotating the samples for 30 minutes at 4°C on a rotator, tubes were centrifuged at 16100 rcf for 15 minutes at 4°C and supernatants collected.

2.6 Protein Quantification

Protein concentration was determined using the BCA protein assay. Working reagent was prepared by combining 50 parts of bicinchoninic acid solution (Sigma-Aldrich – B6943) and 1 part of Copper (II) sulphate solution (Sigma-Aldrich - C2284). To create a standard curve, BSA was diluted in PBS to obtain a range of protein concentrations between 0 to 2 mg/ml. 10 µl of samples (diluted 1:10 in PBS) negative control or BSA standards were plated, in triplicate, in a 96-well plate with 200 µl of working reagent and incubated at 37°C for 30 minutes. The optical density was measured at 595 nm and the concentration of each sample was interpolated from the standard curve.

2.7 Enzyme-linked immunosorbent assay (ELISA)

ELISA kits from BD biosciences were used to measure the level of IL-12p40 (Cat. No 555165), IL-6 (Cat. No 555240), TNF-a (Cat. No 558354) and IL-10 (Cat. No 555157). The assay was performed in 96-wells microplates from Costar (Cat. No 3690), according to the manufacturer's guidelines. Briefly, capture antibody was diluted 1:250 in PBS, added to each well and incubated overnight at 4°C. On the following day, the plate was washed three times in washing buffer (PBS with 0.05% of Tween-20). In order to block any specific binding, the assay diluent (PBS with 10% FBS) was added to each well and incubated for 1 hour at room temperature. Then, standard solutions of each cytokine were prepared by serial dilution to obtain the following concentrations 1000, 500, 250, 125, 62.5 31.3 and 15.6 pg/mL. After discarding the assay diluent and washing three times the plate, samples and standards were added to each well and incubated for 2 hours at room temperature. The plate was then washed five times with washing buffer and subsequently the working detector solution [detection antibody and horseradish peroxidase (HRP)] was added to the plate and incubated for 1 hour at room temperature. At the end of the incubation, the plate was washed seven times and then substrate solution, tetramethylbenzidine (TMB) and hydrogen peroxide from the TMB substrate reagent set (BD Pharmagen, Cat. No 555214) were added and incubated in the absence of light until the appropriate colour change was observed. The reaction

was stopped by adding 25 ul of 1M of H_3PO_4 in each well. Plates were analysed on a plate reader at 450 nm.

2.7.1 CX3CL1 ELISA

To determine the presence and concentration of CX3CL1 I used the Mouse CX3CL1/Fractalkine Quantikine ELISA Kit (R&D system - MCX310). Briefly, tumour protein lysates and plasmas were allowed to thaw on ice. Tumour samples were diluted in calibrator diluent RD5-3, to obtain 85 µg of protein/sample, while plasma samples were diluted in 1:1 or 1:10. In each well, of a 96 well plate, 50 µl of Assay Diluent RD1W were added to 50 µl of standards, control, or samples. After two hours of incubation at room temperature, samples were washed 5 times in washing buffer. Then, 100 µl of mouse fractalkine conjugate was added to each well and incubated for two hours at room temperature. After 5 washes in washing buffer, 100 µl of substrate solution was added to each well and incubated for 30 minutes at room temperature. Finally, 100 µl of stop solution was added to each well and the plate was read at 450 nm with wavelength correction, set to 540 nm.

2.8 RNA extraction

30 mg of tumour samples were homogenised in 600 µl of RLT buffer with 4% b-mercaptoethanol using a gentleMACS homogeniser. RNA was obtained using the RNeasy microkit (Qiagen - 74004) according to manufacturer guidelines. Briefly, each sample was centrifuged for 3 minutes at 13200 rcf, the supernatant was collected and pipetted directly into a QIAshredder spin column placed in a 2 ml collection tube, and centrifuged for 2 minutes 16100 rcf for 3 minutes at 4°C. After collecting the supernatant, equal volume of 70% ethanol was added and sample transferred to an RNA binding column placed in a 2 ml collection tube, centrifuged 20 seconds at 9300 rcf and flow-through discarded. Then, 350 µl of RW1 buffer was added, and tubes centrifuged for 20 seconds at 9300 rcf and the flow-through was discarded. Next, 80 µl of RDD buffer DNAse solution (70 µl of RDD buffer with 10 µl of DNase) was added and incubated for 10 minutes. After, 350 µl of RW1 buffer

was added and the column centrifuged for 20 seconds at 9300 rcf and flow-through was discarded. Then, 500 µl of RPE buffer was added and columns were centrifuged for 20 seconds at 9300 rcf and the flow-through discarded. Finally, a washing step with 500 µl of 80% EtOH was performed and columns were centrifuged for 2 minutes at 9300 rcf, and the flow-through placed in a new 2 ml tube and centrifuged for 5 minutes at 16100 rcf.

RNA was eluted by transferring the column into a 1.5 ml tube and adding 14 µL of H_2O directly onto the membrane. The flow through was collected after centrifugation of 1 minute at 16100 rcf. Total amount and quality of RNA was determined for each sample using a Nanodrop D- UB-Vis spectrophotometer (Termo Scientific).

2.9 Complementary DNA (cDNA) synthesis

Single stranded cDNA was synthesised from mRNA using a commercial high-capacity cDNA reverse transcription kit (Life Sciences Solutions, Cat: 4368813). For each sample reaction a 2x reverse transcription (RT) master mix was prepared containing 2 µl 10x RT buffer, 0.8 µl 25x dNTP mix (100mM), 2 µl 10x RT random primers, 1 µl MultiScribe™ reverse transcriptase, and 4.2 µl nuclease-free H_2O. In a 96-well reaction plate 12 µl of RNA samples, diluted in nuclease-free H_2O to contain equal amounts of RNA, were added to wells containing 8 µl of 2X RT master mix and mixed by pipetting. The reaction plate was sealed using an adhesive film and centrifuged at 1500 rpm for 1 minute to remove air bubbles. qRT-PCRs were performed using a thermal cycler (BIO-RAD, Model#: T100, Cat#: 186-1096), program conditions below (Table 2.4).

	Step 1	**Step 2**	**Step 3**	**Step 4**
Temperature (°C)	25	37	85	4
Time	10	120	5	∞

Table 2.4 cDNA synthesis program
A table displaying the information used to perform reverse transcription on a thermal cycler. For each step of the reaction the temperature and duration is given.

2.10 Quantitative reverse transcriptome polymerase chain reaction (qRT-PCR)

Synthesised single strand cDNA products were diluted (1:50) with nuclease-free H_2O. A qRT-PCR reaction master mix was prepared for each gene of interest containing 10 µl iTaq™ universal probes supermix (2X qRT-PCR master mix) (BIO-RAD, Cat: 172-5135), 1 µl 20X target gene FAM labelled TaqMan gene expression assay (Life Sciences Solutions, Cat: See Table 4). In a 96-well reaction plate, 11 µl of qRT-PCR reaction master mix was added to 9 µl of diluted cDNA. The reaction plate was sealed using an adhesive film and centrifuged at 500 rcf for 1 minute to remove air bubbles. qRT-PCRs were performed using a Real-Time PCR system (Life Sciences Solutions, Model: StepOnePlusTM, Cat: 4376600).

Gene	**Company**	**Cat number**
Cx3cr1	Applied biosystem	Mm00438354_m1
Cx3cl1	Applied biosystem	Mm00436454_m1
Csf1	Applied biosystem	Mm00432686_m1
Ccl2	Applied biosystem	Mm00441242_m1
Csf1R	Applied biosystem	Mm01266652_m1
TNF-α	Applied biosystem	Mm00443258_m1
IL-1b	Applied biosystem	Mm00434228_m1
3.12IL-6	Applied biosystem	Mm00446190_m1
IFN-γ	Applied biosystem	Mm99999071_m1
IL-10	Applied biosystem	Mm00439616_m1
IL-12a	Applied biosystem	Mm00434169_m1
Nos2	Applied biosystem	Mm01309898_m1
Mrc1	Applied biosystem	Mm01329362_m1
Arg1	Applied biosystem	Mm00475991_m1

Table 2.5 List of primer for qRT-PCR
Table describing the primers used for qRT-PCR including company and catalogue number.

2.11 Gemcitabine treatment

Mice were recruited when tumours were palpable. Gemcitabine were obtained from Fresenius Kabi and diluted PBS (SIGMA - D8537). Mice were treated with gemcitabine, which was injected intra-peritoneal twice a week during two weeks at 100mg/kg. Mice where daily monitored and body weighed recorded twice a week. After two weeks of treatment with gemcitabine mice were sacrificed and pancreatic tumours harvested for analysis.

2.12 RNA sequencing and analysis

Pancreatic tumour samples from 6 CKPC mice were used for RNA extraction and sequencing (RNA-Seq). RNA extraction was performed as described in 2.8 and RNA quality assessment was carried out using the Agilent RNA 6000 Nano chip (Agilent Technology – Cat. No 5067-1511). In briefly, the nano dye (1:65) was added to an aliquot of filtered gel. The gel/dye mix was spun for 10 minutes at room temperature at 13,000 rcf and then allowed to equilibrate at room temperature for 30 minutes. The gel was then dispensed into the RNA nano chip. 5 µl pico marker, 1 µl pico ladder and 1 µl of each sample were dispensed into the appropriate wells of the chip. After 1 minute the chip was inserted into the Agilent 2100 Bioanalizer. The 2100 expert software was used to calculate RNA concentration and RNA integrity number (RIN) for each sample.

RNA sequencing was performed by the Wellcome Trust Centre for Human Genetics (University of Oxford, UK) on rRNA depleted samples to ~40x mean depth, on the Illumina HiSeq4000 platform, generating 150bp paired-end reads. RNA-Seq reads were mapped to the mouse genome (mm10, Genome Reference Consortium GRCm38) using hisat2 in strand-specific mode. The number of reads aligning to the exonic region of each gene were counted using htseq-count based on Ensembl annotation. Only genes that achieved at least one read count per million reads (CPM) in at least 25% of the samples were kept. X-Y genes were excluded. Conditional quantile normalisation (cqn) was performed counting for gene length and gc content and a $\log_2$ transformed RPKM expression matrix was generated.

Differential expression was performed in R using the edgeR package (version 3.8.6) (Robinson, McCarthy et al. 2010). The generalised linear model (GLM) approach was used for the differential analysis (McCarthy, Chen et al. 2012). Adjusted p-values were calculated using the Benjamini-Hochberg method. Principal component analysis (PCA), volcano plots and heatmaps of differentially expressed genes were plotted using R in-built functions and ggplot2 (version 1.0.1) (Wickham 2009). Conversion of ensemble gene IDs to HUGO gene nomenclature (hgnc) was carried out using biomaRt (version 2.22.0) (Durinck, Moreau et al. 2005, Thurber, Haynes et al. 2009). Classification of protein-coding genes was performed using the web-based tool PANTHER (version 11.1) (Mi, Muruganujan et al. 2013).

Chapter 3 The CKPC mouse model

3.1 Introduction

To study the role of CX3CR1 in pancreatic cancer I used a mouse model obtained by crossing the GFP-CX3CR1 mouse, which expresses GFP under control of the endogenous CX3CR1 locus, with the KPC mouse. The result of the crossing is a mouse with the genotype $CX3CR1^{GFP/GFP}$LSL-$KRAS^{G12D/+}$LSL$Trp53^{R172H/+}$Pdx1-Cre. This was named the CKPC mouse model. In these mice the CX3CR1 protein was absent as they expressed eGFP instead of CX3CR1. This allowed the identification of cell types that would usually express CX3CR1.

3.2 Characterisation of the $CX3CR1^{GFP/GFP}$ mouse model

The GFP-CX3CR1 mouse model was first established by S Jung (S. Jung et al. 2000). In this study, they reported that mice lacking CX3CR1 had no evidence of developmental defects. Moreover, they showed that none of the green-fluorescent cell populations were impaired in the comparison between $CX3CR1^{+/GFP}$ and $CX3CR1^{GFP/GFP}$ mice. Despite these results, I decided to compare the distribution of leukocytes in $CX3CR1^{GFP/GFP}$ and wild-type (WT) age-matched littermate control mice using the mice that I had generated.

Blood, spleen, bone marrow, pancreas and mesenteric lymph nodes (MLN) were analysed by flow cytometry. Single cell suspensions from each tissue were stained with fluorescence antibodies against markers able to discriminate between myeloid and lymphoid cell populations. These markers are shown in Table 3.1. A fixable viability dye (FVD) was added in the antibody pool to eliminate dead cells from the analysis.

Immune cell subsets	Phenotype markers	Tissues analysed
Leukocytes	$CD45^+$	Pancreas, spleen, blood, bone marrow and MLN
Myeloid cells	$CD45^+CD11b^+$	Spleen, blood, bone marrow and MLN
Inflammatory monocytes	$CD45^+CD11b^+Ly6G^-$ $LY6C^{high}$	Spleen, blood, bone marrow
Granulocytes	$CD45^+CD11b^+Ly6G^+LY6C^+$	Spleen, blood, bone marrow
Macrophages	$CD45^+Ly6G^-LY6C^-F4/80^+$	Spleen and bone marrow
B cells	$CD45^+CD11b^-CD3^-CD19^+$	Spleen, blood, bone marrow and MLN
$CD4^+$ T cells	$CD45^+CD11b^-CD19^-$ $CD3^+CD4^+$	Spleen, blood, bone marrow and MLN
$CD8^+$ T cells	$CD45^+CD11b^-CD19^-$ $CD3^+CD8^+$	Spleen, blood, bone marrow and MLN

Table 3.1 Cell surface markers used to identify different cell populations by flow cytometry
Single cell suspensions from each tissue were stained with a pool of antibodies for the markers listed in the table and quantified by flow cytometry analysis.

3.2.1 Leukocyte cells in the pancreas of wild type and CX3CR1$^{GFP/GFP}$ mice

The pancreas has both endocrine (islets of Langerhans) and exocrine (acinar and ductal cells) functions. The exocrine pancreas is involved in the production and secretion of digestive enzymes and pancreatic juice into the small intestine, whereas the endocrine pancreas is responsible for producing hormones crucial for glucose homeostasis and metabolism (Cleveland, Sawyer et al. 2012).

The presence of immune cells in the pancreas was assessed by flow cytometry analysis. The gating strategy is shown in Figure 3.1.

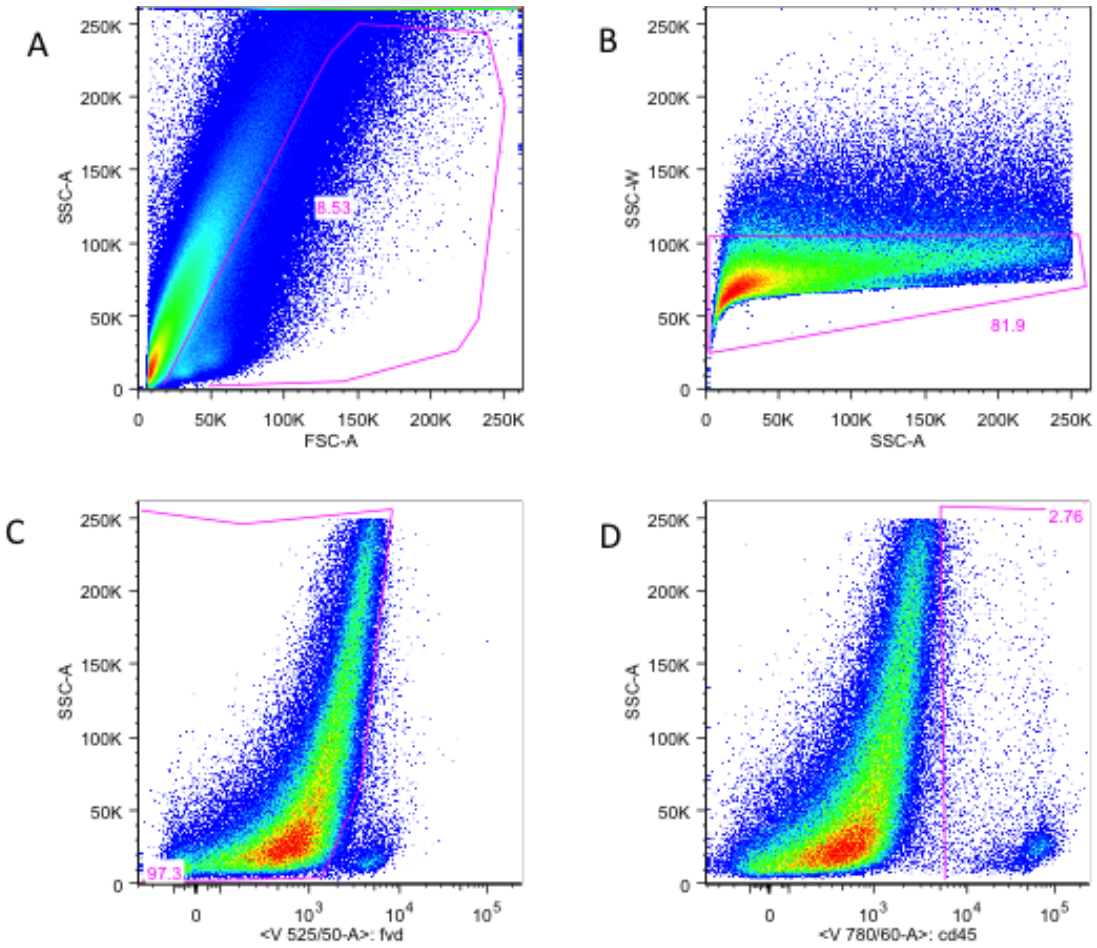

Figure 3.1 Representative gating strategies for the resident immune cells in the pancreas by flow cytometry
Single cell suspensions from the pancreas were stained with a pool of fluorescence-conjugated antibodies and analysed by flow cytometry. Acquired cells were gated to eliminate (A) debris, (B) doublets and (C) dead cells to obtain (D) $CD45^+$ cells.

Leukocytes, defined as $CD45^+$ cells, represented less than 5% of viable cells in the pancreas. There was no significant difference in the leukocytes wild-type and $CX3CR1^{GFP/GFP}$ mice, as shown in Figure 3.2.

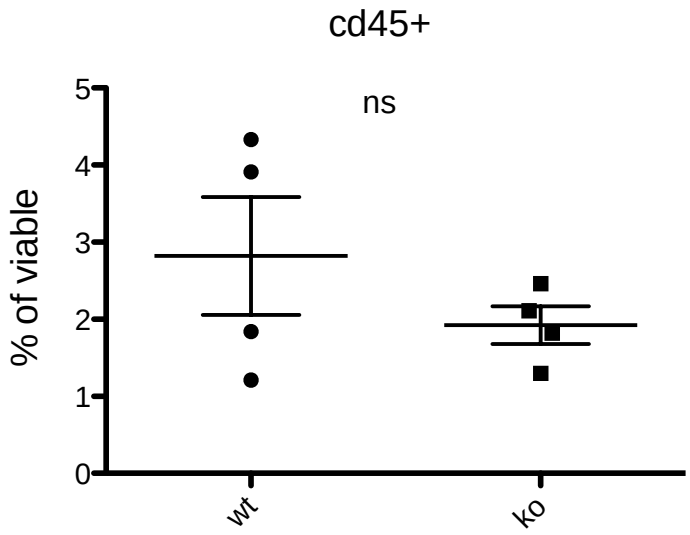

Figure 3.2 Frequency of leukocytes populations in the pancreas
Flow cytometric analysis of leukocytes from the pancreas of wild-type (WT) and CX3CR1$^{GFP/GFP}$ (KO) mice. Values for individual mice are shown as dots and a horizontal line represents mean of the values. Statistical significance was determined by unpaired t-test. N = 4 per group. ns: not significant.

3.2.2 Leukocyte subsets in the spleen of wild-type and CX3CR1$^{GFP/GFP}$ mice

The spleen is the largest secondary lymphoid organ; it acts primarily as a blood filter. It holds a reserve of blood, which can be valuable in case of hemorrhagic shock. The spleen is involved in the immune response by detecting foreign particles and pathogens, such as bacteria, and producing white blood cells in response.
Interestingly the spleen contains about one-fourth of the body's lymphocytes.
It also removes old red blood cells and platelets and also recycles iron (Mebius and Kraal 2005).

Figure 3.3 shows the gating strategy used to analyse the leukocyte subsets in the spleen.

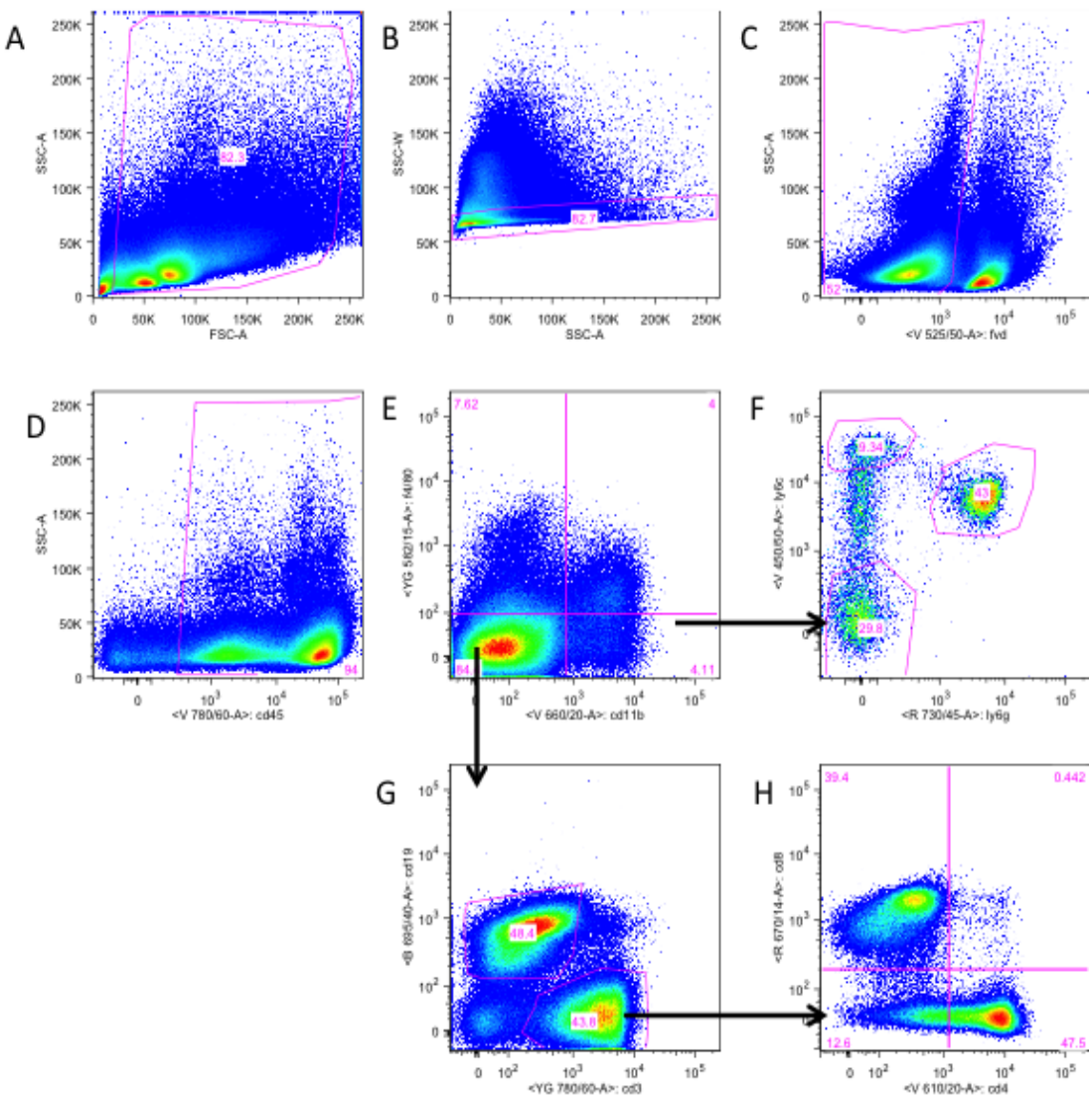

Figure 3.3 Representative gating strategy for leukocyte subsets in the spleen by flow cytometry
Total spleen single cell suspensions were stained with a pool of fluorescence-conjugated antibodies and analysed by flow cytometry. Acquired cells were gated to eliminate (A) debris, (B) doublets and (C) dead cells to obtain (D) CD45$^+$ cells. CD45$^+$ cells were analysed for the expression of (E) F4/80 and CD11b allowing to distinguish between different cell populations. CD11b$^+$ cells were analysed in (F) for the expression of Ly6C and Ly6G. Lymphoid cells were analysed in (G) for the expression of CD19 and CD3. (H) CD3$^+$ cells were further analysed for the expression of CD4 and CD8.

In the spleen, CD45$^+$ cells constituted more than 90% of viable cells (Figure 3.4A), of which around 75% consisted of lymphocytes whilst about 15% were myeloid cells.

Flow cytometric analysis of splenic myeloid cells revealed no significant difference in F4/80$^+$ macrophages (Figure 3.4B), Ly6C$^+$Ly6G$^+$ granulocytes (Figure 3.4C) and Ly6c^{high} monocytes (Figure 3.4D) between wild-type mice and CX3CR1$^{GFP/GFP}$ mice.

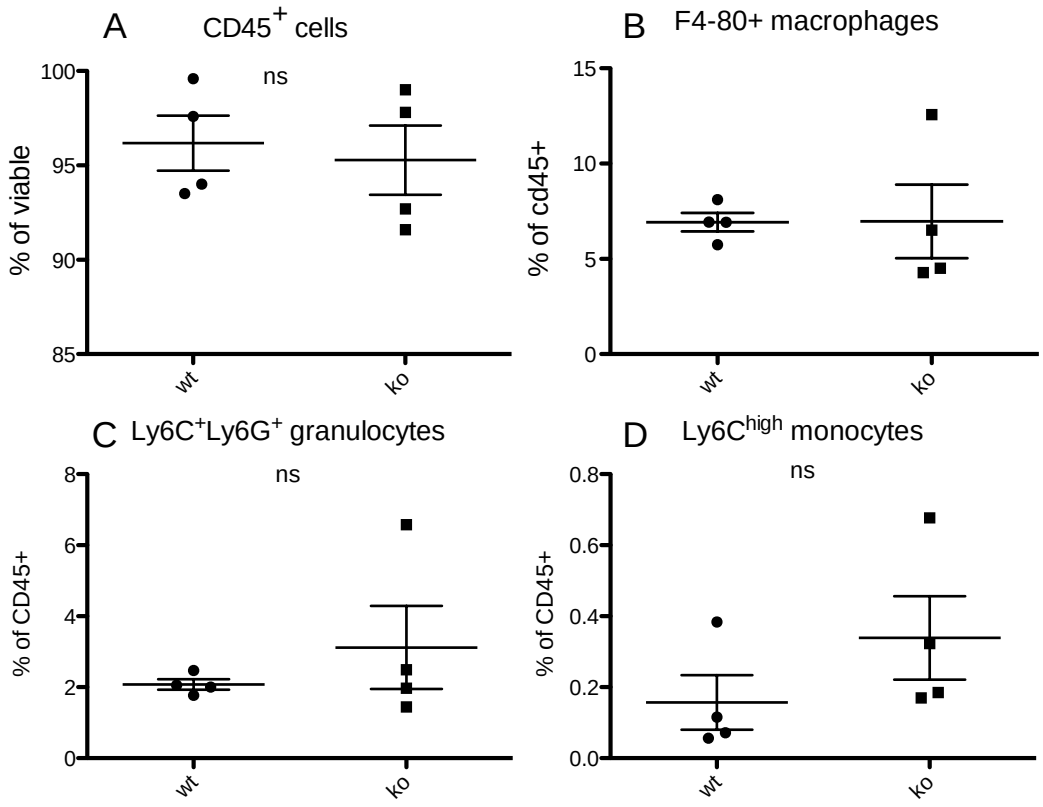

Figure 3.4 Frequency of myeloid cells in the spleen from wild type and CX3CR1$^{GFP/GFP}$ mice
Flow cytometric analysis of leukocytes from spleen of wild-type (WT) and CX3CR1$^{GFP/GFP}$ (KO) mice. (A) Percentages of total CD45$^+$ cells (B) F4/80$^+$ macrophages, (C) Ly6C$^+$Ly6G$^+$ granulocytes and (D) Ly6C^{high} monocytes. Values for individual mice are shown as dots and a horizontal line represents mean of the values. Statistical analysis was determined by unpaired t-test. N = 4 per group. ns: not significant.

Flow cytometric analysis showed also no significant difference in CD19$^+$ B cells between wild-type and CX3CR1$^{GFP/GFP}$ mice (Figure 3.5A).

The percentage of CD3$^+$ T lymphocytes was decreased, but was not significantly different; in CX3CR1$^{GFP/GFP}$ mice compared wild-type mice (Figure 3.5B). Analysis of CD3$^+$ T cell subsets revealed that the CD4$^+$ T cells (Figure 3.5C) and CD8$^+$ T cells distribution (Figure 3.5D) was not significantly different in in CX3CR1$^{GFP/GFP}$ mice compared to wild-type mice.

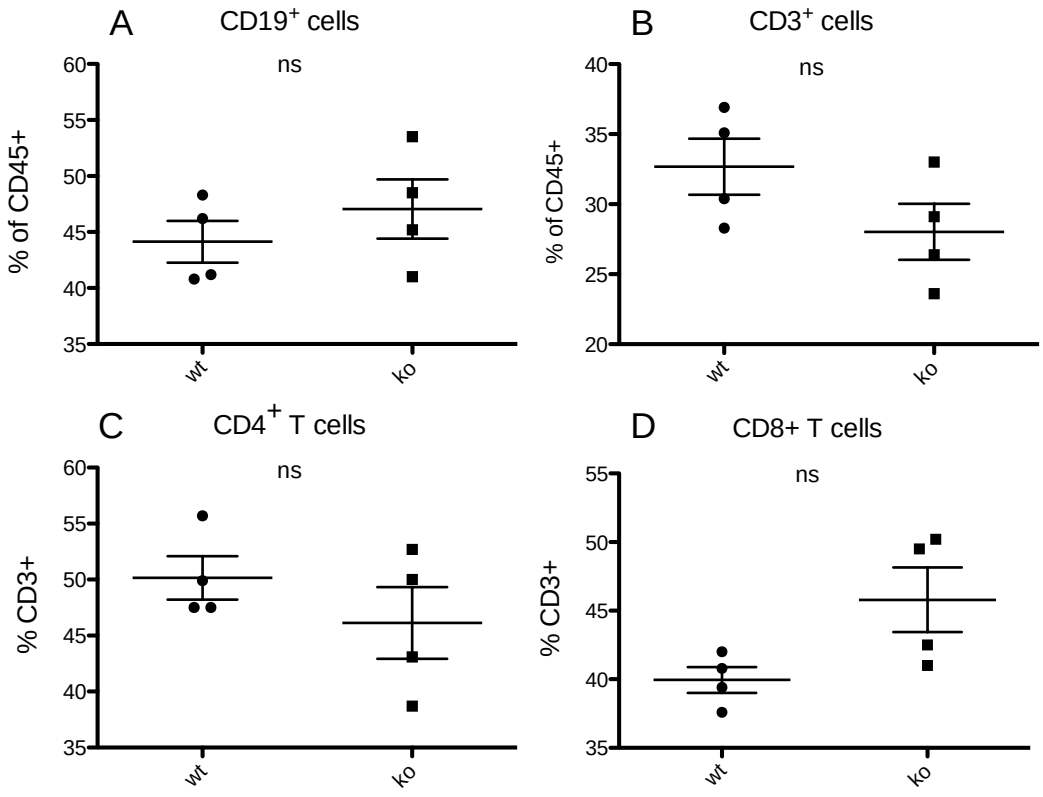

Figure 3.5 Frequency of lymphoid cells in the spleen from wild type and CX3CR1$^{GFP/GFP}$ mice
Flow cytometric analysis of leukocytes from spleen of wild-type (WT) and CX3CR1$^{GFP/GFP}$ (KO) mice. (A) Percentages of CD19^{+} cells, (B) CD3^{+} cells, (C) CD4^{+} cells and (D) CD8^{+} cells. Values for individual mice are shown as dots and a horizontal line represents mean of the values. Statistical analysis was determined by unpaired t-test. N = 4 per group. ns: not significant.

3.2.3 Leukocyte subsets in the blood of wild type and CX3CR1$^{GFP/GFP}$ mice

Immune cells circulate in the blood, through the body, monitoring the presence of pathogens and foreign substances.

Figure 3.6 shows the gating strategy used to investigate the leukocyte populations in the blood.

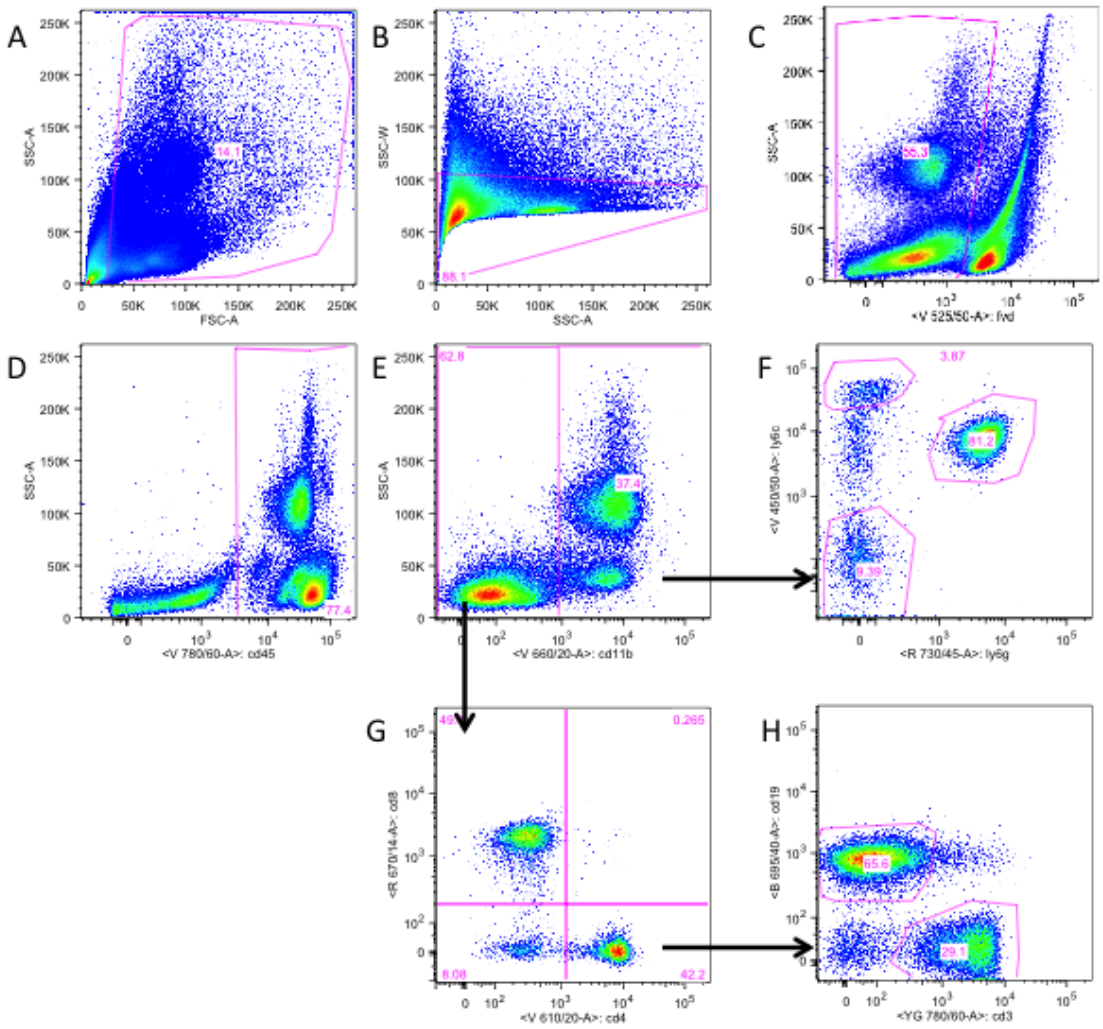

Figure 3.6 Representative gating strategy for the leukocytes subsets in the blood by flow cytometry

Single cell suspensions of peripheral blood leukocytes were stained with a pool of fluorescence-conjugated antibodies and analysed by flow cytometry. Acquired cells were gated to eliminate (A) debris, (B) doublets and (C) dead cells to obtain (D) $CD45^+$ cells. $CD45^+$ cells were discriminated between myeloid and lymphoid subset by the expression of (E) CD11b. Myeloid cells were analysed in (F) for the expression of Ly6C and Ly6G. Lymphoid cells were analysed in (G) for the expression of CD19 and CD3. (H) $CD3^+$ cells were further analysed for the expression of CD4 and CD8.

Flow cytometric analysis showed no difference in the amount of $CD45^+$ cells between wild-type and $CX3CR1^{GFP/GFP}$ mice (Figure 3.7A). $CD11b^+$ myeloid cells represented approximately 30% of leukocytes in both groups (Figure 3.7B). $Ly6C^{high}$ monocytes (Figure 3.7D) and $Ly6C^+Ly6G^+$ granulocytes (Figure 3.7C) showed no difference between groups.

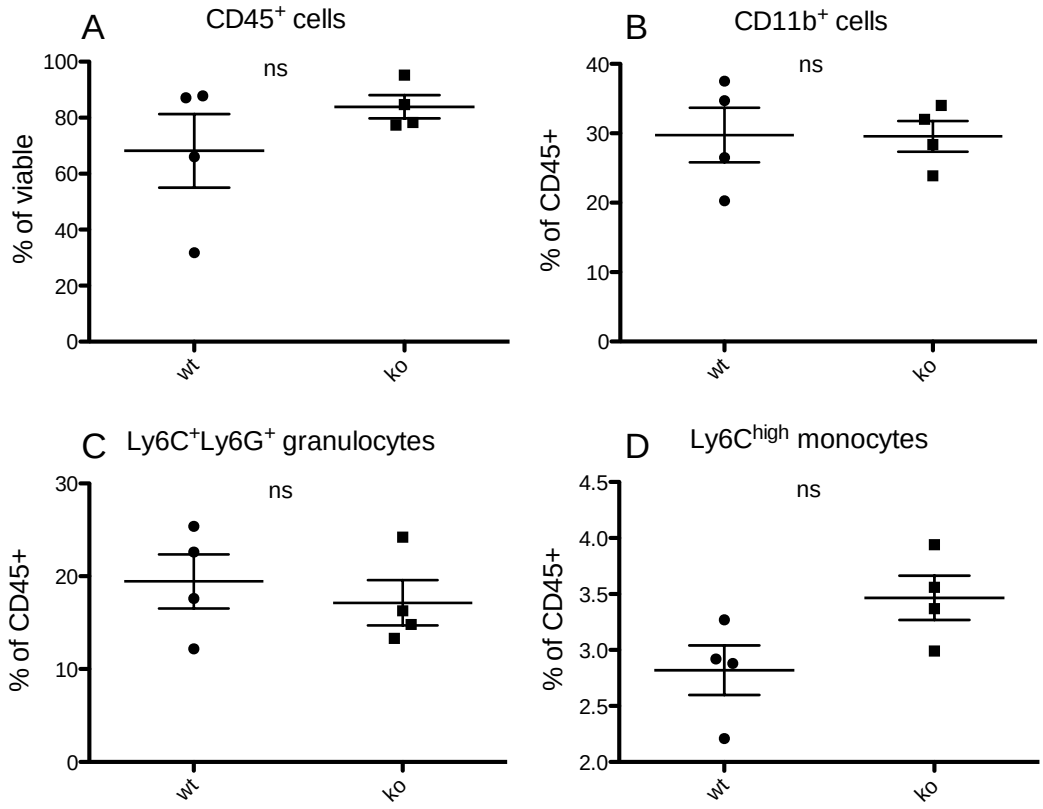

Figure 3.7 Frequency of myeloid cells in the blood of wild type and CX3CR1$^{GFP/GFP}$ mice

Flow cytometric analysis of leukocytes from peripheral blood of wild-type (WT) and CX3CR1$^{GFP/GFP}$ (KO) mice. (A) Percentages of total CD45$^+$ cells (B) CD11b$^+$ myeloid cells, (C) Ly6C$^+$Ly6G$^+$ granulocytes and (D) Ly6C^{high} monocytes. Values for individual mice are shown as dots and a horizontal line represents mean of the values. Statistical analysis was determined by unpaired t-test. N = 4 per group. ns: not significant.

CD19$^+$ B cells were the most abundant cells in the blood, approximately 50% in both CX3CR1$^{GFP/GFP}$ and wild type mice (Figure 3.8A). The percentage of CD3$^+$ T lymphocytes (Figure 3.8B) and the distribution between CD4$^+$ T cells (Figure 3.8C) and CD8$^+$ T cells (Figure 3.8D) was not different between groups.

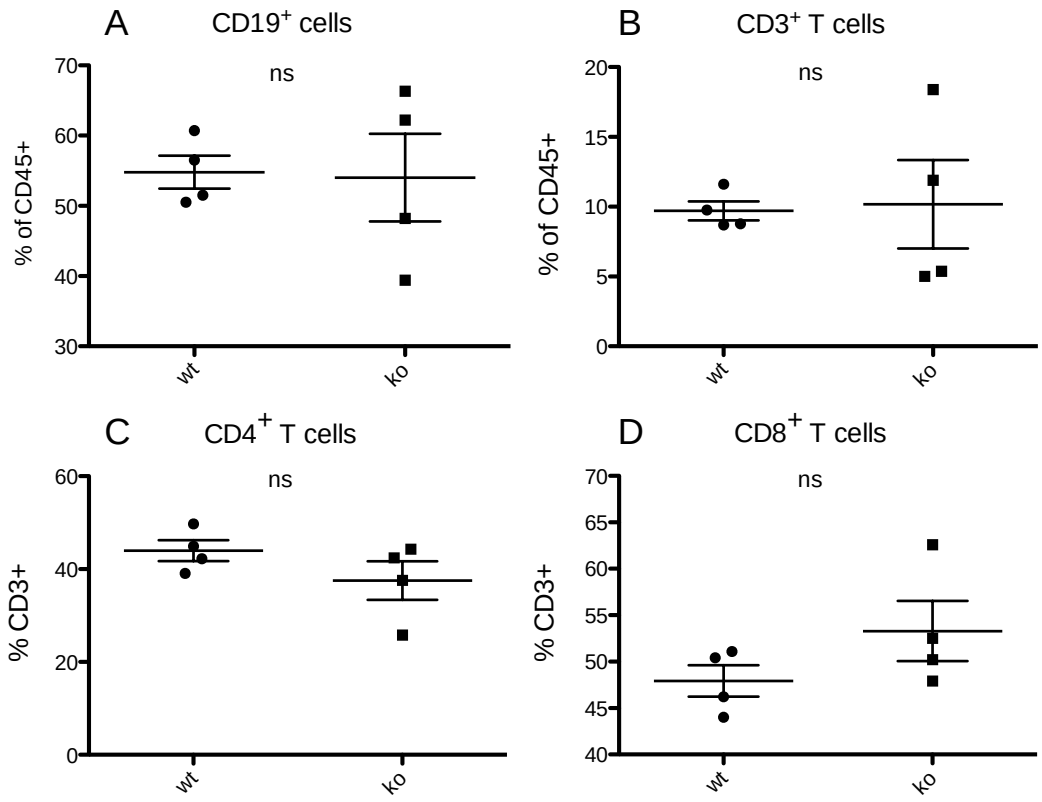

Figure 3.8 Frequency of lymphoid cells in the peripheral blood of wild type and CX3CR1$^{GFP/GFP}$ mice

Flow cytometric analysis of leukocytes from peripheral blood of wild-type (WT) and CX3CR1$^{GFP/GFP}$ (KO) mice. (A) Percentages of CD19^{+} cells, (B) CD3^{+} cells, (C) CD4^{+} cells and (D) CD8^{+} cells. Values for individual mice are shown as dots and a horizontal line represents mean of the values. Statistical analysis was determined by unpaired t-test. N = 4 per group. ns: not significant.

3.2.4 Leukocyte subsets in MSL of wild type and CX3CR1$^{GFP/GFP}$ mice

The lymph nodes are small bean shaped secondary lymphoid organs. They are present widely throughout the body and linked by lymphatic vessels. Lymph nodes act as filters that screen for foreign substances and antigens and are essential for the interactions between antigen presenting cells and lymphocytes (Girard, Moussion et al. 2012). Mesenteric lymph nodes, MLN, are lymph nodes that are located in the walls of the intestines and stomach, between the layers of the mesentery. MLNs play a role in maintaining an active homeostasis during steady

state conditions but quickly enlarges in response to infection with intestinal pathogens.

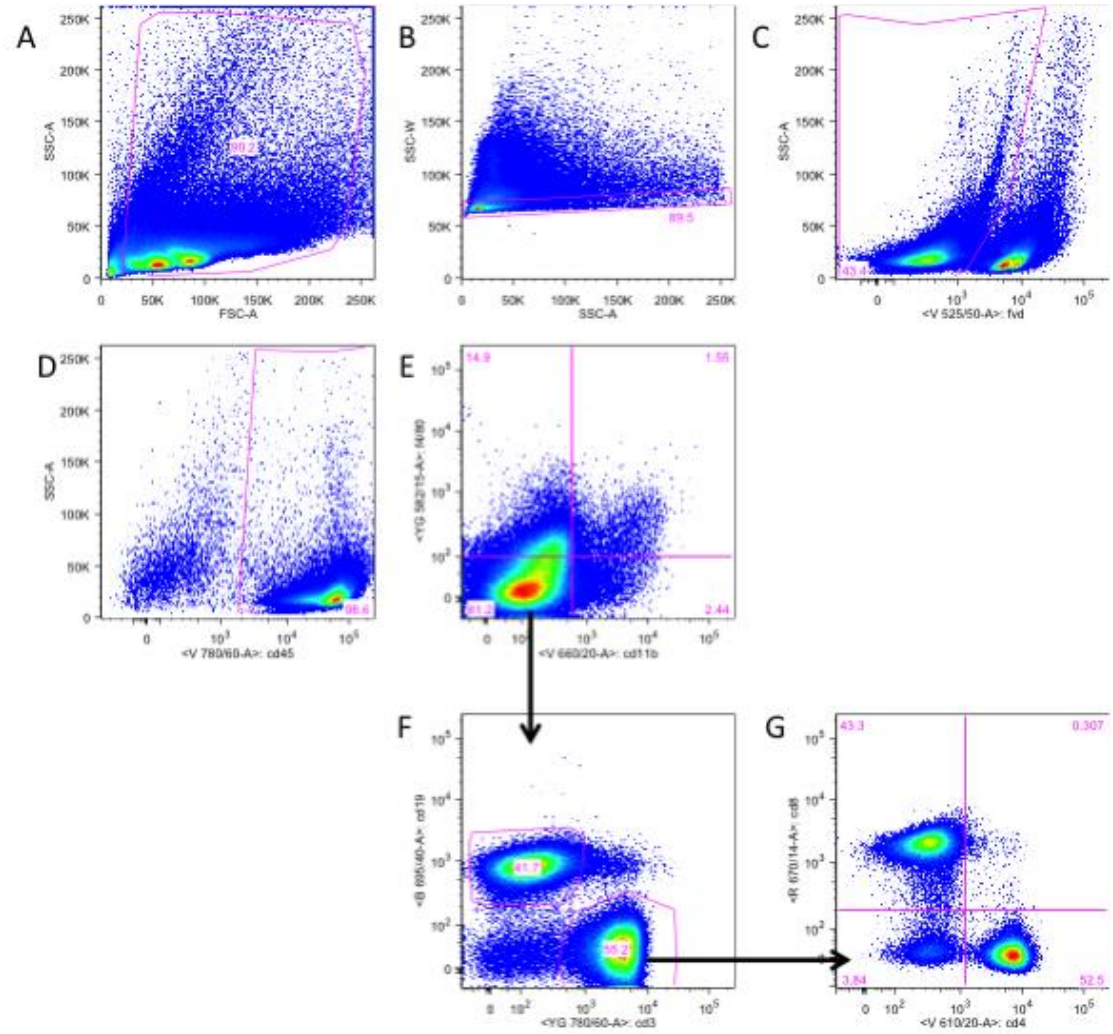

Figure 3.9 Representative gating strategy for the leukocytes in the MLN by flow cytometry

Total MLN single cell suspensions were stained with a pool of fluorescence-conjugated antibodies and analysed by flow cytometry. Acquired cells were gated to eliminate (A) debris, (B) doublets and (C) dead cells to obtain (D) $CD45^+$ cells. $CD45^+$ cells were analysed for the expression of (E) F4/80 and CD11b allowing discrimination between myeloid and lymphoid subsets. Lymphoid cells were analysed in (F) for the expression of CD19 and CD3. (G) $CD3^+$ cells were further analysed for the expression of CD4 and CD8.

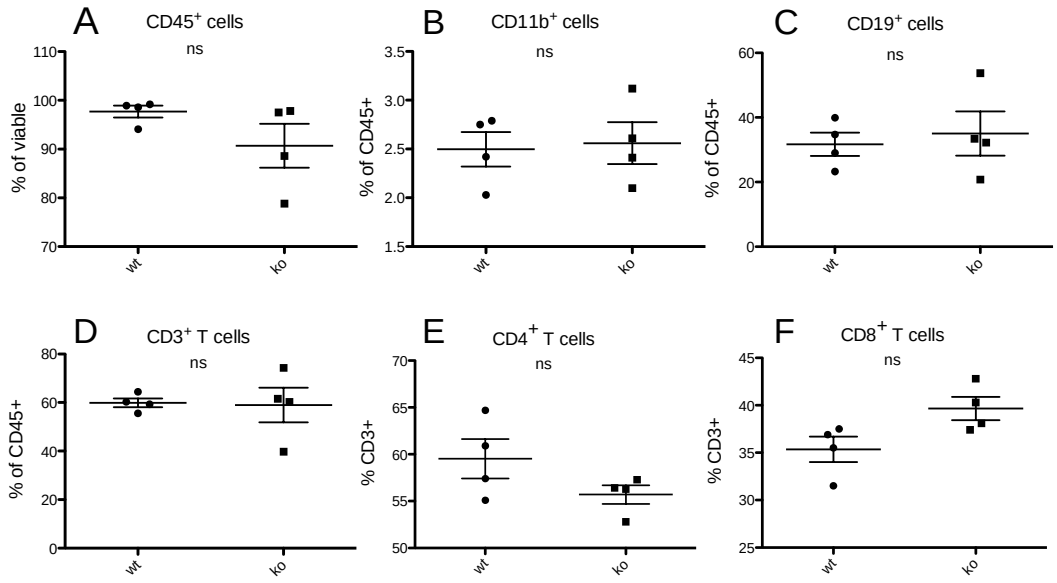

Figure 3.10 Frequency of leukocytes cells in the MLN of wild type and CX3CR1$^{GFP/GFP}$ mice

Flow cytometric analysis of leukocytes from MLN of wild-type (WT) and CX3CR1$^{GFP/GFP}$ (KO) mice. (A) Percentage of total viable CD45$^+$ cells, (B) CD11b$^+$ myeloid cells, (C) CD19$^+$ cells, (D) CD3$^+$ cells, (E) CD4$^+$ cells and (F) CD8$^+$ cells. Values for individual mice are shown as dots and a horizontal line represents mean of the values. Statistical analysis was determined by unpaired t-test. N = 4 per group. ns: not significant.

MLN analysis by flow cytometry (gating strategy illustrated in Figure 3.9) showed no difference in the percentage of CD45$^+$ cells between wild-type and CX3CR1$^{GFP/GFP}$ mice (Figure 3.10A). CD11b$^+$ myeloid cells were hardly present in lymph nodes, less than 3% in both groups (Figure 3.10B).

Lymphocytes constituted approximately 90% of CD45$^+$ cells, of which 60% were CD3$^+$ T cells (Figure 3.10D), and 30% were CD19$^+$ B cells (Figure 3.10C) in both wild-type and CX3CR1$^{GFP/GFP}$ mice. Percentages of CD3$^+$ T cell subsets showed no difference in CD4$^+$ T cells (Figure 3.5E) and CD8$^+$ T cells (Figure 3.10F) between experimental groups.

3.2.5 Leukocyte subsets in the bone marrow of wild type and CX3CR1$^{GFP/GFP}$ mice

Bone marrow is a tissue in the interior of bones and it is the site haematopoiesis, where all blood cells are generated and differentiated from progenitor cells (Gurkan and Akkus 2008).

Figure 3.9 shows the gating strategy used for the flow cytometry analysis of bone marrow.

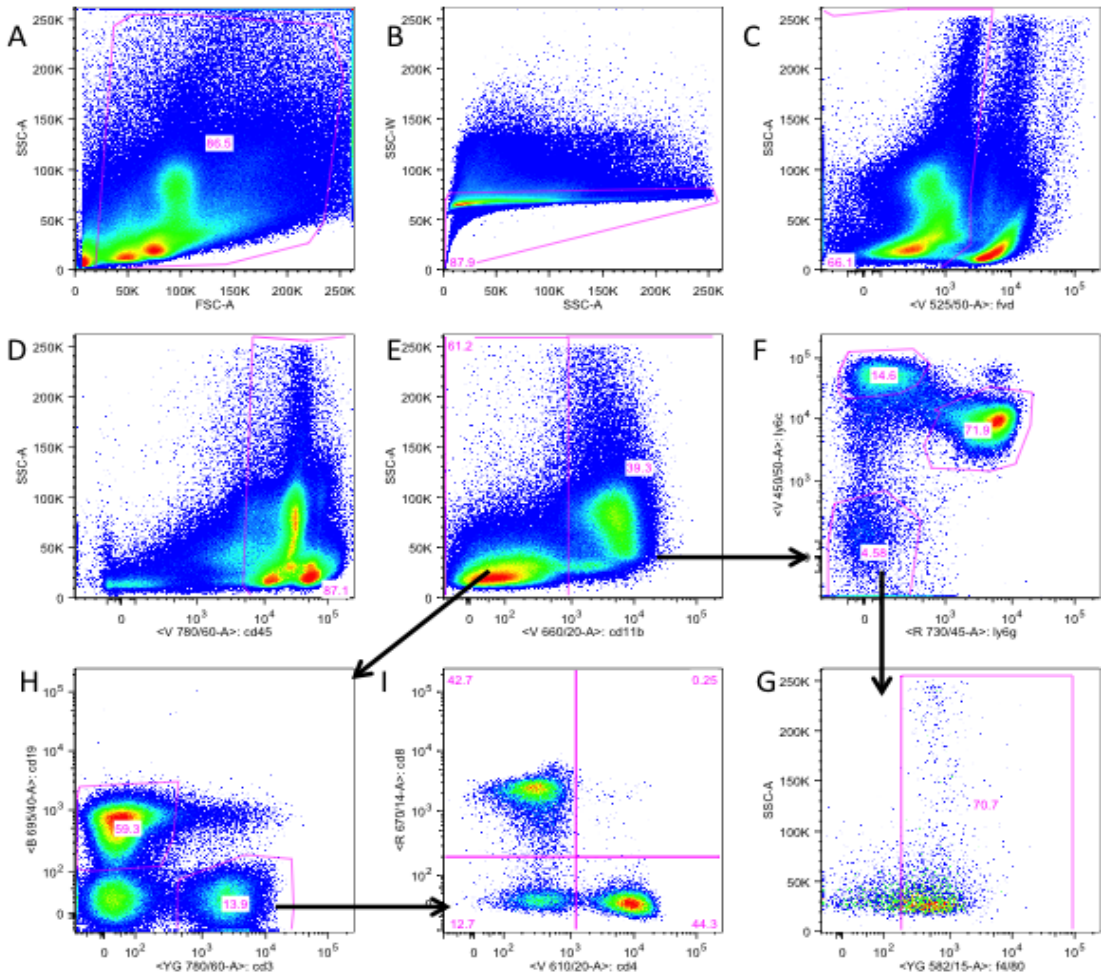

Figure 3.11 Representative gating strategy for the leukocyte subsets in the bone marrow by flow cytometry
Total bone marrow single cell suspensions were stained with a pool of fluorescence-conjugated antibody antibodies and analysed by flow cytometry. Acquired cells were gate to eliminate (A) debris, (B) doublets and (C) dead cells to obtain (D) CD45$^+$ cells. CD45$^+$ cells were analysed for the expression of (E) CD11b allowing discrimination between myeloid and lymphoid subsets. CD11b$^+$ cells were analysed in (F) for the expression of Ly6C and Ly6G and (G) F4/80. CD11b$^-$ lymphoid cells were analysed in (H) for the expression of CD19 and CD3. (I) CD3$^+$ cells were further analysed for the expression of CD4 and CD8.

CD45+ cells showed no difference between wild-type and CX3CR1$^{GFP/GFP}$ mice (Figure 3.12A). Myeloid cells accounted about 37% of CD45+ cells (Figure 3.10B). Ly6C+Ly6G+ cells were present in the same proportions in both KPC and CKPC mice, comprising approximately 28% of the CD45+ population (Figure 3.12C). These cells in the bone marrow identify a subset of immature precursor cells that can give origin to monocytes, macrophages, granulocytes and dendritic cells (Kusmartsev, Nagaraj et al. 2005). Ly6C^{high} monocytes and F4/80+ macrophages were present at 3% and 0.5%, Figure 3.12D and E, respectively, in both wild-type and CX3CR1$^{GFP/GFP}$ mice.

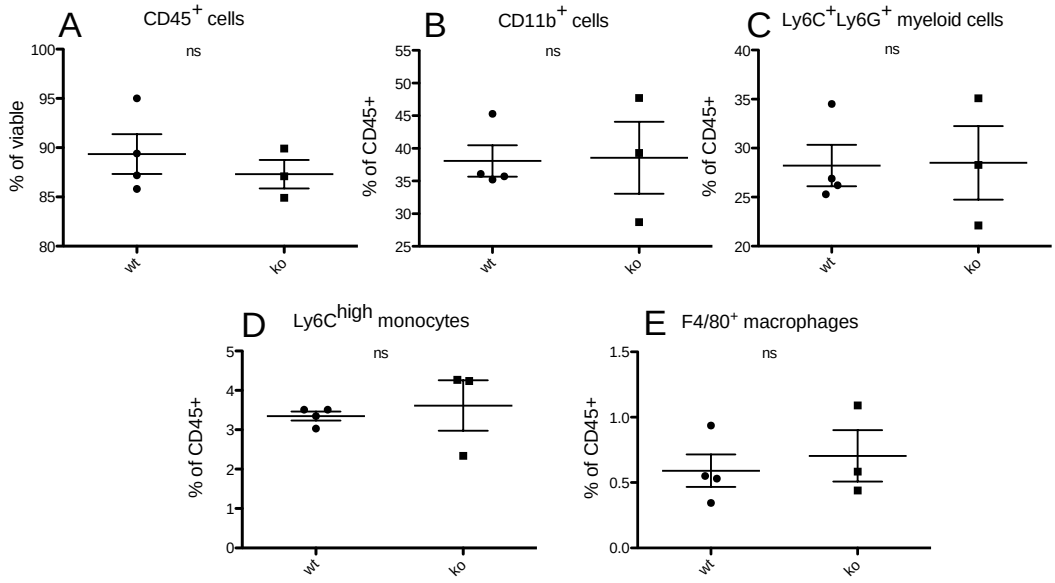

Figure 3.12 Frequency of myeloid cell subsets in the bone marrow of wild type and CX3CR1GFP/GFP mice

Flow cytometric analysis of leukocytes from peripheral blood of wild-type (WT) and CX3CR1$^{GFP/GFP}$ (KO) mice. (A) Percentage of total CD45+ cells (B) CD11b+ myeloid cells, (C) Ly6C+Ly6G+ myeloid cells, (D) Ly6C^{high} monocytes and (E) F4/80+ macrophages. Values for individual mice are shown as dots and a horizontal line represents mean of the values. Statistical analysis was determined by unpaired t-test. WT N = 4 KO, N = 3. ns: not significant.

Analysis of the lymphocytic subsets revealed no significant difference in CD19+ B cells (Figure 3.13A) and CD3+ T cells (Figure 3.13B), between wild-type and CX3CR1$^{GFP/GFP}$ mice. The CD3+, CD4+ T cells (Figure 3.13C) and CD8+ T cells (Figure 3.13D) showed no difference between groups.

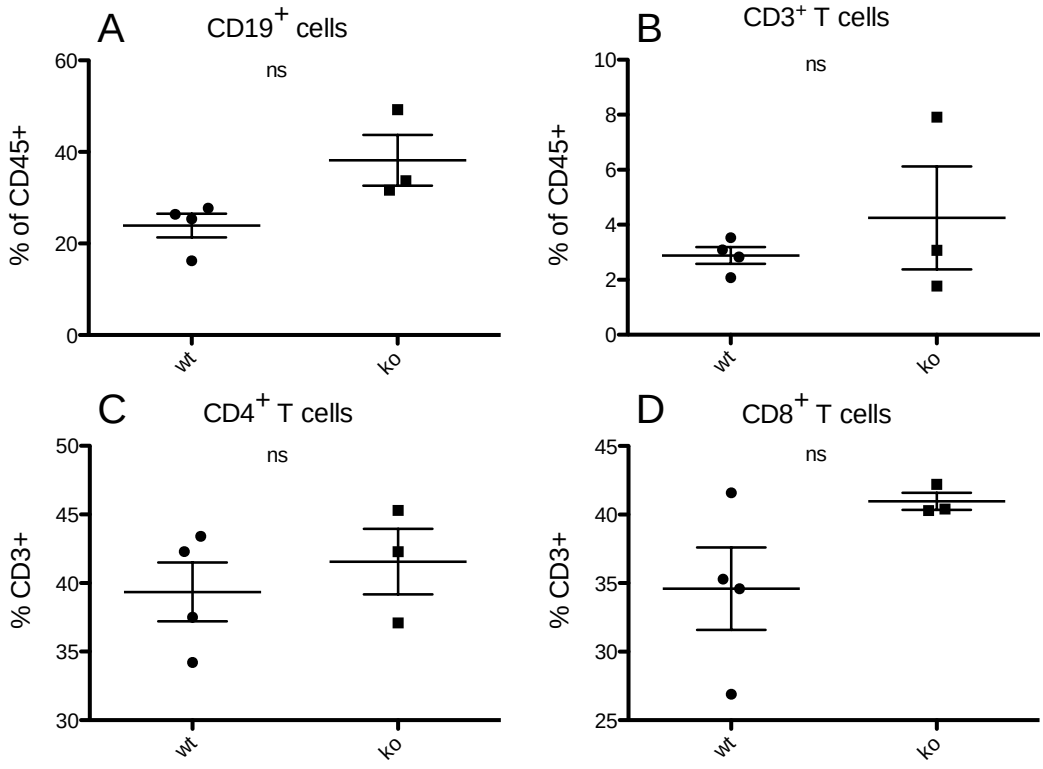

Figure 3.13 Frequency of lymphoid cells in the bone marrow of wild type and CX3CR1$^{GFP/GFP}$ mice

Flow cytometric analysis of lymphocytes from bone marrow of wild-type (WT) and CX3CR1$^{GFP/GFP}$ (KO) mice. (A) Percentages of CD19^{+} cells, (B) CD3^{+} cells, (C) CD4^{+} cells and (D) CD8^{+} cells. Values for individual mice are shown as dots and a horizontal line represents mean of the values Statistical analysis was determined by unpaired t-test. WT N = 4, KO N = 3. ns: not significant.

In summary, my analysis of the distribution of leukocytes in CX3CR1$^{GFP/GFP}$ mice compared to wild-type control mice showed that the lack of CX3CR1 did not cause any significant difference in the myeloid and lymphoid cell subsets analysed. Notably, the proportion of CD45^{+} leukocytes was comparable in each organ analysed.

3.2.6 GFP expression in leukocyte populations of CX3CR1$^{GFP/GFP}$ mice

As the CX3CR1$^{GFP/GFP}$ mice express GFP instead of functional CX3CR1 protein, I was able to identify the cells which would express CX3CR1 in wild-type conditions. I quantified the expression of GFP in CX3CR1$^{GFP/GFP}$ mice in different leukocyte populations by flow cytometry.

The expression of GFP-CX3CR1 in myeloid and lymphoid cell populations was investigated in spleen, blood, mesenchymal lymph nodes and bone marrow. The values of geometrical mean intensity of GFP are expressed in Figure 3.14.

Analysis of the level of GFP-CX3CR1 showed that myeloid and lymphoid cells differed in its expression. In fact, myeloid cells expressed a higher level of GFP-CX3CR1 compared to lymphoid cells.

As shown in Figure 3.14, CD19^{+} B cells had the lowest level of GFP-CX3CR1 in all the tissues analysed. CD4^{+} and CD8^{+} T cells expressed the same level of GFP-CX3CR1 in the spleen (Figure 3.14B), MLN (Figure 3.14C) and bone marrow (figure 3.14D), while in the blood (Figure 3.14A) CD4^{+} T cells showed higher GFP-CX3CR1 amount compared CD8^{+} T cells.

Interestingly, each myeloid cell subset expressed different levels of GFP-CX3CR1 in each tissue. In blood (Figure 3.14A) and spleen (Figure 3.14B) the highest levels of GFP-CX3CR1 were expressed by Ly6C^{high} monocytes followed by F4/80^{+} macrophages. In contrast, in the bone marrow (Figure 3.14D) the highest level of GFP-CX3CR1 was expressed by F4/80^{+} macrophages and then Ly6C^{high} monocytes. Finally, granulocytes expressed lower levels of GFP-CX3CR1 compared the other myeloid cell subsets in all the tissues analysed (Figure 3.14).

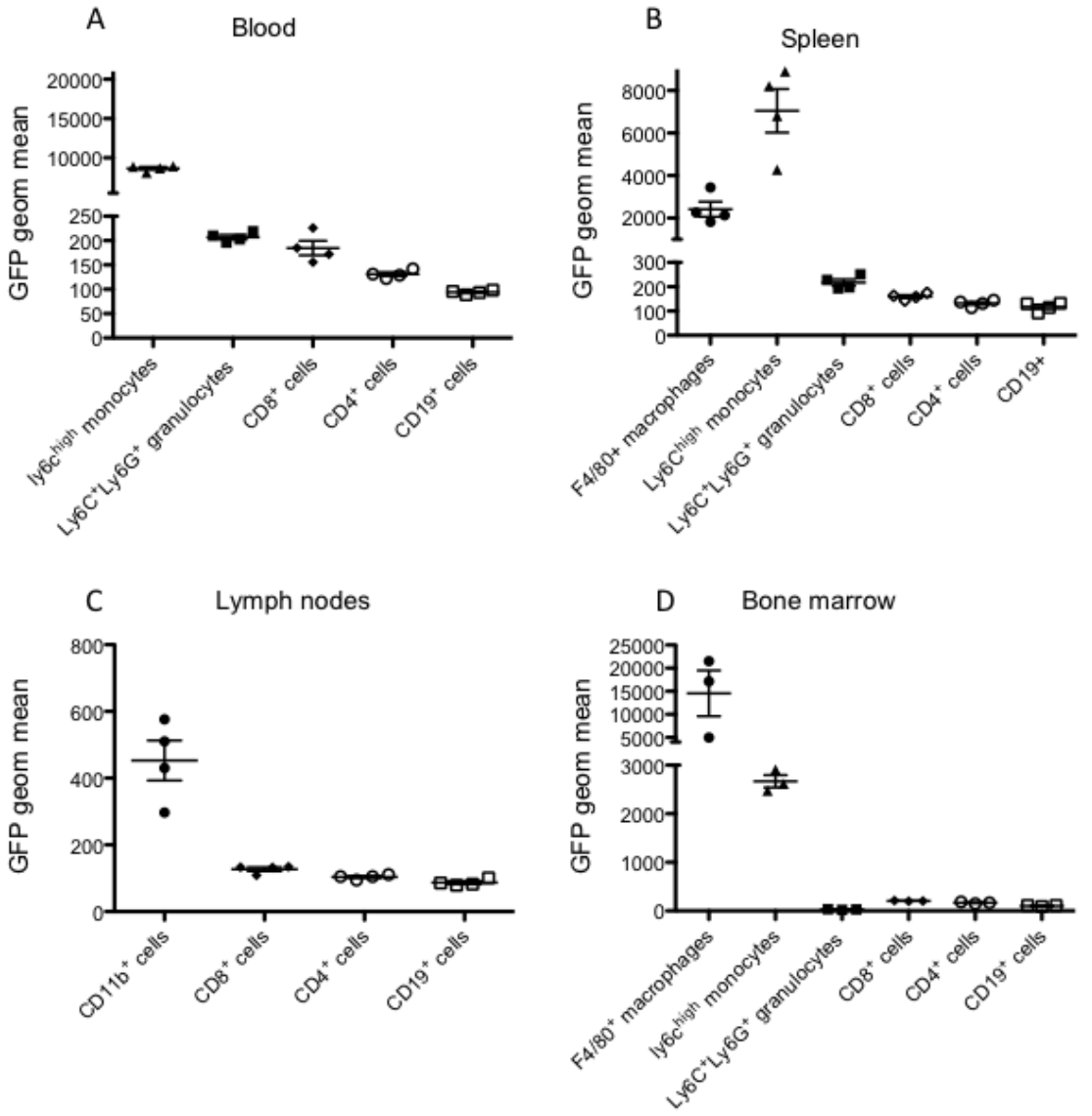

Figure 3.14 GFP expression in leukocyte populations in the spleen, blood, mesenteric lymph nodes and bone marrow
GFP expression was determined by flow cytometry and quantified as geometrical mean intensity of GFP. Leukocytes were gated as described in chapter 3.1.2. GFP intensity were analysed in (A) spleen, (B) blood, (C) mesenteric lymph nodes and (D) bone marrow. Values for individual mice are shown as dots and a horizontal line represents mean of the values.

In summary, the analysis of GFP levels in the CX3CR1$^{GFP/GFP}$ mice showed that it was expressed predominantly by myeloid cells. However, not all the myeloid subsets expressed GFP at the same amount. In fact, while both Ly6C^{high} monocytes and F4/80^{+} macrophages expressed high levels of GFP, Ly6C^{+}Ly6G^{+} granulocytes expressed levels of GFP comparable with the lymphoid cell populations.

3.3 Characterization of the CX3CR1$^{GFP/GFP}$-KPC (CKPC) mouse model

The GFP-CX3CR1 mice were crossed with KPC mice to obtain CX3CR1$^{GFP/GFP}$LSL-KRAS$^{G12D/+}$LSLTrp53$^{R172H/+}$Pdx1-Cre (CKPC) mice. In order to assess if these mice expressed GFP in tumour cells, immunofluorescence was performed on malignant pancreas tissue. Sections of CKPC (Figure 3.14A) and KPC (Figure 3.14B) pancreas were stained for GFP, E-cadherin and DAPI. The GFP expression was observed only in the CKPC mice but not in the KPC mice. Moreover, I observed that the E-cadherin positive cells co-expressed eGFP, further confirming that the pancreatic tumour cells express GFP-CX3CR1, in CKPC as described in Figure 3.14A.

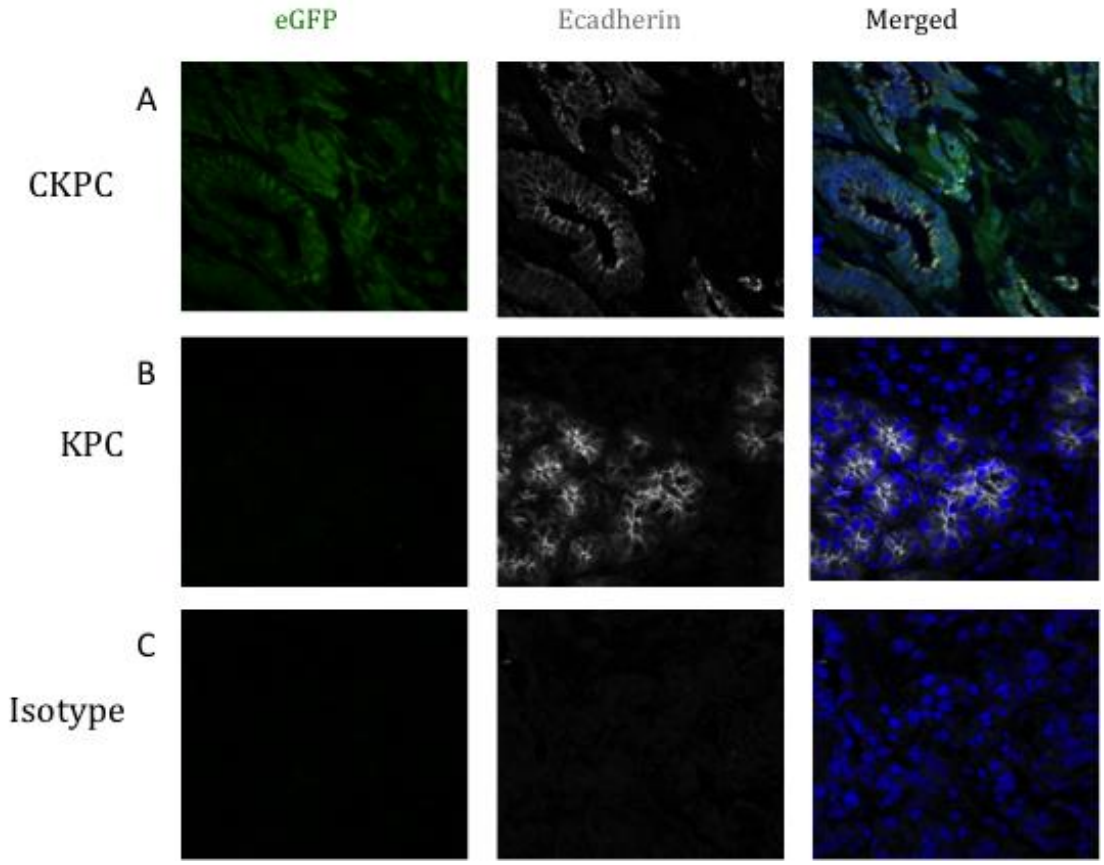

Figure 3.15 Immunofluorescence for GFP in pancreas tissue

Frozen 7 µm sections of CKPC and KPC pancreatic tissue were stained for GFP and E-cadherin. DAPI was used as a nuclear marker. Rabbit IgG and rat IgG1 isotype controls were stained on CKPC pancreas tissue. Images were taken on a LSM710 microscope at 40X magnification. Representative image for N=3 per group and isotype n=1.

3.3.1 GFP expression in tumour and leukocyte populations of CKPC mice

The CKPC mice, as the CX3CR1$^{GFP/GFP}$ mice, express GFP instead of a functional CX3CR1 protein, allowing the identification of cell populations which would express CX3CR1.

CKPC mice were analysed not only to identify which cells express GFP-CX3CR1, but also to quantify its level of expression in different leukocyte subsets.

The expression of GFP-CX3CR1 in myeloid and lymphoid cell populations was investigated in tumour, blood, spleen, MLN and bone marrow. The values of GFP geometrical mean intensity are shown in Figure 3.16.

As in the CX3CR1$^{GFP/GFP}$ mice (Figure 3.14), GFP-CX3CR1 levels were different in myeloid and lymphoid cell populations. In particular, myeloid cells expressed higher levels of GFP-CX3CR1 as compared to lymphoid cells.

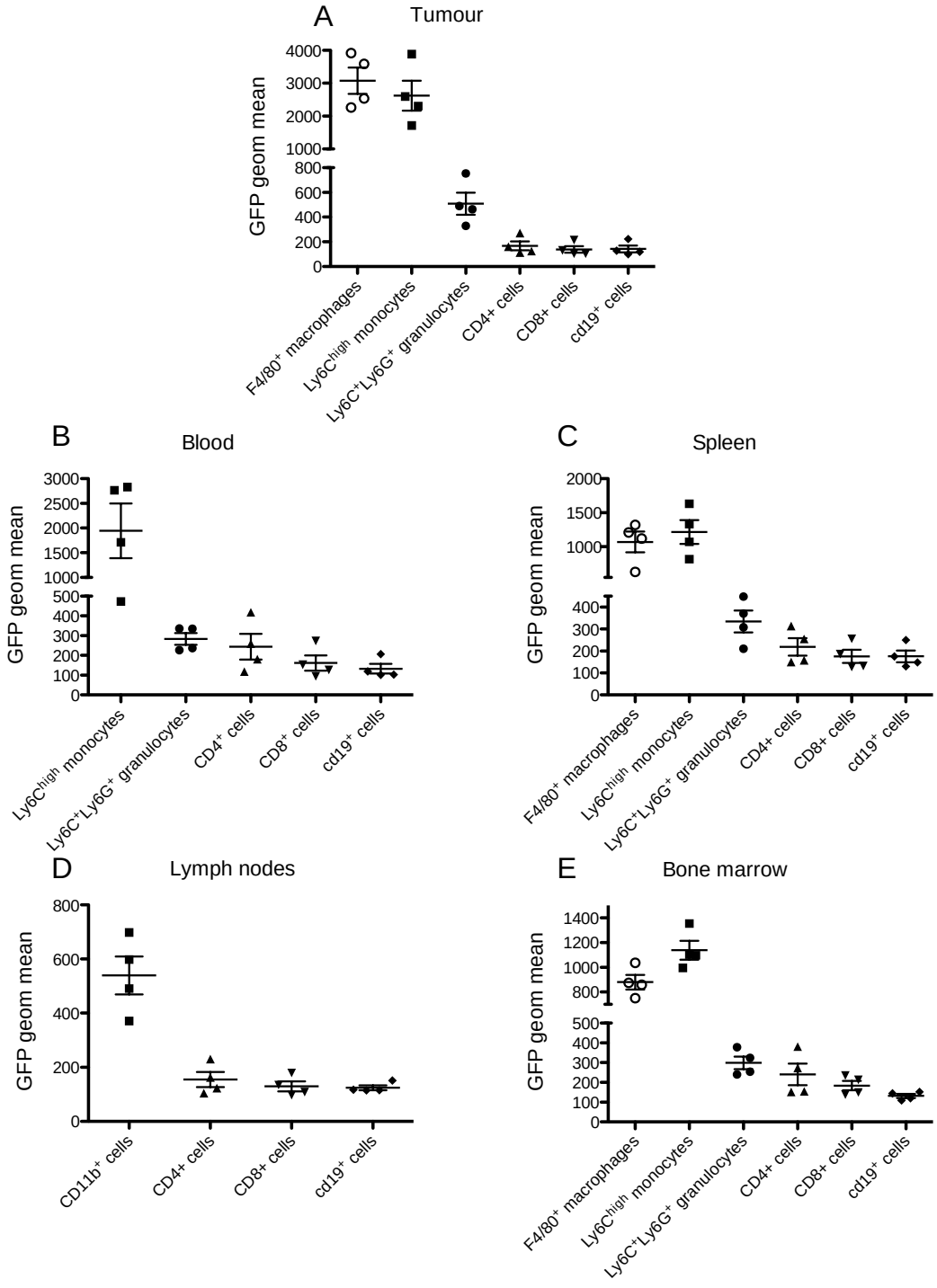

Figure 3.16 GFP expression in leukocyte populations in the tumour, spleen, blood, mesenchymal lymph nodes and bone marrow of CKPC mice

GFP expression was determined by flow cytometry and quantified as geometrical mean intensity of GFP. Leukocytes were stained as described in chapter 3.1.2. GFP intensity were analysed in (A) tumour, (B) spleen, (C) blood, (D) mesenchymal lymph nodes and (E) bone marrow. Values for individual mice are shown as dots and a horizontal line represents mean of the values.

Figure 3.16 showed that $CD19^+$ B cells had the lowest level of GFP-CX3CR1 in all the tissues analysed.

$CD4^+$ and $CD8^+$ T cells expressed the same level of GFP-CX3CR1 in the tumour (Figure 3.16A), MLN (Figure 3.16D), while in the blood (Figure 3.16B), spleen (Figure 3.16C) and bone marrow (Figure 3.14E) $CD4^+$ T cells showed higher GFP-CX3CR1 amount compared $CD8^+$ T cells.

Interestingly, as observed in $CX3CR1^{GFP/GFP}$ mice, each myeloid cell subset expressed different levels of GFP-CX3CR1. In blood (Figure 3.16B), spleen (Figure 3.14C) and bone marrow (Figure 3.16E) the highest levels of GFP-CX3CR1 were expressed by $Ly6C^{high}$ monocytes, followed by $F4/80^+$ macrophages. In the tumour (Figure 3.16A) the highest level of GFP-CX3CR1 was expressed by $F4/80^+$ macrophages and then $Ly6C^{high}$ monocytes. Finally, granulocytes expressed lower level of GFP-CX3CR1 compared the others myeloid cells subsets in all the tissues analysed (Figure 3.16).

The analysis on the GFP levels in the CKPC mice was similar to $CX3CR1^{GFP/GFP}$ mice. In fact, in both mice myeloid cells express more GFP in all the organs analysed. Moreover, in both models $Ly6C^{high}$ monocytes were the cells expressing higher GFP level in the blood and spleen, whilst in $Ly6C^+Ly6G^+$ granulocytes GFP was expressed at low levels in all organs analysed, where the GFP level was comparable with what observed in the lymphoid cell subsets.

3.4 Discussion

Chemokines and their receptors mediate a variety of functional activities in several immunological processes, such as chemotaxis and haematopoiesis. In cancer they have been implicated in regulation of angiogenesis, metastasis and recruitment of immune cells (Raman, Sobolik-Delmaire et al. 2011). The chemokine receptors CX3CR1 and its unique ligand CX3CL1 are known to modulate the migration of leukocytes under physiological and pathological conditions. In my study I have

investigated the effects of CX3CR1 on immune cell trafficking and tumour cell growth in pancreatic cancer.

As mentioned above, chemokine receptors are involve in chemotaxis of immune cells also in steady state condition, for this reason I investigated if the lack of CX3CR1 has an effect in the immune cells profile of different lymphoid organs. I analysed different subset of myeloid and lymphoid cells in blood, spleen, bone marrow and MLN and I observed no significant difference when I compared the $CX3CR1^{GFP/GFP}$ and wild-type mice. These results are in agreement with the results of S. Jung et al. when they established the $CX3CR1^{GFP/GFP}$ mice model (Jung, Aliberti et al. 2000).

In some experiments in this chapter the number of mice analysed in each group was just three, the minimum sample size to perform statistical analysis. However, our results, which showed no difference in the percentages immune cell populations between CX3CR1GFP/GFP and WT mice, are consistent with was already published by S. Jung (Jung, Aliberti et al. 2000).

After I analysed the leukocyte profiles in the $CX3CR1^{GFP/GFP}$ mice in steady state conditions I crossed them with the KPC mice. First, I confirmed that the CKPC mice, but not KPC mice, express GFP. Then I looked at the GFP levels in the leukocytes populations in the different lymphoid organs. Interestingly, in both $CX3CR1^{GFP/GFP}$ and CKPC mice the GFP levels were comparable when looked at the same organ.

3.5 Summary

- No difference in myeloid and lymphoid population in the pancreas, blood, spleen, mesenteric lymph nodes and bone marrow between $CX3CR1^{GFP/GFP}$ and $CX3CR1^{+/+}$ mice
- Myeloid cells express highest levels of GFP-CX3CR1 compared to lymphoid cells in $CX3CR1^{GFP/GFP}$ mice tumours
- Myeloid cells express highest level of GFP-CX3CR1 compared to lymphoid cells in CKPC mice

3.6 Conclusion

In this chapter, I characterised the CX3CR1$^{GFP/GFP}$ mice model looking at the leukocyte composition in the pancreas, blood, spleen, mesenchymal lymph nodes and bone marrow. I also looked at the level of GFP expression by these cells in both the CX3CR1$^{GFP/GFP}$ and CKPC mice. These results will allow a better understanding of the role of CX3CR1 in the tumour microenvironment of KPC and CKPC mouse models, the subject of the next chapter.

Chapter 4 The role of CX3CR1 in pancreatic cancer

4.1 Introduction

Several studies have reported an up-regulation of CX3CR1 in different cancers, such as prostate (Shulby, Dolloff et al. 2004, Jamieson, Shimizu et al. 2008), breast (Andre, Cabioglu et al. 2006, Jamieson-Gladney, Zhang et al. 2011) and pancreatic (Marchesi, Piemonti et al. 2008, Celesti, Di Caro et al. 2013). In pancreatic cancer CX3CR1 expression is associated with increased migration and metastasis formation (Marchesi, Piemonti et al. 2008, Marchesi, Locatelli et al. 2010). CX3CR1 is highly expressed in both human pancreatic tumour cell lines and in primary PDAC tumour tissues, whilst 'benign' epithelial pancreatic duct cell lines and 'normal' exocrine pancreas do not express the receptor (Marchesi, Piemonti et al. 2008).

The chemokine receptor, CX3CR1 forms a high-affinity axis with its unique ligand CX3CL1 and is expressed on monocytes, macrophages and T cells. CX3CR1 is also present on pancreatic malignant cells, where it has been associated with metastasis formation.

The KPC (LoxP-Stop-LoxP-K-ras$^{G12D/+}$;LSL-Trp53$^{R172H/+}$;Pdx-1-Cre) mouse model is the most commonly used mouse model for pancreatic cancer. The KPC mouse recapitulates the pathological, histological, genomic and clinical signatures of human pancreatic cancer (Hingorani, Wang et al. 2005) with some of the critical genetic mutations involved in human pancreatic cancers (Herreros-Villanueva, Hijona et al. 2012, Westphalen and Olive 2012). As described in Chapter 3, the KPC genetic mouse model of pancreatic cancer was crossed to the CX3CR1$^{GFP/GFP}$ mice to make the CKPC mice to investigate if genetic loss of CX3CR1 affects PDAC formation, development and the TME composition.

In this chapter I aim to investigate if genetic loss of CX3CR1 affects PDAC formation and progression in the KPC mouse model. In particular, I will examine if loss of CX3CR1 expression affects cells of the tumour microenvironment.

4.2 Lack of CX3CR1 does not affect mouse survival in the KPC model

In order to evaluate the role played by CX3CR1 in pancreatic cancer, the survival rates of KPC mice and CKPC mice were compared. All mice included in the experiment developed pancreatic cancer (Figure 4.1A 4.1B). Most of the mice showed macro-metastasis in the peritoneum and in the liver (Figure 4.1C).

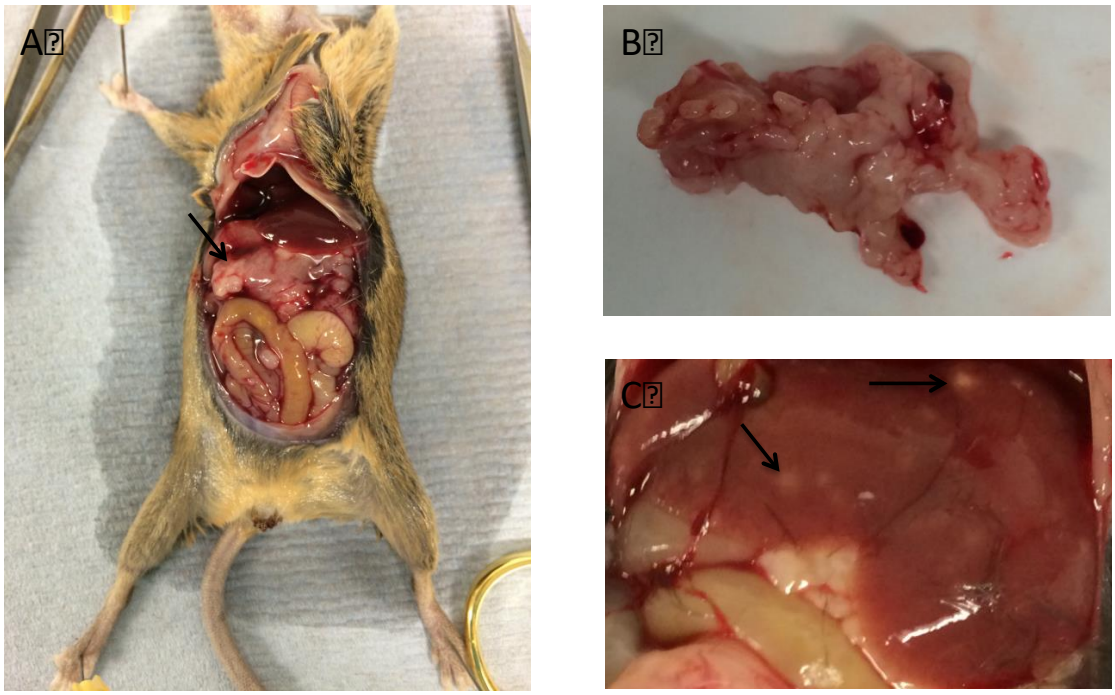

Figure 4.1 CKPC pancreatic tumour and metastasis
Representative images from a CKPC mouse at tumour end-point stage. Mice at end point stage were scarified and autopsy was performed. Images show the A) peritoneum cavity with pancreatic tumour (arrow) B) pancreatic tumour and C) liver metastasizes (arrows).

Overall survival was statistically indistinguishable between KPC and CKPC mice (data collection with the help of Dr Juliana Candido). The median lifespan of mice was 119.5 days and 110.6 days for KPC and CKPC, respectively (Figure 4.2).

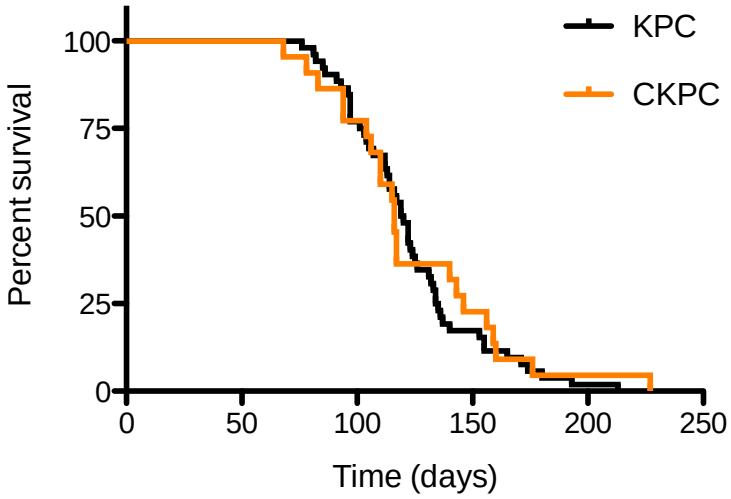

Figure 4.2 Survival of KPC and CKPC mice
Loss of CX3CR1 did not affect survival of mice which develop pancreatic tumours. Kaplan–Meier analysis of survival of KPC and CKPC mice monitored until they reached the end point. N=52 KPC mice, N=22 CKPC mice. Statistical significance was determined by Log-Rank test.

4.3 CX3CR1 and CXC31 expression in KPC and CKPC

Next, I investigate how the loss of CX3CR1 affects various aspect of the TME. In these experiments, tumours were collected when mice reached the end point stage, unless otherwise specified.

First of all, I looked at the expression of CX3CR1 at mRNA level and its ligand CX3CL1, both at mRNA and protein level, in the tumour and in the blood of KPC and CKPC mice.

4.3.1 mRNA levels of *Cx3cr1* and *Cx3cl1* in KPC and CKPC tumours

To confirm that *Cx3cr1* was not expressed at the mRNA level in the pancreatic tumours of CKPC mice I used qRT-PCR. Figure 4.3A shows that in the pancreas of CKPC mice the expression of *Cx3cr1* was absent.

Moreover, I evaluated if loss of the chemokine receptor *Cx3cr1* had an effect on the expression of its only known ligand *Cx3cl1*. There was no significant difference in *Cx3cl1* mRNA expression in KPC tumours compared to the CKPC (Figure 4.3B).

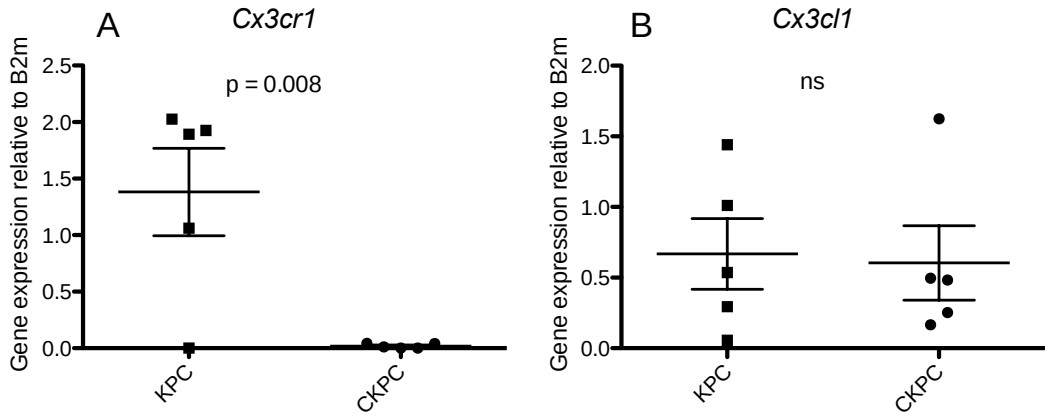

Figure 4.3 *Cx3cr1* and *Cx3cl1* mRNA expression level
RNA was extracted from frozen pancreas tumours of KPC and CKPC mice and qRT-PCR was performed. A) *Cx3cr1* and B) *Cx3cl1* mRNA expression level relative to β2 microglobulin (*B2m*) were plotted. Values for individual mice are shown as dots and a horizontal line represents mean of the values. Statistical significance was determined by unpaired t-test. N=5 per group. ns: not significant.

4.3.2 CX3CL1 protein in tumour and plasma of KPC and CKPC mice

After observing no significant changes at the mRNA level for *Cx3cl1* in the tumours of CKPC mice compared to KPC, the protein level of CX3CL1 was assessed. CX3CL1 levels were measured by ELISA in tumour protein lysates and in the plasma of KPC and CKPC mice, as described in Methods.

Both in the tumours and plasma of KPC mice I found low expression of CX3CL1. However, it was highly expressed in the CKPC mice in both tumour lysates (Figure 4.4A) and plasma (Figure 4.4B) and the differences were statistically significant. I observed that CKPC mice express 10 times more CX3CL1 compared KPC mice ($p = 0.0131$) in the tumour and 300 times more in the plasma ($p = <0.0001$).

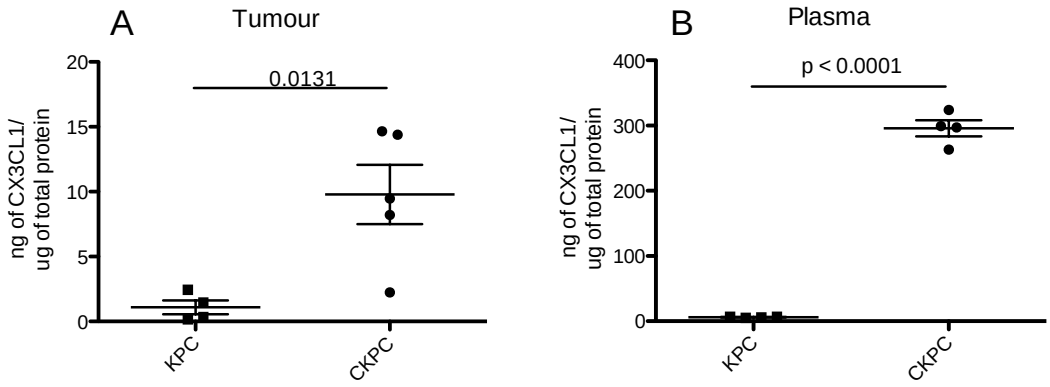

Figure 4.4 CX3CL1 protein levels in tumour and plasma of KPC and CKPC mice
The levels of CX3CL1 in KPC and CKPC mice were determined by ELISA. A) 85 μg of protein lysate from frozen tumours was tested and values are shown as ng of CX3CL1/μg of total protein. B) 50 μl of plasma (diluted 1:1 with water) was analysed and values are shown as ng of CX3CL1/1 ml of plasma. Values for individual mice are shown as dots and a horizontal line represents mean of the values. Statistical significance was determined by unpaired t-test. N = 5 in Figure A) N=4 in Figure B. P-values are shown on the graphs.

4.4 Immune infiltration in pancreatic tumours

I next assessed whether CX3CR1 has a role in regulating immune infiltration into PDAC tumours. Infiltration of both myeloid and lymphoid cells in KPC and CKPC pancreatic tumours was analysed by flow cytometry. Single cell suspensions from each pancreatic tumour were stained with fluorescence-labelled antibodies against a panel of markers able to discriminate between myeloid and lymphoid cell populations as described in Methods. The different immune cells were identified based on the gating strategy shown in Figure 4.5.

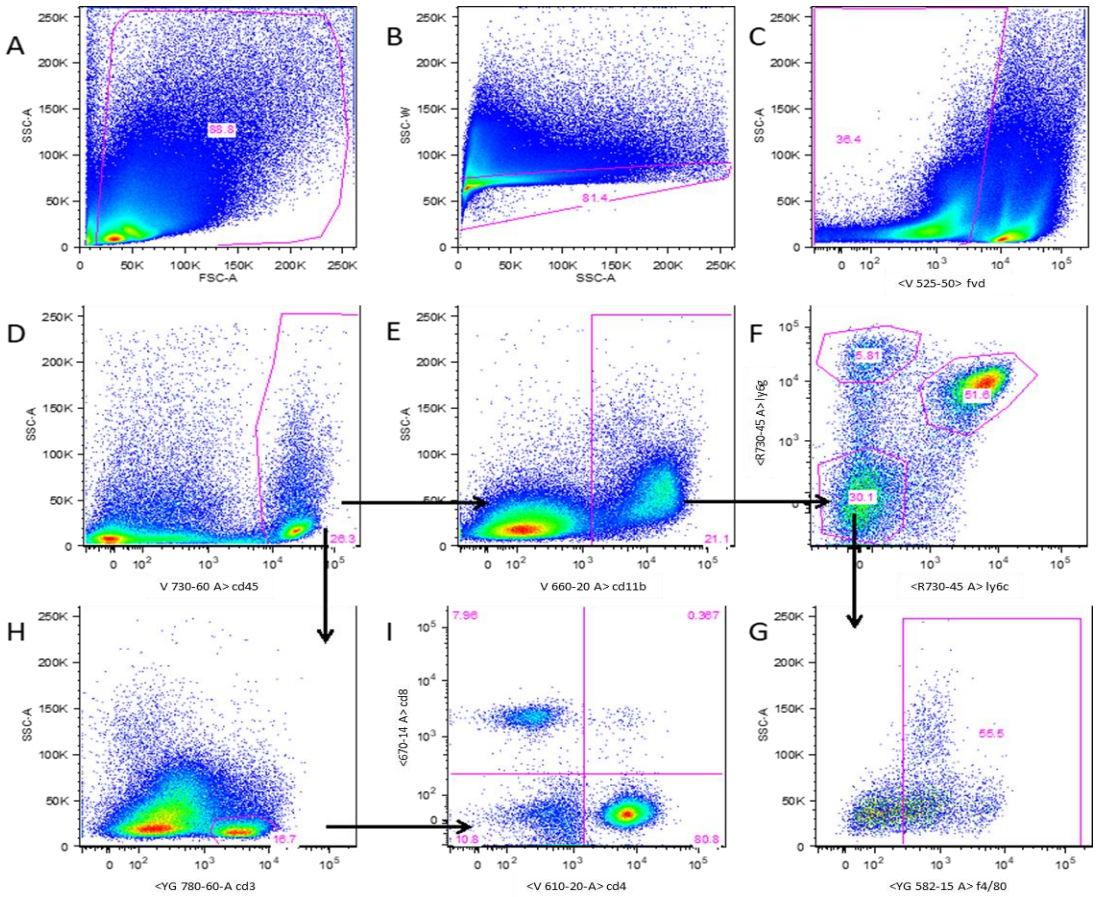

Figure 4.5 Representative gating strategy for the leukocyte subsets in the tumour by flow cytometry
Total pancreatic tumour single cell suspensions were stained with a pool of fluorescence-conjugated antibody antibodies and analysed by flow cytometry. Acquired cells were gate to eliminate (A) debris, (B) doublets and (C) dead cells to obtain (D) CD45$^+$ cells. CD45$^+$ cells were analysed for the expression of (E) CD11b and (H) CD3$^+$ allowing discrimination between myeloid and lymphoid subsets. CD11b$^+$ cells were analysed in (F) for the expression of Ly6C and Ly6G and (G) F4/80. (I) CD3$^+$ cells were further analysed for the expression of CD4 and CD8

Infiltration of CD45$^+$ cells was not significantly different between KPC and CKPC tumours (Figure 4.6A). The frequency of myeloid cells, based on CD11b expression, was not statistically increased in the CKPC compared to the KPC mice, (mean value of 40% and 20% respectively) (Figure 4.6B). Ly6C$^+$Ly6G$^+$ granulocytes and Ly6C^{high} monocytes were slightly increase in CKPC compared to KPC mice (Figure 4.6C and D, respectively). F4/80$^+$ macrophages, accounted for ~ 20% of the CD45$^+$ cells and showed no major difference between KPC and CKPC (figure 4.6E).

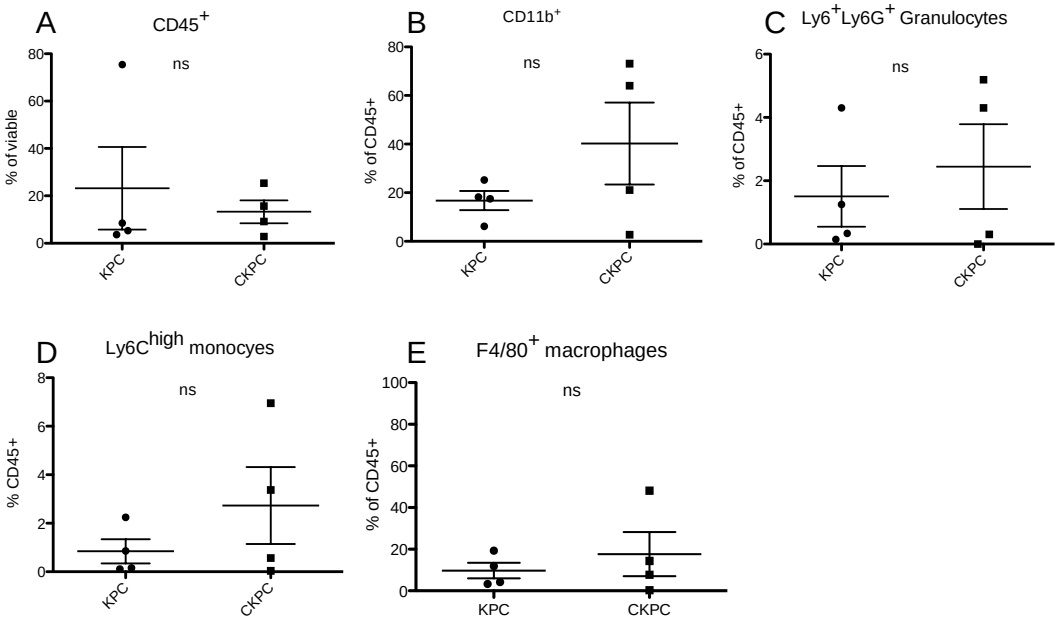

Figure 4.6 Percentage of myeloid cell subsets in KPC and CKPC tumours
Flow cytometric analysis of myeloid cells from KPC and CKPC tumours. Cells were gated as shown in Figure 3.9. Value for individual mice are shown as dots and a horizontal line represents mean of the values. Statistical significance was determined by unpaired t-test. N = 4 per group. ns: not significant.

Interestingly, $CD3^+$ T lymphocytes were significantly decreased in CKPC mice compared to KPC mice. There were 12% and 4% of $CD3^+$ T cells in KPC and CKPC respectively (p value =0.494) (Figure 4. 7A). However, I observed no significant difference in the proportion of $CD4^+$ T cells (Figure 4.7B) and $CD8^+$ T cells (Figure 4.7C) within the $CD3^+$ T cell population.

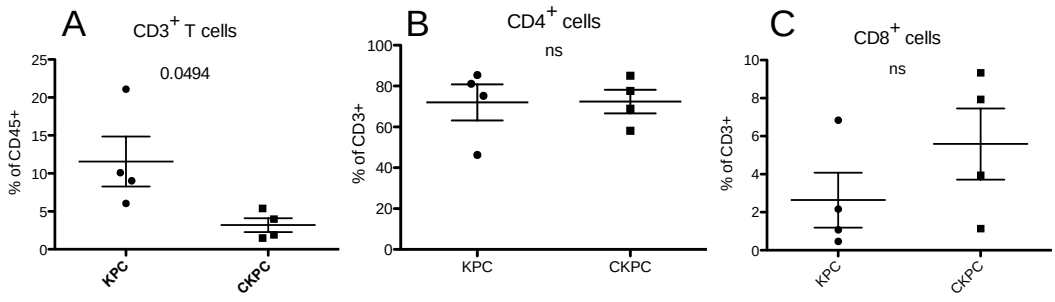

Figure 4.7 Percentage of myeloid cell subsets in KPC and CKPC tumours
Flow cytometric analysis of lymphoid cells from KPC and CKPC tumours. Cells were gated as shown in Figure 3.9. Value for individual mice are shown as dots and a horizontal line represents mean of the values. Statistical significance was determined by unpaired t-test. N = 4 per group. ns: not significant.

4.5 CCL2, CSF1 and CSF1R expression in KPC and CKPC tumours

After observing the changes in the levels of CX3CL1 in the plasma and tumours of CKPC mice along with the subtle alterations in myeloid cell frequencies, I next assessed the expression of CCL2, mediator of myeloid cells chemotaxis, as well as CSF1 and CSF1R, involved in myeloid cells proliferation and differentiation.

CCL2 is a chemokine that leads to the recruitment of monocytes, memory T cells, and NK cells to the sites of inflammation (Deshmane, Kremlev et al. 2009). CSF1 is a cytokine involved in the proliferation, differentiation, and survival of monocytes into macrophages (Stanley and Chitu 2014). CSF1R is a membrane protein receptor for CSF1 and IL-34; it is expressed on monocytes and macrophages and it plays a role in their differentiation and function (Hamilton 2008).

I found no statistical difference in the expression of *Csf1* and *Ccl2* and *Csf1R* at transcript level in the tumours (Figure 4.8A, B and C respectively).

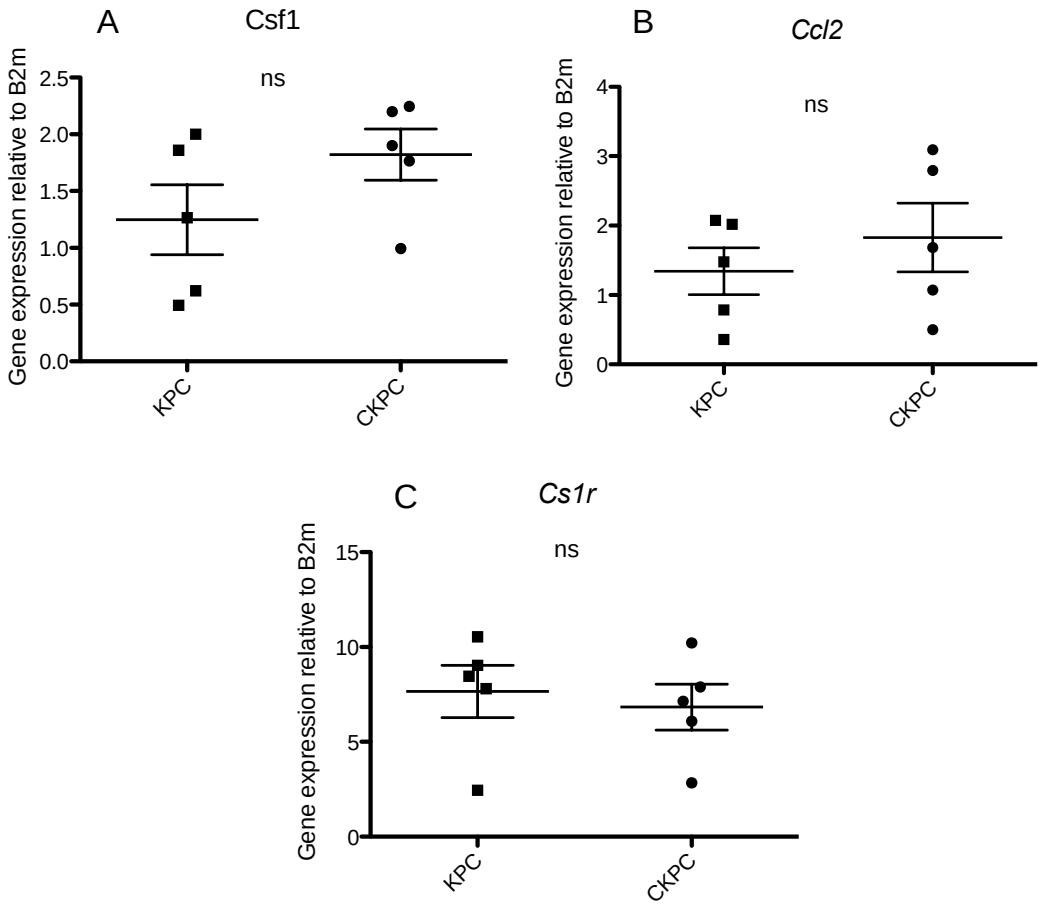

Figure 4.8 *Csf1*, *Ccl2* and *Csf1r* expression in KPC and CKPC tumours
RNA from frozen pancreas tumours from KPC and CKPC mice was extracted and qRT-PCR was performed. A) *Csf1*, B) *Ccl2* and C) *Csf1r* mRNA expression level relative to *B2m* were plotted. Values for individual tumours are shown as dots and a horizontal line represents mean of the values. Statistical significance was determined by unpaired t-test. N=5 tumours per group. ns: not significant.

4.6 The inflammatory environment in KPC and CKPC mice

The binding of chemokines to their respective receptors initiates a series of cellular events: changes in cell shape leading to enhanced locomotion; secretion of lysosomal enzymes, and production of cytokines (Griffith, Sokol et al. 2014). Therefore, the KPC mice might have a different inflammatory microenvironment compared to CKPC mice. In particular, the levels of inflammatory cytokine expression were analysed to verify if there were any difference between KPC and CKPC mice. I next examined potential alterations in expression of the major pro-

inflammatory cytokines TNF-α, IL-1β and IL-6 as well as the anti-inflammatory IL-10. These were assessed in pancreatic tumour lysates from KPC and CKPC mice at gene (*Il6*, *Il12a*, *Il10* and *Tnf*) and protein level (TNF-α, IL-1β, IL-6 and IL-12) by qRT-PCR and ELISA.

There were no significant differences at the mRNA expression levels of *Il10*, *Tnf*, *Il1b* and *Il6*, in tumour lysates from KPC and CKPC mice (Figure 4.9 A-D).

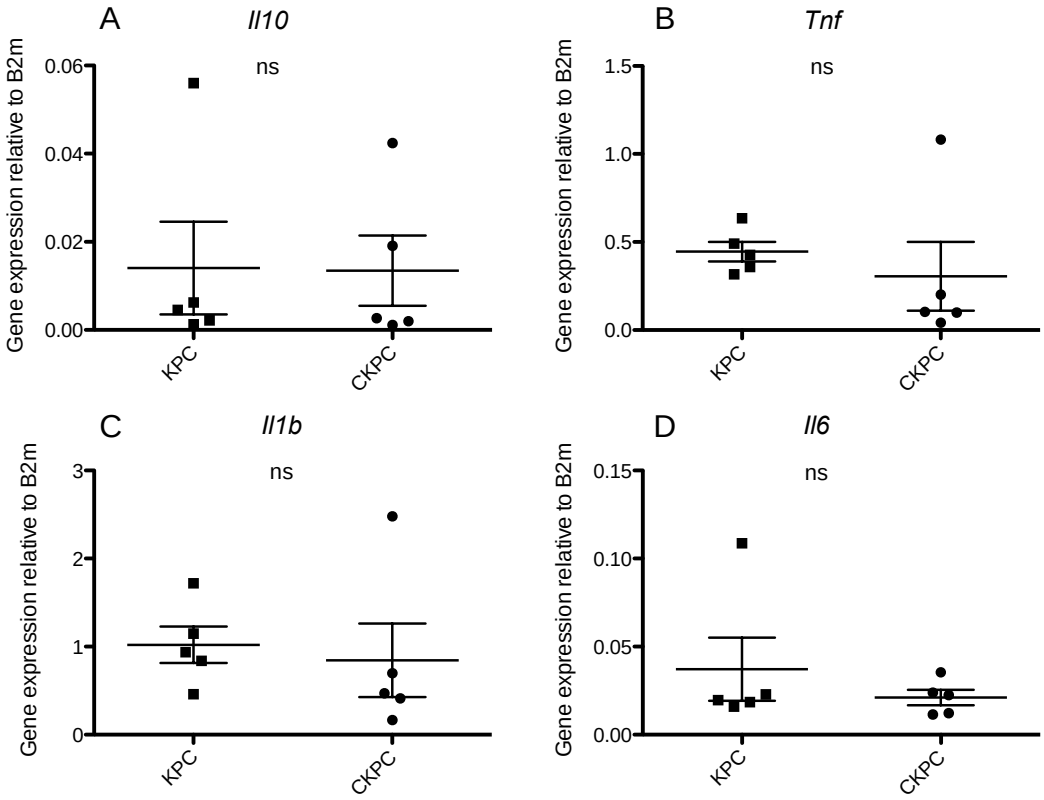

Figure 4.9 mRNA expression of *Il10, Tnf*, *Il6 and Il1b* expression in KPC and CKPC tumours

RNA from frozen pancreatic tumours of KPC and CKPC mice were extracted and qRT-PCR was performed for A) *Il10*, B) *Tnf*, C) *Il1b* and D) *Il6* mRNA expression level relative to *B2m* were plotted. Values for individual mice are shown as dots and a horizontal line represents mean of the values. Statistical significance was determined by unpaired t-test. N=5 per group. ns: not significant.

IL-10, TNF-α, IL-6 and IL12p40 were measured at protein level by ELISA. IL-10 levels were significantly higher in CKPC compared to KPC mice, p = 0.0460 (Figure 4.10A). TNF-α and IL-6 were not statistically increased in CKPC compared to KPC

mouse tumours (Figure 4.10B and C, respectively). IL-12 subunit beta (IL-2p40) levels were comparable between KPC and CKPC mice (Figure 4.10D).

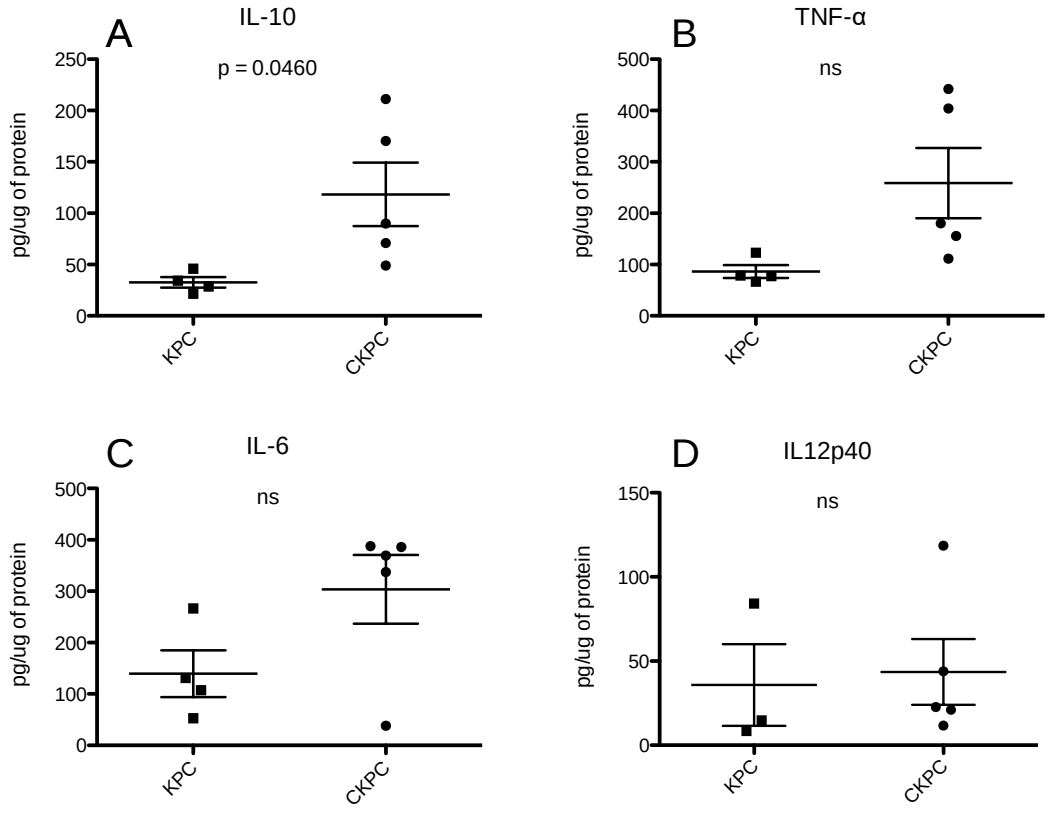

Figure 4.10 Protein expression of IL-10, TNF-α, IL-6 and IL-12p40 in KPC and CKPC tumours

Protein levels of inflammatory cytokines in the tumours were determined by ELISA. 85 μg of protein lysates from frozen tumours were tested and value are shown as ng of cytokines/μg of total protein. A) IL-10, B) TNF-α, C) IL-6 and D) IL-12p40. Values for individual mice are shown as dots and a horizontal line represents mean of the values. Statistical significance was determined by unpaired t-test. N = 5 per group (KPC IL12p40 = 3). ns: not significant.

4.7 mRNA profiles of FACS-sorted tumour-infiltrating cells from KPC and CKPC mice

CKPC tumours showed some subtle changes in the TME compared to KPC, primarily a reduction in the frequency of $CD3^+$ T cells and an increase in IL-10 levels (Figure 4.7 and 4.10). I next sought to examine in more detail expressional

profiles of inflammatory on FACS-sorted tumour infiltrated immune cells namely F4/80$^+$ macrophages, Ly6C$^+$Ly6G$^+$ granulocytes and CD3$^+$ T cells. I chose to analyse F4/80$^+$ macrophages because those are the cells have the highest levels of CX3CR1, CD3$^+$ T cells because they were significantly decreased in CKPC mice compared to KPC mice, and Ly6C$^+$Ly6G$^+$ granulocytes because those are the myeloid cells at highest density after the F4/80$^+$ macrophages in the tumour microenvironment of KPC and CKPC mice.

4.7.1 F4/80$^+$ macrophages

Figure 4.11 shows mRNA levels *Cx3cr1*, *Tnf*, *Il6*, *Il12a*, *Il1b*, *Il10*, *Nos2* and *Arg1* in sorted F4/80$^+$ macrophages from KPC and CKPC mice. The expression of CX3CR1 was measured to confirm its KO in CKPC-tumour macrophages (Figure 4.9A). *Tnf*, *Il6, IL12a, IL1b* and *Il10* cytokines were analysed but no significant difference was found between macrophages from KPC and CKPC mice (Figure 4.11B, C, D, E and F, respectively).

Additionally, two macrophage activation markers nitric oxide synthases-2 (NOS2) and Argenase-1 (Arg1) were analysed. NOS2 and Arg1 are classic M1 and M2 markers, respectively (Jablonski, Amici et al. 2015). *Nos2* and *Arg1* mRNA showed no significant differences seen between KPC and CKPC mice (Figure 4.11G and H respectively)

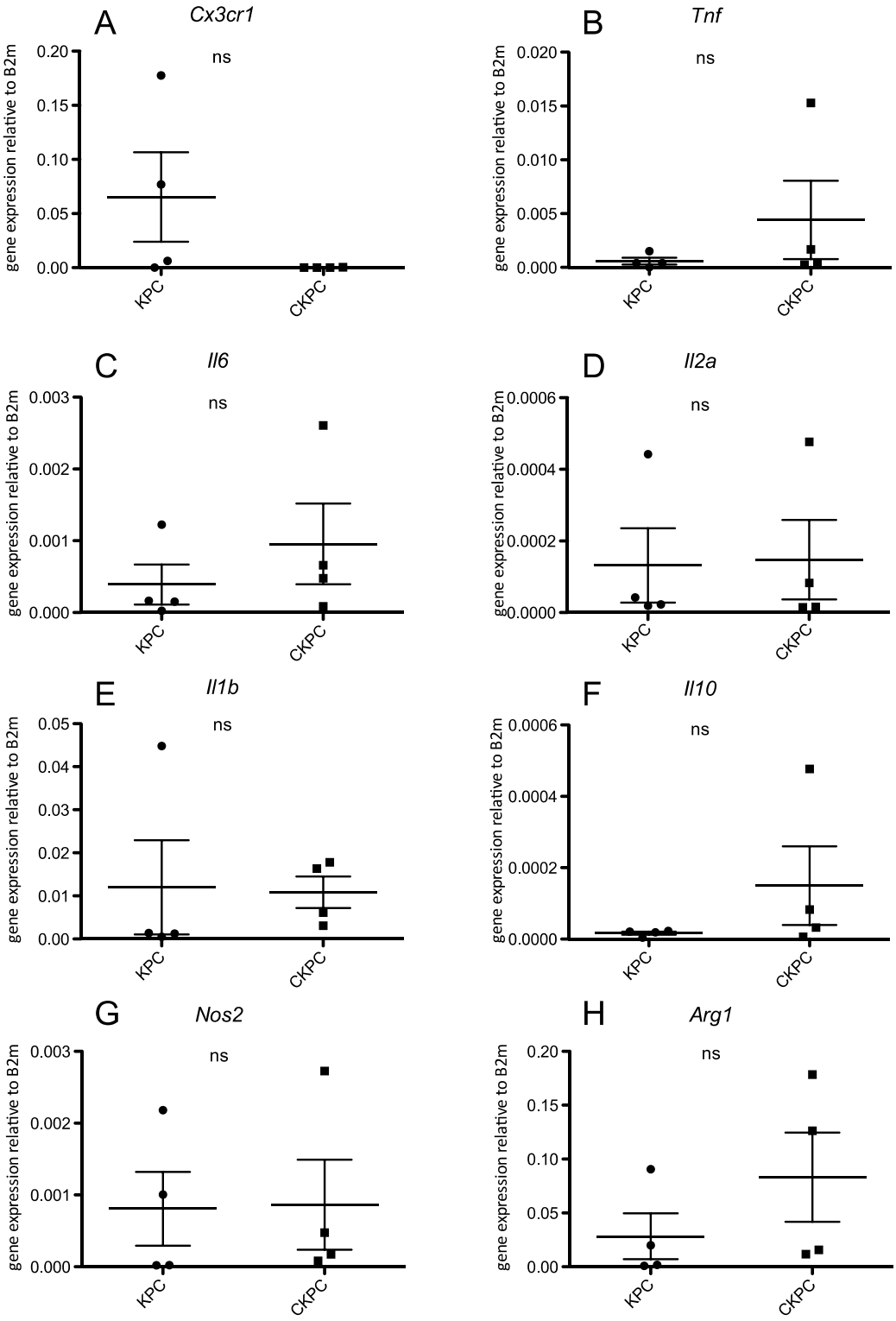

Figure 4.11 mRNA expression *Cx3cr1*, *Tnf*, *Il6*, *Il12a*, *Il1b*, *Il10*, *Nos2* and *Arg1* in F4/80⁺ macrophages from KPC and CKPC tumours

RNA from F4/80⁺ macrophages FACS-sorted from tumour of KPC and CKPC mice was extracted and qRT-PCR was performed for A) *Cx3cr1*, B) *Tnf*, C) *Il6*, D) *Il12a*, E) *Il1b*, F) *Il10*, G) *Nos2* and H) *Arg1* mRNA expression levels relative to B2m were plotted. Values for individual mice are shown as dots and a horizontal line represents mean of the values. Statistical significance was determined by unpaired t-test. N=4 per group. ns: not significant.

4.7.2 Ly6c$^+$Ly6G$^+$ granulocytes

Figure 4.11 shows the mRNA levels of sorted Ly6C$^+$Ly6G$^+$ granulocytes from KPC and CKPC mice. The KO of CX3CR1 was confirmed also in CKPC Ly6c$^+$Ly6G$^+$ granulocytes, (Figure 4.12A). In 3 out of 4 KPC Ly6C$^+$Ly6G$^+$ granulocytes C*x3cr1* expression was not detected, due to the fact that this cell population express low level of CX3CR1 (Figure 3.16A).

As with F4/80$^+$ macrophages, I observed no significant difference in the expression of cytokines and activation markers in Ly6c$^+$Ly6G$^+$ granulocytes between KPC and CKPC mice (Figure 4.12D and E respectively). *Tnf*, *Il6, IL12a, IL1b* and *Il10* and mRNA levels were equal in granulocytes from KPC and CKPC tumours (Figure 4.12B, C, D, E and F, respectively). Moreover, Ly6c$^+$Ly6G$^+$ granulocytes from CKPC tumours expressed the same amount of *Nos2* and *Arg1* in KPC and CKPC tumours (Figure 4.12G and H, respectively).

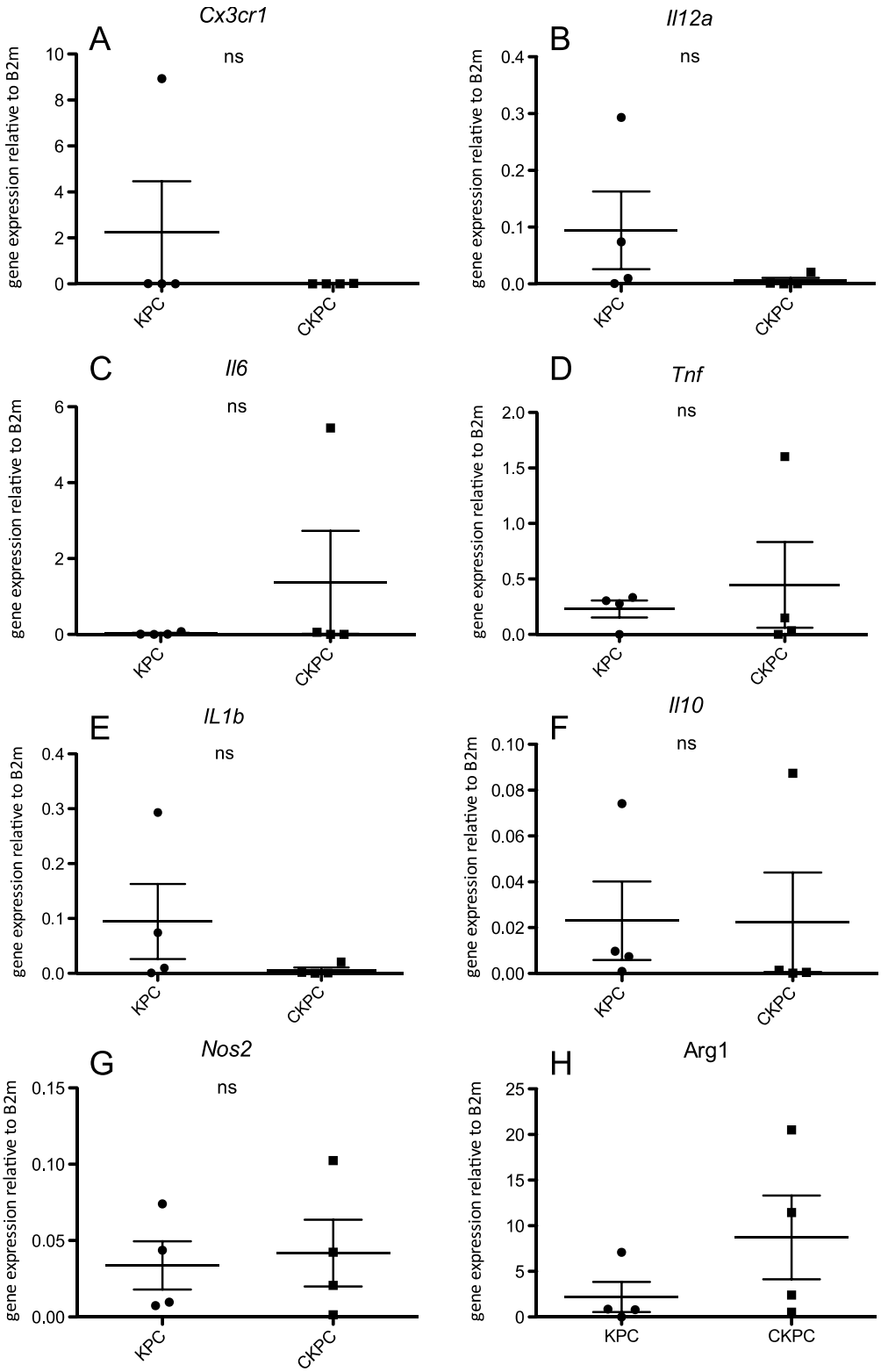

Figure 4.12 mRNA expression *Cx3cr1*, *Tnf*, *Il6*, *Il12a*, *Il1b*, *Il10*, *Nos2* and *Arg1* in Ly6c$^+$Ly6G$^+$ granulocytes from KPC and CKPC tumours

RNA from frozen Ly6C$^+$Ly6G$^+$ granulocytes sorted from tumours of KPC and CKPC mice were extracted and qRT-PCR was performed for A) *Cx3cr1*, B) *Tnf*, C) *Il6*, D) *Il12a*, E) *Il1b*, F) *Il10*, G) *Nos2* and H) *Arg1* mRNA expression levels relative to B2m were plotted. Values for individual mice are shown as dots and a horizontal line represents mean of the values. Statistical significance was determined by unpaired t-test. N=4 per group. ns: not significant.

4.7.3 CD3$^+$ T cells

FACS-sorted CD3$^+$ T cells from KPC and CKPC mice were analysed for expression of *Cx3cr1*, *Tnf*, *Il6*, *Il12a*, *Il1b* and *Il10* as shown in Figure 4.13. The absence of CX3CR1 mRNA expression was observed also in CD3$^+$ T cells from CKPC mice (Figure 4.13A). There was no significant difference in the mRNA expression of any of inflammatory cytokines analysed. However, in CD3$^+$ T cells sorted from CKPC I observed slightly more *Tnf*, (Figure 4.13B).

CD3$^+$ T cells from KPC and CKPC tumours showed equal mRNA levels of *Il6*, *Il12a, Il1b* and *Il10*, Figure 4.13C, D, E and F, respectively.

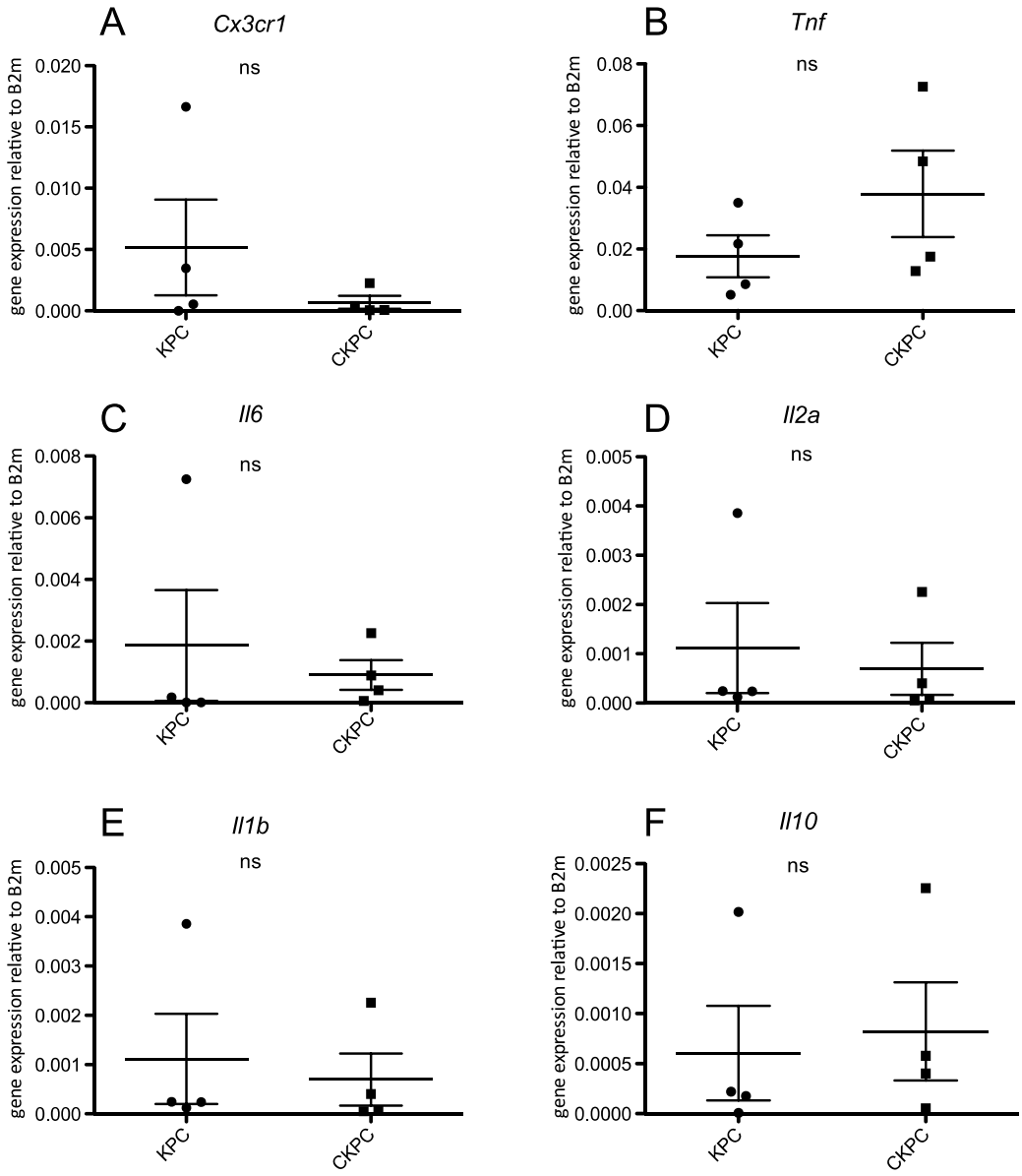

Figure 4.13 mRNA expression *Cx3cr1*, *Tnf*, *Il6*, *Il12a*, *Il1b* and *Il10* in CD3⁺ T cells from KPC and CKPC tumours

RNA from CD3⁺ T cells sorted from tumours of KPC and CKPC mice was extracted and qRT-PCR was performed for A) *Cx3cr1*, B) *Tnf*, C) *Il6*, D) *Il12a*, E) *Il1b* and F) *Il10*, mRNA expression levels relative to B2m were plotted. Values for individual mice are shown as dots and a horizontal line represents mean of the values. Statistical significance was determined by unpaired t-test. N=4 per group. ns: not significant.

4.8 The effects of chemotherapy on KPC and CKPC tumours

The experiments above showed that absence of CX3CR1 appeared to have no impact on tumour development in the KPC mouse model and also that there were only a few quite subtle differences in the TME. It is known that chemotherapy not only affects tumour cells but can also alter the TME. For example, chemotherapy can modify both the composition and functions of immune cells in circulation and into the tumour (Galluzzi, Buque et al. 2015, Tsuchikawa, Takeuchi et al. 2016); as showed in a study by Soeda et al, where patients treated for three weeks with gemcitabine exhibited an increase in circulating $CD11c^+$ DC and $CD14^+$ monocytes (Soeda, Morita-Hoshi et al. 2009). Moreover, the effect of chemotherapy on the function of the immune cells can be either immuno-suppressive or immuno-stimulatory (Galluzzi, Zitvogel et al. 2016).

I questioned if administration of chemotherapy in CKPC mice would have an effect on tumour growth or could influence the tumour-infiltration of immune cells differently to KPC. I chose to treat the animals with gemcitabine, since it is a chemotherapy frequently used in clinic to treat patients with pancreatic tumours (Kim 2008). Gemcitabine is a cytosine nucleoside analog, which is incorporated in DNA during its replication, inducing apoptosis (Noble and Goa 1997). Mice were used when their tumours were palpable and then treated twice a week for two weeks with gemcitabine administered intra-peritoneally at a dose of 100mg/kg of mouse. After two weeks of treatment with gemcitabine mice were sacrificed and pancreatic tumours were harvested for analysis.

Firstly, the collected tumours were weighed. As showed in Figure 4.14 pancreatic tumours from KPC and CKPC mice did not show any significant differences. Notably, the mice at the end of the experiment were not at end-point stage and did not show any sign of discomfort and sickness.

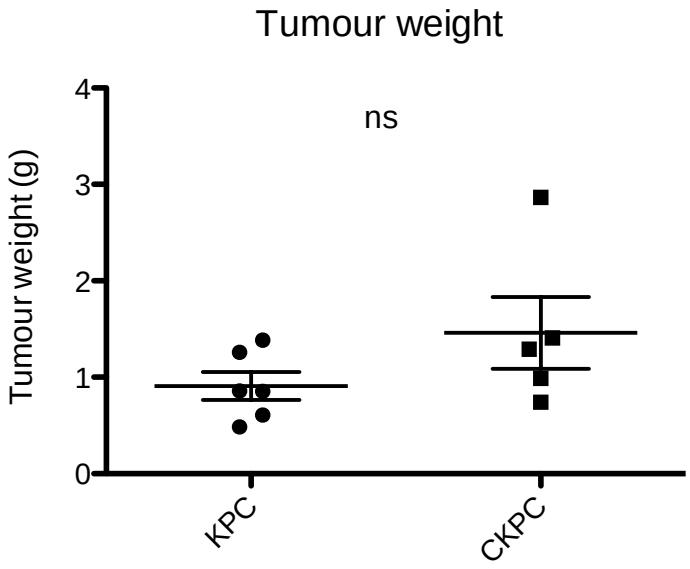

Figure 4.14 Tumour weight of KPC and CKPC mice treated with gemcitabine
Pancreatic tumours were collected from KPC and CKPC mice after being treated with gemcitabine and weighed. Mice were treated twice a week for two weeks with gemcitabine administered intra-peritoneally at a dose of 100mg/kg of mouse. Values for individual mice are shown as dots and a horizontal line represents mean of the values. Statistical significance was determined by unpaired t-test. KPC N=6 for and CKPC N=5. ns: not significant.

Pancreatic tumours were then analysed by flow cytometry. Single cell suspensions from each tissue were stained with fluorescent antibodies against markers able to discriminate between myeloid and lymphoid cell populations. The gating strategy is shown in Figure 4.5.

Overall, the infiltration of $CD45^+$ cells was not significantly different between KPC and CKPC mice (Figure 4.15A). The percentages of myeloid cells, based on CD11b expression, were decreased in the CKPC compared to the KPC mice, 43% versus 70% respectively (Figure 4.15B). However, the difference was again not statistically significant. When I looked into the myeloid subsets I observed that $Ly6C^+Ly6G^+$ granulocytes and $Ly6C^{high}$ monocytes were equal between KPC and CKPC mice (Figure 4.15 and 4.15D, respectively). $F4/80^+$ macrophages were decreased, but again not significantly, in CKPC compared to KPC mice (Figure 4.15E).

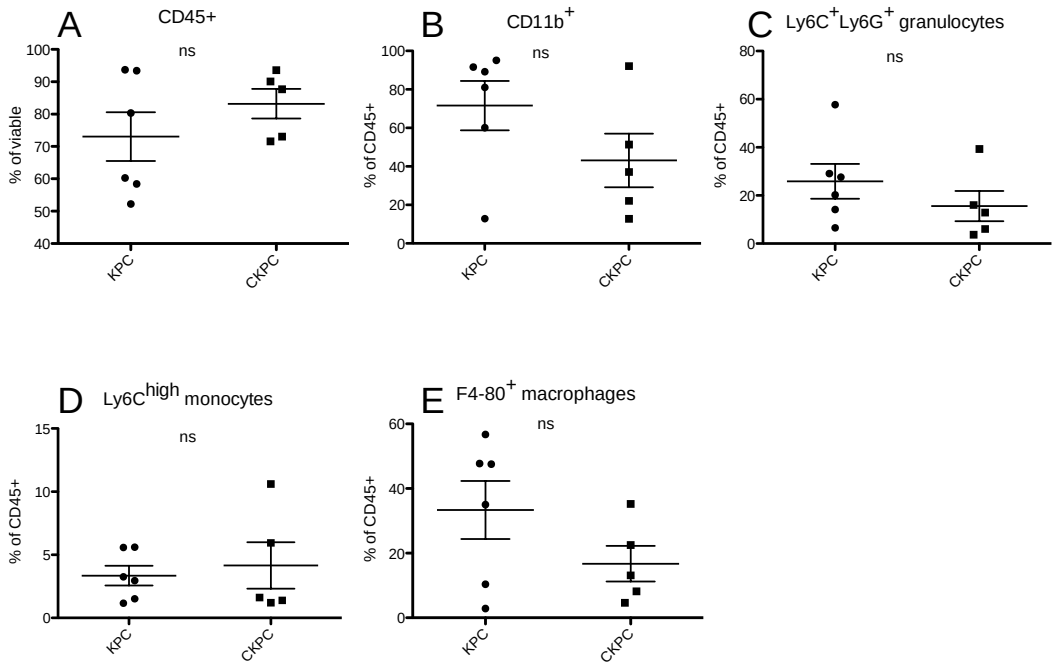

Figure 4.15 Percentage of myeloid cell subsets in the tumour of KPC and CKPC mice treated with gemcitabine

Flow cytometric analysis of myeloid cells from the tumour of KPC and CKPC mice treated with gemcitabine. Cells were gated as outline in Figure 3.9. Value for individual mice are shown as dots and a horizontal line represents mean of the values. Statistical significance was determined by unpaired t-test. KPC N=6 for and CKPC N=5. ns: not significant.

$CD3^+$ T lymphocytes were slightly increased in CKPC mice compared to KPC mice, 40% and 25% of $CD45^+$ cells, respectively (Figure 4.16A). There was no difference in the proportion of $CD4^+$ T lymphocytes (Figure 4.16B) and $CD8^+$ T lymphocytes (Figure 4.16C) within the $CD3^+$ T cells.

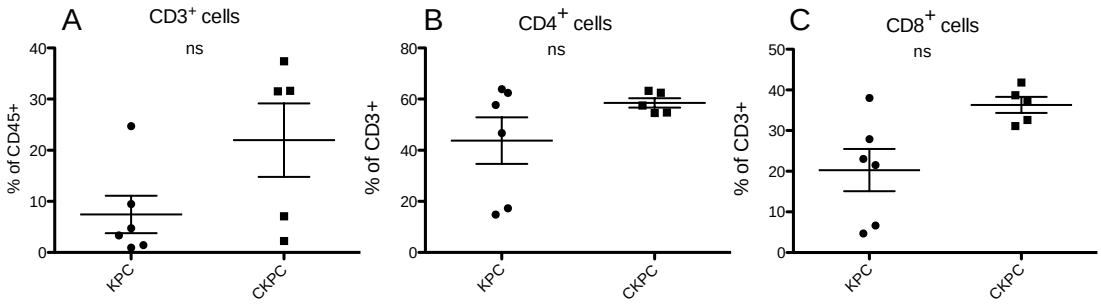

Figure 4.16 Percentage of lymphoid cell subsets in the tumour of KPC and CKPC mice treated with gemcitabine
Flow cytometric analysis of lymphoid cells from the tumour of KPC and CKPC mice treated with gemcitabine. Cells were gated as outline in Figure 3.9. Value for individual mice are shown as dots and a horizontal line represents mean of the values. Statistical significance was determined by unpaired t-test. KPC N=6 for and CKPC N=5. ns: not significant.

4.9 Discussion

In the previous chapter I have showed that the immune cells infiltrated into pancreatic tumours, and expressed CX3CR1 to different extent. Next, I wanted to examine if the lack of the CX3CR1 receptor had an effect in the tumour microenvironment within the pancreas tumours.

First, I compared the survival of KPC and CKPC mice and I found that the lack of CX3CR1 had no effect on the survival of mice with pancreatic tumours (Figure 4.2). In PDAC patients, the correlation between CX3CR1 and overall survival was investigated by Merchesi et al. In their study they showed that the tumour expression of CX3CR1 has no effect on overall survival in relapsed PDAC patients (Marchesi, Piemonti et al. 2008). At this stage, the pancreas of all the mice showed no healthy tissue, becoming a large malignant mass. The vast majority of mice exhibited metastasis in the peritoneum and liver. I also observed metastasis in the diaphragm, spleen, lungs and kidneys. Some mice developed ascites in the peritoneum.

CX3CL1 is the only known ligand for CX3CR1, so I expected that the absence of CX3CR1 in the CKPC mice might have an effect on the levels of CX3CL1. In fact, it has been already observed by Shah et al. that in CX3CR1 KO mice exhibited higher levels of circulating CX3CL1 when fed under chow or high-fat diet (Shah, O'Neill et

al. 2015). Our results confirmed this hypothesis showing that in CKPC mice the amount of CX3CL1 was much higher compared KPC mice both in tumour lysates and plasma (Figure 4.3). In the KPC mice, I barely found any expression of CX3CL1. However, when I looked at the mRNA level of CX3CL1 I observed its expression in KPC tumours, but there was no difference compared to CKPC mice. This may suggest, that KPC and CKPC produced similar amount of CX3CL1, but in the CKPC mouse CX3CL1 could have accumulated over time because there was no receptor to bind to.

Then I compared infiltration of myeloid and lymphoid cells in KPC and CKPC tumours. Our result showed no difference in the overall amount of leukocytes infiltrated into the tumour (Figure 4.6). The percentage of T cells within the tumour was significantly lower in CKPC mice compared KPC mice (Figure 4.7). However, the proportion of $CD4^+$ cells and $CD8^+$ T cells was comparable between CKPC and KPC mice. The decrease of $CD3^+$ T cells could be caused by a direct lack of CX3CR1 on T cells, which impair their recruitment in the tumour microenvironment or induced their death. Otherwise, the decrease in the percentages of $CD3^+$ T cells could be caused indirectly. Changes in one or more populations of the TME, might be the responsible for blocking the recruitment of $CD3^+$ T cells or for promoting their death. CX3CR1 is expressed by a subset of cytotoxic T cells (Nishimura, Umehara et al. 2002) and by a small subset of $CD3^+$ T cells, $CD8^+$ memory T cells with cytotoxic but not proliferative capability (Bottcher, Beyer et al. 2015). Therefore, considering that these populations constitute a small proportion of the total of $CD3^+$ T cells, it seems unlikely that their decrease in CKPC mice is caused by the direct lack of CX3CR1.

CX3CR1 is mostly involved in monocyte survival and differentiation into macrophages (Landsman, Bar-On et al. 2009). I wanted to verify if the lack of CX3CR1 induced compensatory mechanisms changing levels of other chemokines/chemokine receptors. CSF1 and CCL2 are critical for the recruitment of macrophages. I looked at the mRNA levels of *Csf1* and *Ccl2* and I observed that CKPC expressed a not significant higher amount of both chemokines. This result

may support our hypothesis of a compensatory mechanism mediated by CCL2 and CSF1 to explain the comparable levels of macrophages in CKPC and KPC mice.
There is a growing appreciation that inflammation is the root cause of many cancers.

I looked to see if CKPC mice had a different inflammatory microenvironment compared to KPC mice. I analysed several inflammatory cytokines, both at mRNA and protein levels. Interestingly, I did not observe any significant differences between KPC and CKPC mice when I look at the mRNA levels but I observed difference at protein levels. In particular, I observed a significant increase in IL-10 and no significant changes in TNF-α and IL-6 in CKPC mice compared to KPC mice.

I was interested to identify which cells were responsible for the production of these cytokines. To assess this I isolated F4/80$^+$ macrophages, Ly6C$^+$Ly6G$^+$ granulocytes and CD3$^+$ T cells and measured the mRNA levels of these inflammatory cytokine. Our results showed a slight not significant increase in the mRNA levels of *Il0*, *Il6* and TNF-α produced by F4/80$^+$ macrophages and CD3$^+$ T cells. These results indicated that the increase in *Il10* in CKPC tumours was produced by other cell subsets in the tumour microenvironment. In fact, IL-10 can be produced by tumour cells, tumour suppressive myeloid cells and B cells. Otherwise, it is also possible that the increase in IL-10 in CKPC tumours it is caused by its production by two or more cell subsets.

Chemotherapy can modify the TME by altering the cytokine and chemokine milieu as well as frequencies of immune cell populations and their effector function (Tsuchikawa, Takeuchi et al. 2016). For this reason I analysed the effects of a two-week gemcitabine treatment on immune infiltration in KPC and CKPC tumours. There was no difference in tumour weight between KPC and CKPC mice at the end of the treatment. After two week of gemcitabine treatment I observed a not significant decrease in the frequency of CD11b$^+$ cells and an increase in CD3$^+$ T cells, both CD4$^+$ and CD8$^+$ T cells, in CKPC compared to KPC. Increase in CTL after treatment with gemcitabine was already been observed by Pei et al. and it is mediated by DCs (Pei, Pan et al. 2014).

Moreover, I observed difference in the immune infiltration, in both KPC and CKPC mice, between tumours at end point stages (Figure 4.6 and 7 and tumours after gemcitabine treatment (Figure 4.15 and 16). These differences could be caused either by the gemcitabine treatment itself or by the different stage of the tumours. Several studies have reported that chemotherapy treatment, such as gemcitabine, induce immune-modulatory effects (Pei, Pan et al. 2014, Chang, Jiang et al. 2016). This might support that gemcitabine was indeed responsible in the changes I observed in the in the TME. For example, increase in CTL activity after treatment with gemcitabine was already been observed by Pei et al. In this study pancreatic tumour cells treated with gemcitabine stimulated DC maturation, which in turn promoted T cells proliferation and a CTL antitumor immune response (Pei, Pan et al. 2014).

As in chapter 3, the results described here were obtained from analysis of small numbers of mice in each experimental group. This could explain why, even if some of my results showed several fold differences between the experimental groups, they were not statistically significant. Moreover, the experiments used both male and female mice. The use of same-sex mice in the experiments could have given more consistent results, in particular when chemokine and chemokine receptors levels were analysed. In fact, some chemokines are expressed at different levels in male and females (Madalli, Beyrau et al. 2015).

4.10 Summary

- No difference in the survival of CKPC compared to KPC mice
- Significant decrease in $CD3^+$ T cells in CKPC mice compared to KPC mice
- Significant increase in the amount of CX3CL1 in the tumour and in the plasma of CKPC mice
- Significant increase in the amount of IL-10 in CKPC mice compared to KPC mice

- KPC and CKPC mice treated for two weeks with gemcitabine have no difference in immune infiltration.

4.11 Conclusion

Briefly, this chapter compares the TME between KPC and CKPC mice. In particular, I looked at the survival, the immune infiltration and the production of cytokines and chemokines in both KPC and CKPC mice. The results obtained showed that the lack of CX3CR1 caused subtle in the TME. Finally, I analysed the effects of chemotherapy on immune infiltration into the TME. In order to better understand these results RNA sequencing of KPC and CKPC mice was performed and it will be analysed in the next chapter.

Chapter 5 RNA sequencing of KPC and CKPC tumours

5.1 Introduction

In Chapter 4, I compared different aspects of the TME of KPC and CKPC mice. My results showed that the lack of CX3CR1 caused a significant decrease of $CD3^+$ T cells and increase of IL-10 in the TME. To further understand what caused these changes I decided to perform RNA sequencing on KPC and CKPC tumour samples. I chose to use RNA sequencing because it is a method that would allow analysis of the entire transcriptome, enabling the identification of pathways or genes that were altered when CX3CR1 was not expressed in the TME.

In the RNA sequencing experiment, I compared six CKPC tumour samples with seven KPC tumour samples. The RNA transcriptome from KPC samples was previously obtained by postdoc Dr Juliana Candido. I performed the RNA extraction from the CKPC tumour samples. All tumours were processed at end point and the same analysis pipeline was applied to all sequencing data.

5.2 RNA quality

RNA was extracted from 6 CKPC frozen tumours, collected from end point mice and kept at -80°C until RNA extraction was performed. Table 5.1 summarises the characteristics of each mouse from which the tumour was harvested.

Mouse	Sex	Age (days)
CX3CR1 _K01	Female	98
CX3CR1 _K02	Female	193
CX3CR1 _K03	Female	116
CX3CR1 _K04	Female	165
CX3CR1 _K05	Female	143
CX3CR1 _K06	Male	134

Table 5.1 Characteristics of mice used for RNA sequencing
Table showing the sex and age of each mouse used for the RNA sequencing experiment. Mice were sacrificed at end point. Harvested tumours were snap frozen and kept at -80°C until RNA extraction performed.

RNA integrity was measured using an Agilent RA 6000 nano kit on the Agilent RNA 2100 Bioanalyzer. The software analyses integrity and quality of the RNA in the samples, giving an RNA integrity number (RIN). RIN values range from 1 to 10, reflecting complete RNA degradation (RIN = 1) to high quality, intact RNA (RIN = 10). Figure 5.1 illustrates the results of Agilent analysis on CKPC samples. The quality of RNA was acceptable for further analysis. RIN numbers for the control KPC samples were > 7 and these samples were also taken at end point (data from Dr Juliana Candido).

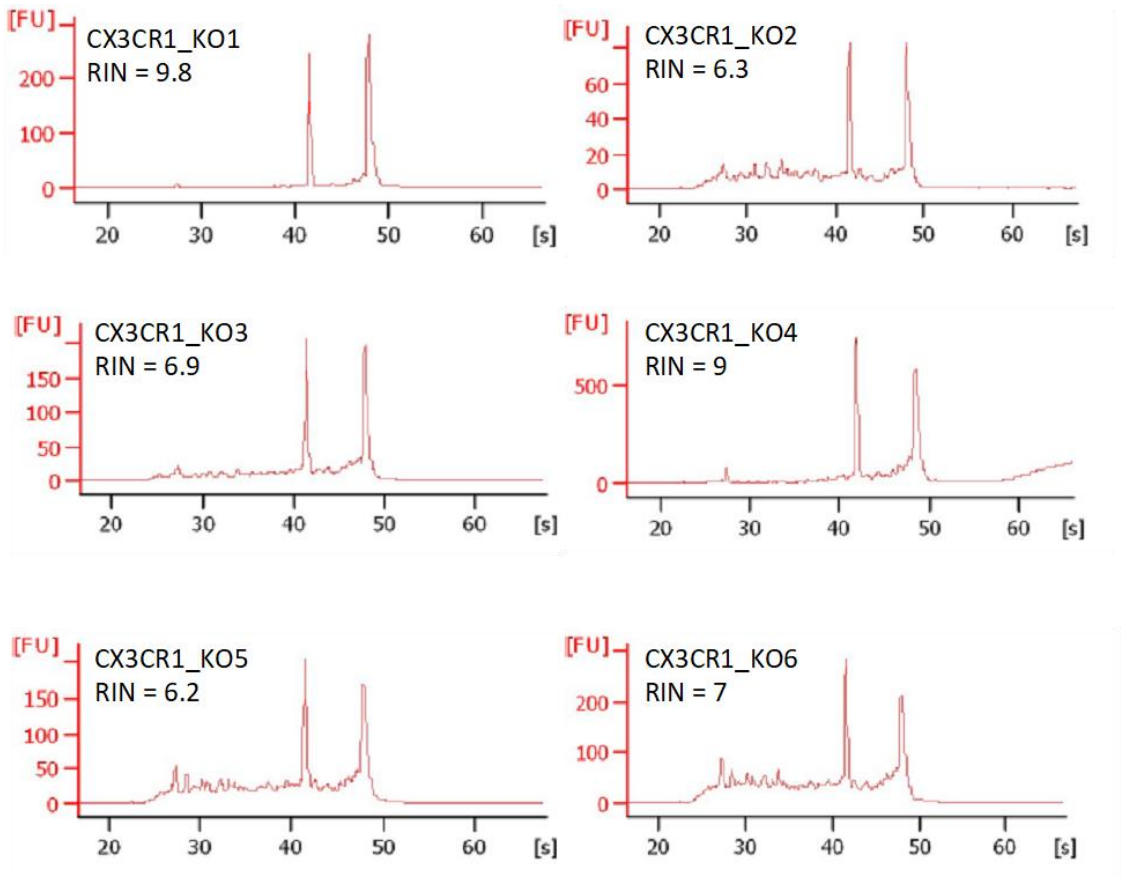

Figure 5.1 RNA quality
RNA profiles using an Agilent RA 6000 nano kit for the six CKPC tumour samples which were sent for RNA sequencing. Each peak represents one of the ribosomal subunits, 18S 28S, respectively. RIN is calculated as the ratio of 18S to 28S subunits. The RIN is shown for each sample. CX3CR1_KO = CKPC.

5.3 Analysis of gene expression composition

All the bioinformatics analysis was performed by Dr Eleni Maniati, a senior postdoctoral fellow in our laboratory, and Dr Ai Nagano from our Bioinformatics Core. The KPC samples were named KPC1-7, while the CKPC samples were named CX3CR1 _KO1-6.

In total 16,388 genes were sufficiently quantified. Among these, 13,817 were protein-coding genes, accounting for the 84% of the transcriptome (Figure 5.2). Pseudogenes, segments of DNA related to real genes that have lost functionality in cellular gene expression or protein-coding ability, represented 5% of total genes (Figure 5.2).
4% of genes were predicted genes with no experimental validation up to date. These genes are transcribed genomic regions potentially representing novel genes, but which need to be confirmed in the laboratory. 2% of total genes were long intergenic non-coding RNA (LincRNA). Linc RNA are a subset of long non-coding RNAs (lncRNAs), containing more than 200 nucleotides with no coding potential, which do not overlap with any known protein-coding genes.

Antisense RNA, processed transcript and immunoglobulin/T cell receptor (IG/TR) genes each accounted for 1% of total genes. Antisense RNAs are single-stranded RNA species, complementary to messenger RNAs (mRNAs). Processed transcripts are non-coding RNA that does not contain an open reading frame (ORF). IG genes codify for B cell receptor or antibody while TC genes codify for the T cell receptors. Finally, the remaining 2% of genes grouped other non-coding RNA species, such as sense intronic, miRNA and ribozyme.

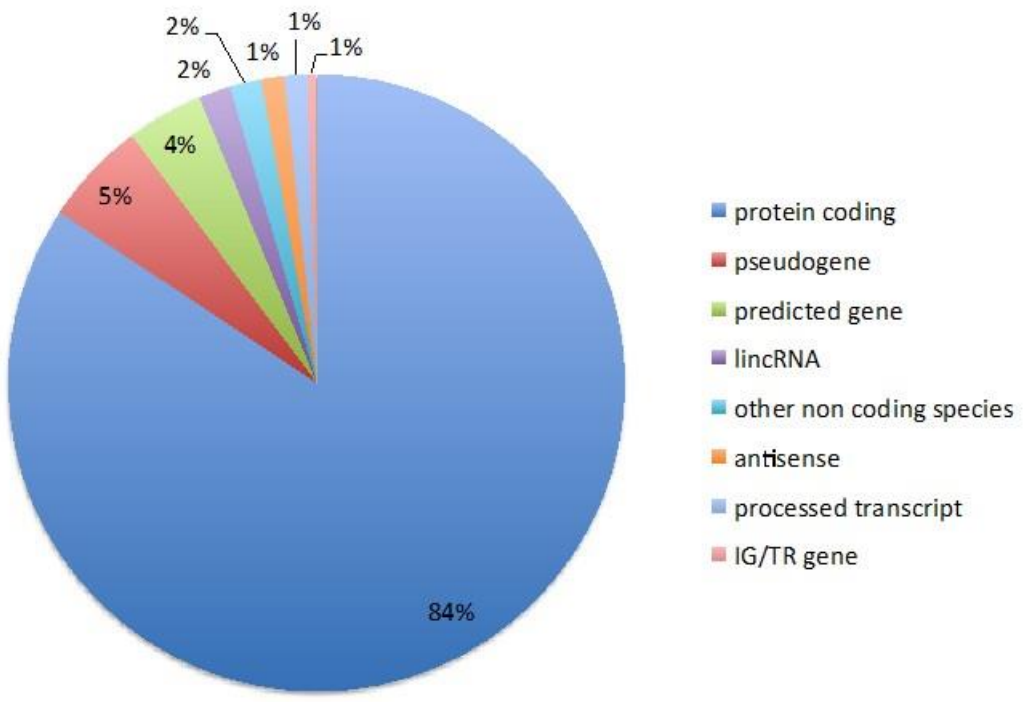

Figure 5.2 Gene species in the dataset
Pie chart showing the distribution of mapped reads to different transcript types and gene regions. IG=immunoglobulin, TR= T cell receptor.

Next, I looked at the classification of protein-coding genes generated by Panther tool. As shown in Figure 5.3 more than 1500 genes belonged to the nucleic acid binding subgroup. I also observed that protein-coding genes codifying for receptor, signalling molecule, cytoskeletal and defence/immune protein were highly present in our dataset.

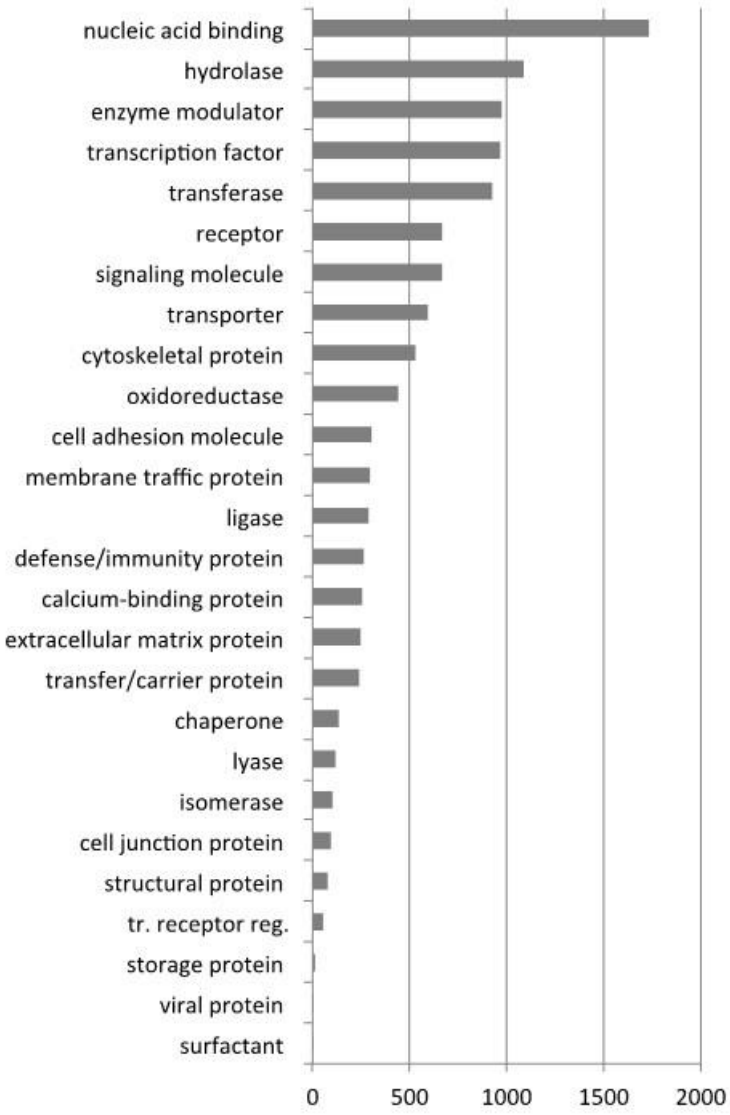

Figure 5.3 Classification of protein coding genes
Bar chart showing the protein class ontology enrichments of protein-coding genes using the Panther tool. The graph displays also the number of proteins (count) identified for each protein class.

5.4 Principal component analysis

Principal component analysis (PCA) is a dimensionality reduction and unsupervised clustering method. PCA allows identification of the relative relationship between each sample in 2 or 3-dimensional coordinate space in order

to visualize sample-to-sample distances. PCA uses linear combinations of the original data to define a new set of unrelated variables (principal components).

The results obtained performing PCA confirmed that our samples clustered in two separated groups, representing the KPC and CX3CR1_KO (CKPC) genotype (Figure 5.4).

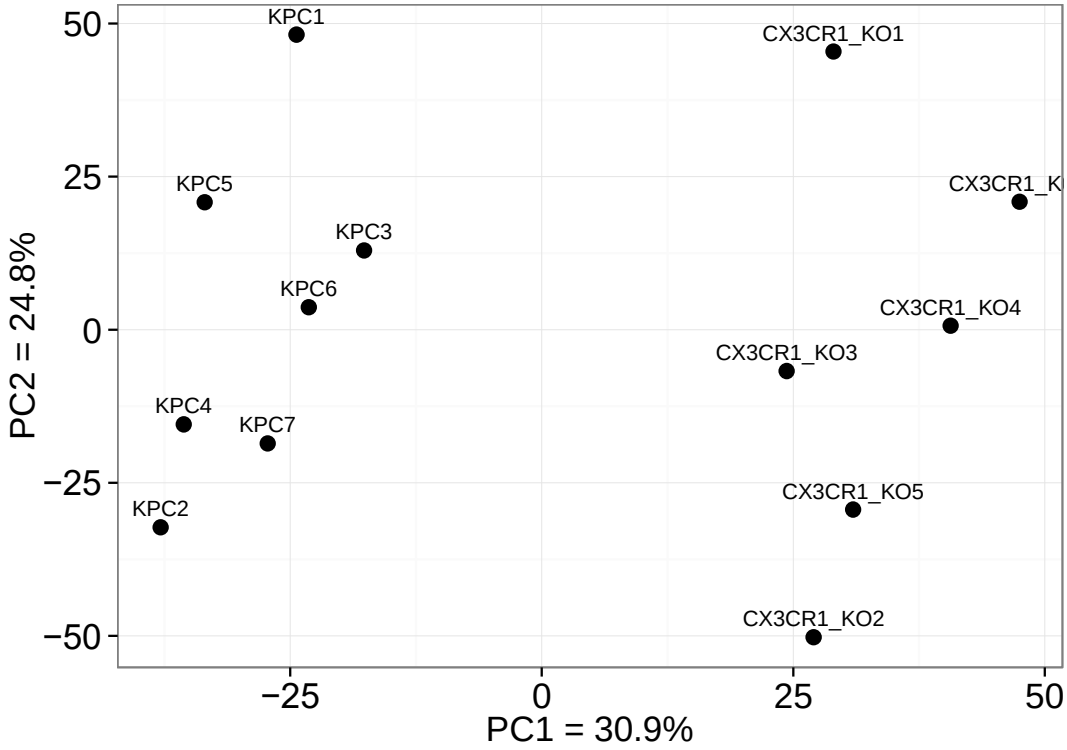

Figure 5.4 Principal component analysis
The graph shows how our 13 samples from KPC and CKPC tumours cluster using principal component analysis (PCA). The x-axis is the direction that separates the data points the most (PC1) and accounts for 30.9% of the variance in the data. The y-axis is a second direction that separates the data most (PC2) and accounts for 24.8% of the variance. CX3CR1_KO= CKPC.

5.5 Differential expression analysis

Differential expression analysis allows identification of genes significantly different between two or more conditions. Using a threshold of adjusted p-value < 0.05 and fold change > 2 ($log_2FC > |1|$) 607 differentially expressed genes were

identified, of which 368 genes were downregulated, while 239 genes were upregulated in CKPC tumour samples compared to KPC (Figure 5.5).

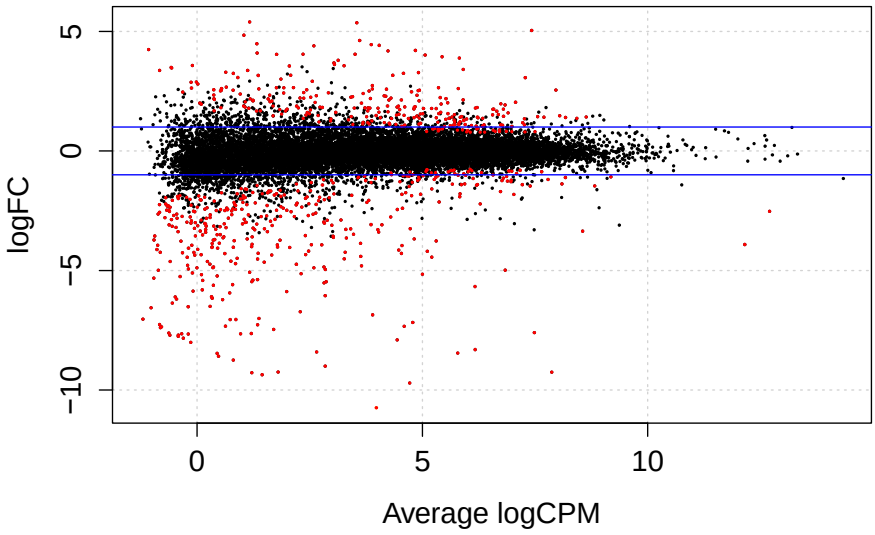

Figure 5.5 Differential expression analyses of KPC and CKPC tumour samples
Visualization of the comparison of transcript expression profiles between KPC and CKPC tumour samples to identify differentially expressed genes. Scattered dot plot illustrating average expression (log counts per million, CPM) vs $\log_2$ fold change. Blue line illustrates $\log_2$FC = 1 and -1.

Next, to visualise the differentially expressed (DE) genes within each sample a heat-map graph was generated. A heat-map is a graphical representation of the gene expression values for each of the 607 genes. Expression values are represented by colours, upregulated genes in CKPC tumour samples were represented in red while green indicated downregulated genes in CKPC tumour samples (Figure 5.6).

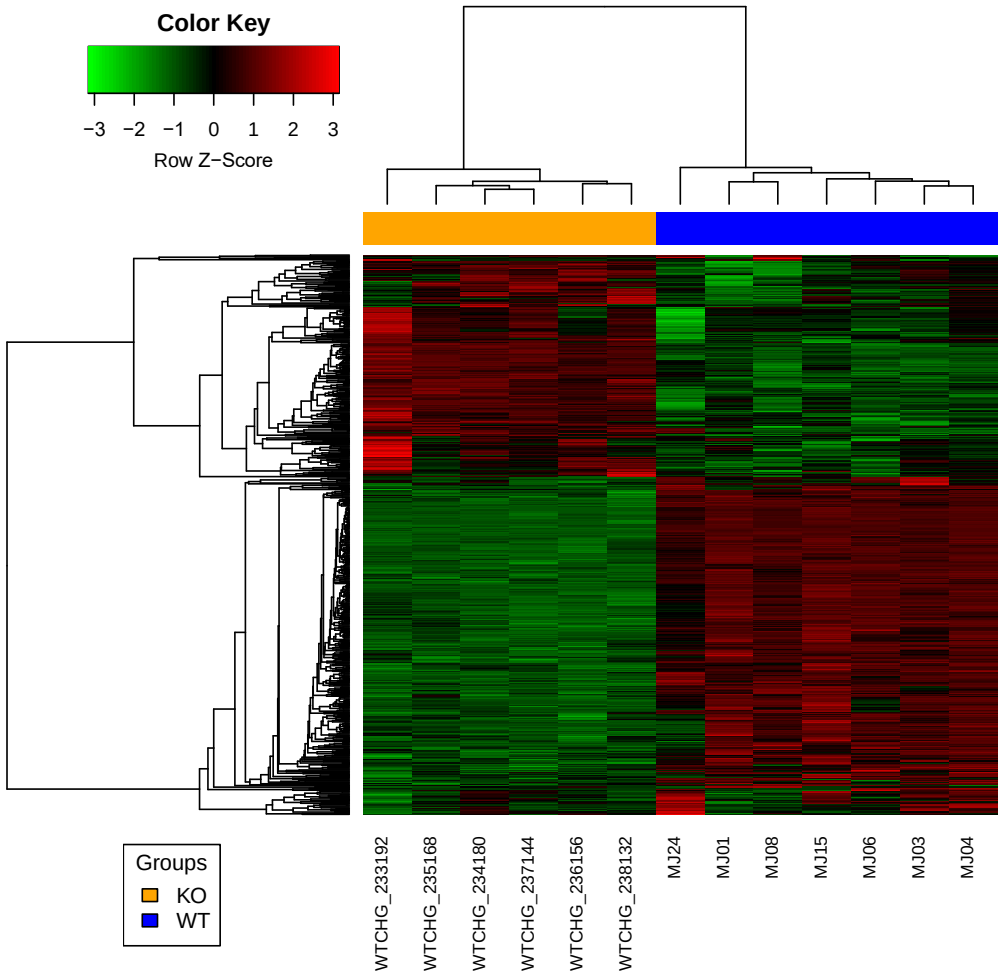

Figure 5.6 Heat-map of the differential expressed genes
Hierarchical clustering heat-map of the 607 differentially expressed (DE) genes with log2FC > |1| and adj. p-value < 0.05. Each column represents one tumour sample, each row represents a single gene. Red represents upregulated genes while green indicates downregulated genes in CKPC compared KPC tumour samples. WTCHG = CKPC samples, MJ = KPC samples.

Of the 607 DE genes only 212 were protein-coding genes, of which 75 were downregulated while 137 were upregulated in CKPC compared KPC tumour samples (Figure 5.7).

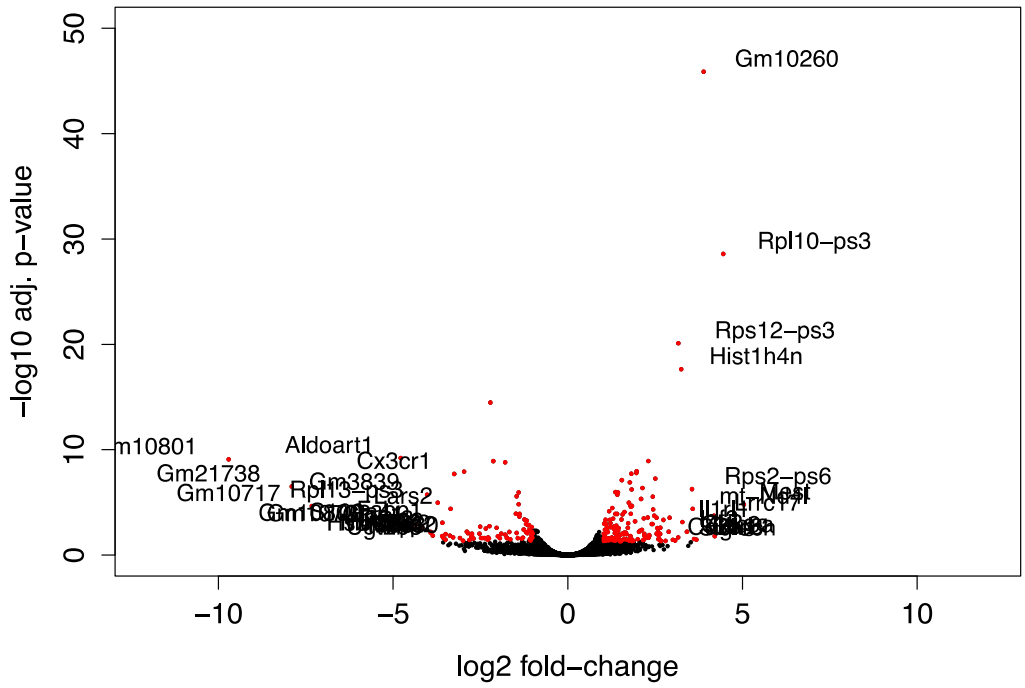

Figure 5.7 Volcano plot of protein-coding genes
Visualization of the comparison of transcript expression profiles between KPC and CKPC tumour samples to identify differentially expressed genes. Volcano plot illustrating $\log_2$ fold change vs –log10 adj. P-value. Coloured in red are differentially expressed genes (adj. p-value < 0.05 and log2FC > |1|)

5.5.1 Analysis of DE protein coding genes

I next examined the classification of the DE protein-coding genes. Genes coding for nucleic acid binding proteins represented the majority of differentially expressed genes (Figure 5.8), in line with the abundance in the entire transcriptome (Figure 5.3).

Approximately 50 DE genes encoded enzymes such as oxidoreductase, hydrolase, transferase, ligase and lyase. Interestingly, although defence/immunity proteins accounted for just eleven genes, six of them were in the top 20 down- and upregulated genes and will be further discussed below.

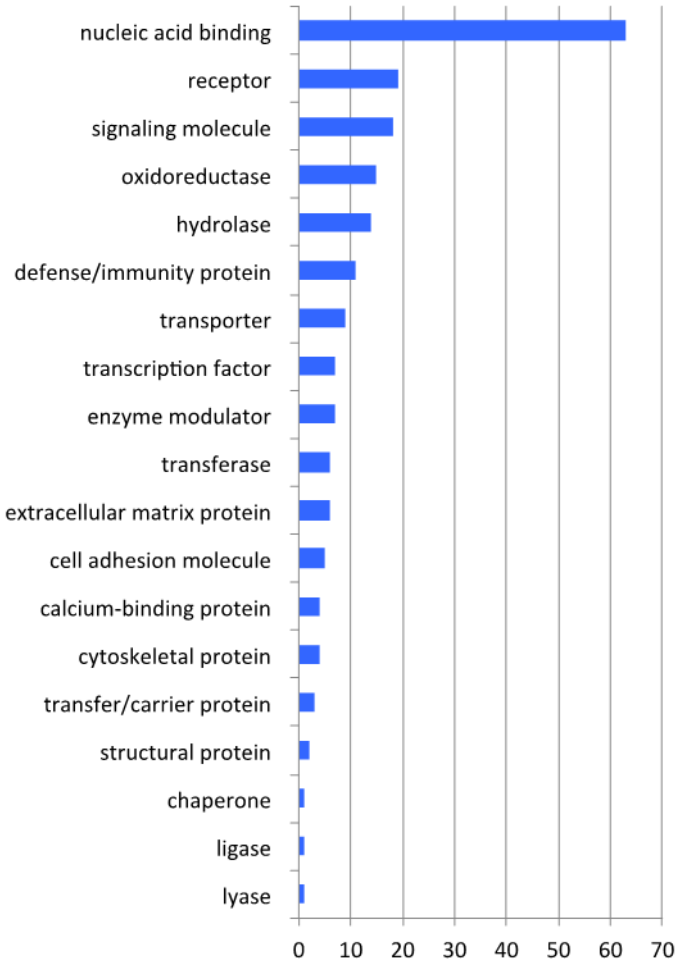

Figure 5.8 Classification of DE protein-coding genes
Bar chart showing the protein class of DE genes using the Panther bioinformatics tool. The graph displays also the number of proteins (count) identified for each protein class.

Subsequently, I also examined which gene ontology biological processes are associated with the DE protein coding genes. Figure 5.9 lists the biological processes of the DE genes. As expected the most common set of genes identified by gene ontology were those involved in cellular process (112 genes). Also of interest, 98 genes were metabolic genes and five DE genes were related to locomotion.

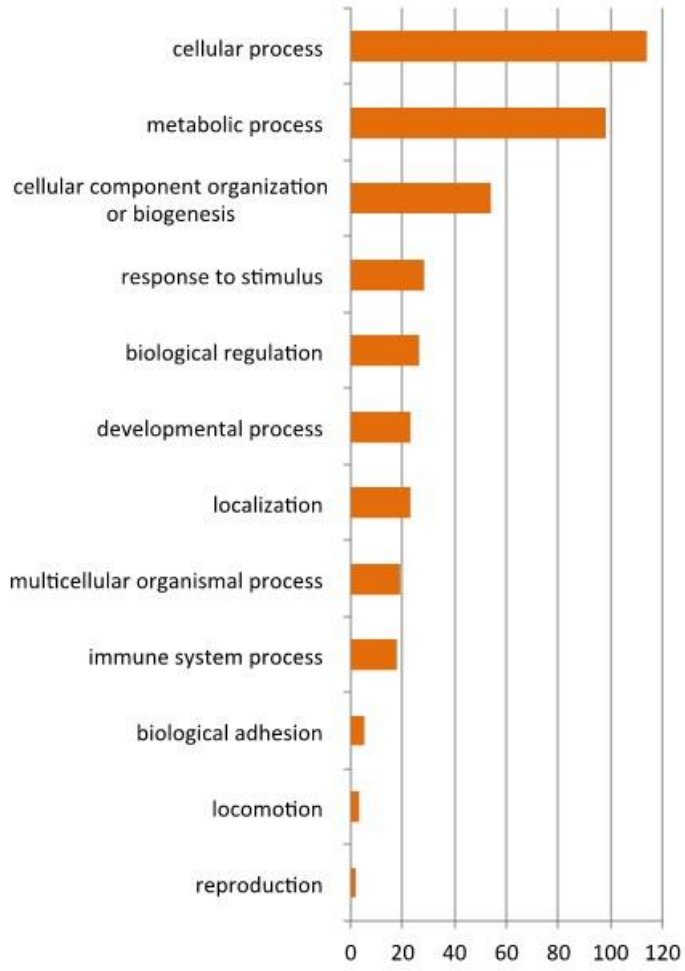

Figure 5.9 Classification of DE protein-coding genes in Gene Ontology biological process
Bar chart showing the gene ontology biological process classification of DE genes using the Panther bioinformatics tool. The graph displays also the number of proteins (count) identified for each biological process.

5.5.2 Top differentially expressed genes

Figure 5.10 shows the top 20 genes downregulated in CKPC compared to KPC tumours, with fold-change illustrated on a $\log_2$ scale. *Cx3cr1* was one of the most downregulated genes, confirming the targeted genetic disruption of *Cx3cr1* in CKPC mice (Figure 5.10 and 5.11A).

The top downregulated gene was *Aldoart1* with approximately a 10-fold change in expression. This gene encodes for an enzyme of the glycolysis pathway illustrating a potential link of *Cx3cr1* with metabolism (Vemuganti, Bell et al. 2007).

Interestingly, some of the most downregulated genes such as *Nlrp10* and *Cd300ld3,* play a role in the regulation of innate immunity. *Nlrp10* is a member of the NLR protein family, a class of pattern recognition receptor. It plays a regulatory role in the innate immune system, being part of the inflammasome. It is expressed by monocytes, macrophages, DCs, neutrophils, $CD4^+$ T and B cells (Damm, Lautz et al. 2013). *Cd300ld3* encodes for the CMRF35-like molecule 3 protein belonging to the Ig superfamily. It is an activating receptor and it is expressed on macrophages and mast cells and plays a role in cytokine production by regulating TLR9 signalling (Wu, Zhu et al. 2011).

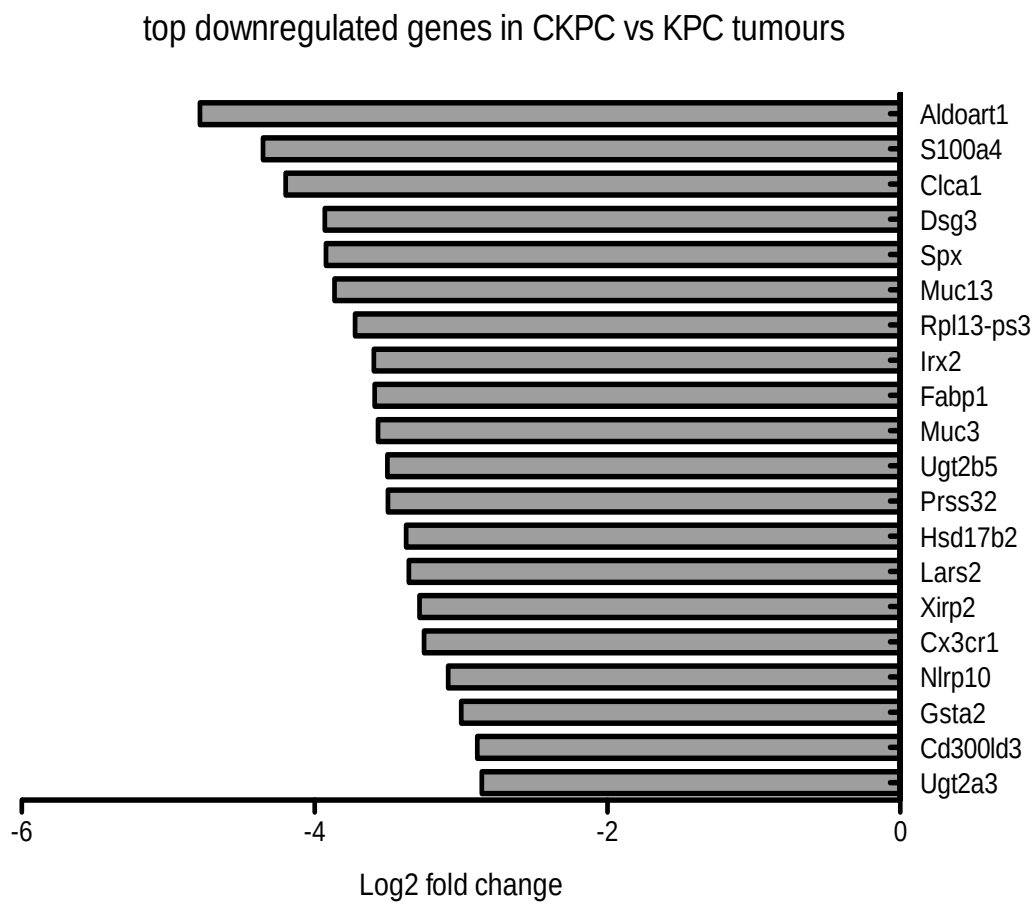

Figure 5.10 Top downregulated genes in CKPC vs KPC tumours
Bar chart showing the top 20 genes that were downregulated in CKPC tumours vs KPC tumours. Values shown as Log2 fold changes.

Furthermore, among the top downregulated genes I found *S100a4,* a calcium binding protein (Figure 5.10 and 5.11B). S100a4 shows no enzymatic activity but exerts its biological function via the interaction with the target proteins. It is

expressed by fibroblasts, immune cells, and cancer cells and is released into the extracellular space in response to various stimuli. S100a4 regulates several cellular processes, such as proliferation, motility, invasion, and tubulin polymerization. Over-expression of S100a4 has been associated with several malignancies, among which pancreatic, breast and lung cancers (Fei, Qu et al. 2017).

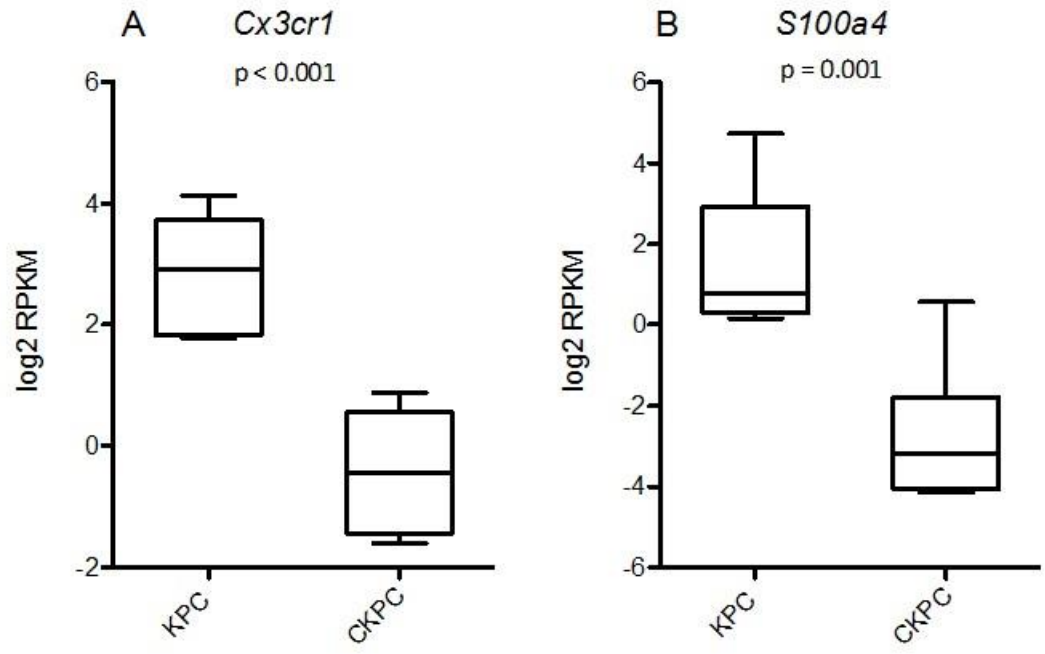

Figure 5.11 Gene expression of *Cx3cr1* and *S100a4*
Boxplots illustrating *Cx3cr1* and *S100a4* gene expression in KPC and CKPC tumours. Values shown as Log2 fold changes and adj. p-value < 0.05.

Using the same criteria, I identified the top 20 up-regulated genes in CKPC compared to KPC tumours, shown in Figure 5.12. The top up-regulated gene was *Mest* coding for Mesoderm-specific transcript homolog protein, a hydrolase associated to the endoplasmic reticulum expressed in foetal tissues and also in lymphocytes (Kosaki, Kosaki et al. 2000).

Igf2, Insulin like growth factor 2, is upregulated more than six-fold in CKPC compared KPC tumours. It is a member of the insulin family of polypeptide growth factors; it has growth-promoting activity and has been associated with cancer (Brouwer-Visser and Huang 2015).

Again, I found that several upregulated genes play a role in the regulation of the immune system, such as *Il1r1*, *Clec9a*, *SiglecH* and *CD5l*. *Il1r1*, Interleukin 1 Receptor Like 1, is a member of the interleukin 1 receptor family and is a mediator involved in inflammatory responses (Schett, Dayer et al. 2016). *Clec9a* is a C-type lectin-like receptor expressed on DCs, involved in the cross-presentation of antigens from dead cells (Macri, Dumont et al. 2016). *Cd5l,* CD5 antigen-like, it is a soluble protein belonging to the SRCR superfamily. It is mostly expressed by macrophages and regulates mechanisms in inflammatory responses (Sanjurjo, Aran et al. 2015). *SiglecH* is a member of the Siglec family which are cell surface immunoglobulin-like lectins that bind sialic acid. It is expressed by pDCs and mediates endocytosis and cross-presentation of antigens (Crocker, Paulson et al. 2007).

Among the most upregulated genes, three were pseudogenes, *Rpl10-ps3*, *Rps2-ps6* and *Rps12-ps3*. All of these pseudogenes were ribosomal proteins.

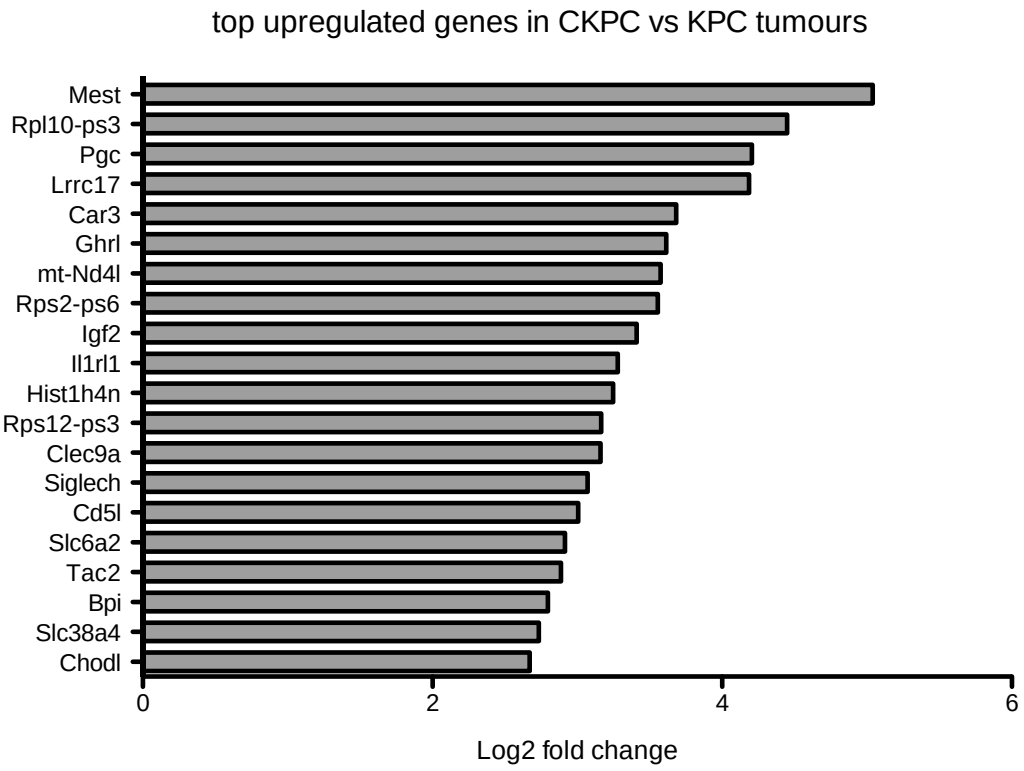

Figure 5.12 Top upregulated genes in CKPC vs KP tumours

Top 20 genes that were upregulated in CKPC tumours vs KPC tumours. Values shown as Log2 fold changes and adj. P-value <0.05.

5.5.3 Immune system related genes

As illustrated in Chapter 4, the differences I observed between the TMEs from KPC and CKPC mice were related to the immune system. For this reason, I looked into the DE genes in order to find changes able to explain the differences between KPC and CKPC mice.

First of all, I found that the lack of CX3CR1 in pancreatic tumours led to the differential expression of two chemokines. The chemokines that were differentially expressed were Cxc*l*10 and *Cxcl12*, both upregulated in CKPC mice compared to KPC mice (Figure 5.13). CXCL10 is secreted by monocytes, endothelial cells and fibroblasts and is involved in the recruitment of monocytes, T cells and NK cells (Figure 5.13A) (Liu, Guo et al. 2011). CXCL12, also known as stromal cell-derived

factor 1 (SDF-1), is produced in response to proinflammatory stimuli, such as TNF and IL-1. It plays a role in the migration of T lymphocytes and monocytes (Figure 5.13B) (Karin 2010).

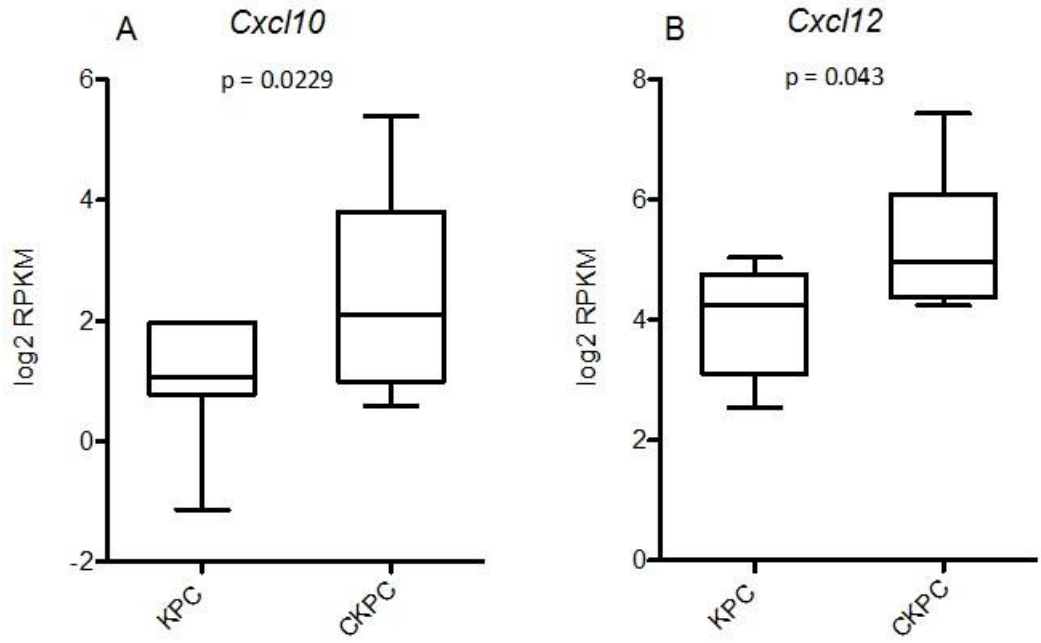

Figure 5.13 Differentially expressed chemokines
Boxplots illustrating *Cxcl10* and *Cxcl12* gene expression in KPC and CKPC tumour. Values shown as Log2 fold changes and adj. p-value < 0.05.

I also observed DE genes that are part of the transcription factor family, *Gata*3 and *Cebpb* (Figure 5.14). Both these transcription factors are expressed by immune cells and are downregulated in CKPC mice compared to KPC mice. Gata-3 (GATA Binding Protein 3) regulates T cell development and induces the differentiation towards T helper 2 (Th2) cells during inflammatory responses (Figure 5.14A) (Wan 2014). C/ebp-β (CCAAT/enhancer-binding protein beta) it is important for macrophage activation and function, regulating M2-associated genes (Figure 5.14B) (Huber, Pietsch et al. 2012).

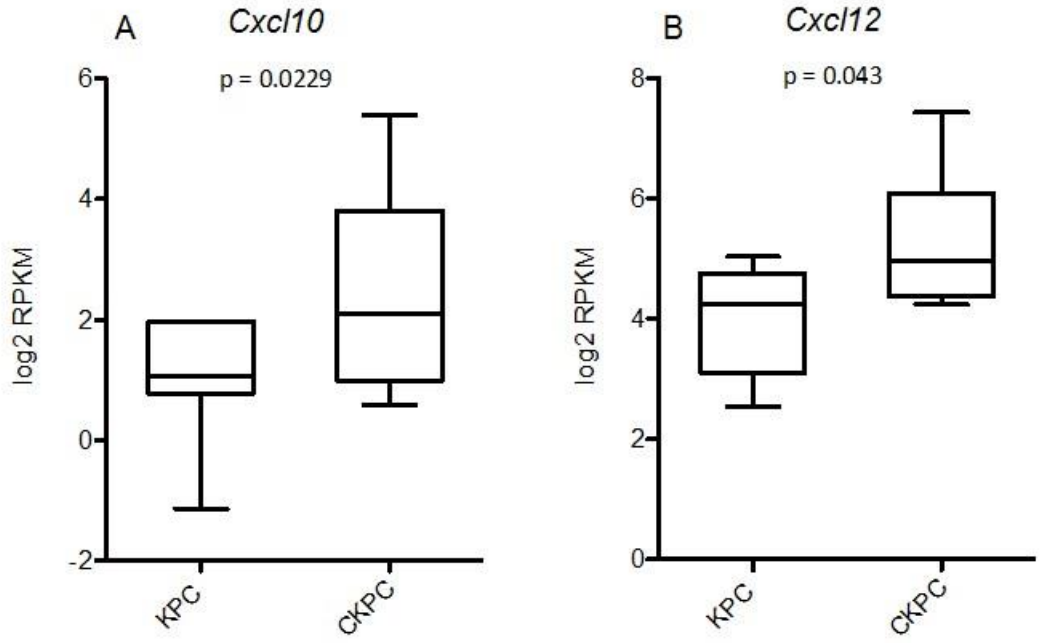

Figure 5.14 Differentially expressed transcription factors
Boxplots illustrating *Gata3* and *Cebpb* gene expression in KPC and CKPC tumour. Values shown as Log2 fold changes and adj. p-value < 0.05.

5.6 Tumour content of the samples

I next examined epithelial malignancy-associated genes *Pdx1*, *Epcam* and *Cdh1* in KPC and CKPC samples and I found no difference (Figure 5.15). This indicated that in KPC and CKPC tumours the malignant component is equal and agrees with the data shown in Chapter 4.

Pdx1 (Pancreatic and duodenal homeobox 1) is a transcription factors that plays an important role in pancreatic development and is expressed by epithelial cells and β-cells, as well in PDAC cells (Figure 5.15A). *Epcam* (Epithelial cell adhesion molecule) is a transmembrane glycoprotein mediating cell–cell adhesion in epithelial cells. It is expressed on most normal epithelial cells and gastrointestinal carcinomas, such as PDAC (Figure 5.15B). Cdh1 (E-cadherin) is a classical member of the cadherin superfamily and it is involved in cell-cell adhesion. It is expressed in many cancers, including PDAC (Figure 5.15C).

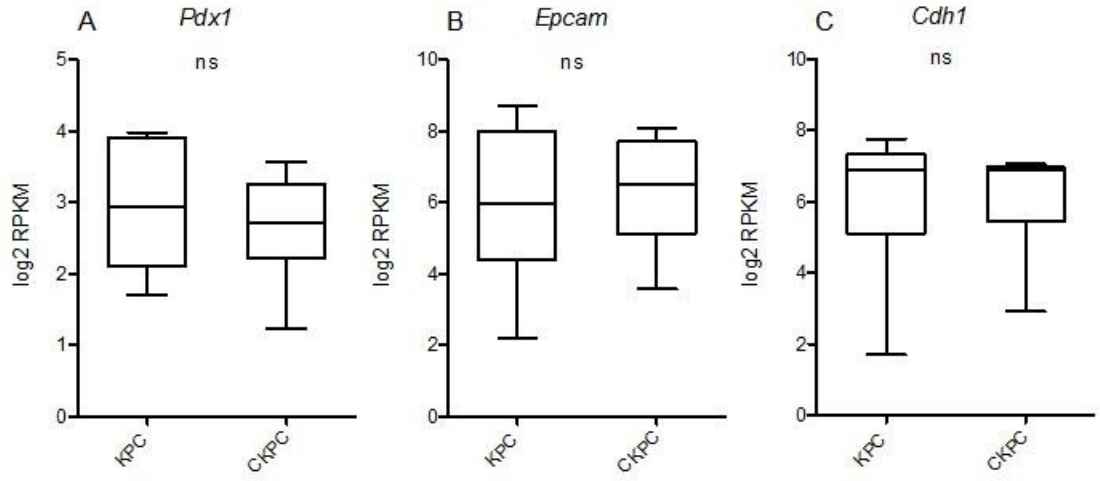

Figure 5.15 Tumour content level
Boxplots illustrating *Pdx1, Epcam* and *Cdh1* gene expression in KPC and CKPC tumours. Values shown as Log2 fold changes. ns: not significant.

5.7 Discussion

The lack of CX3CR1 in pancreatic cancer induced subtle changes in the TME, as shown in Chapter 4, but did not affect overall survival of mice or response to gemcitabine. Likewise, the analysis of the RNA sequencing experiment revealed only 607 differentially expressed genes, of which 368 genes were downregulated and 239 genes were upregulated, between KPC and CKPC tumours.

In order to exclude potential batch effects in the data arising from sequencing the samples on two separate RNAseq runs I examined expression of the tumour-associated genes, *Pdx1*, *Epcam* and *Cdh1* (Figure 5.15). As expected, there was no significant difference in their expression in KPC and CKPC tumours, which confirmed same tumour content and discounted the presence of batch effects in the data. On the other hand, there was a significant reduction in expression of *Cx3cr1* in CKPC mice (Figure 5.11A), which confirmed the genetic disruption of the *Cx3cr1* locus.

The analysis of KPC and CKPC tumour samples identified 16,388 filtered genes, among which, 13,817 were protein-coding genes. I identified 212 differentially

expressed protein–coding genes, of which 75 were downregulated while 137 were upregulated in CKPC compared KPC tumour samples.

The analysis of the DE protein-coding genes using either Panther protein classification or gene ontology biological process indicated that several DE genes encoded for immune system and chemotactic proteins (Figure 5.7 and 5.8, respectively). In particular, using the Panther protein classification, I observed that the lack of CX3CR1 induced the differential expression of receptors, signalling molecules, defense/immunity protein, cell adhesion and cytoskeletal proteins (Figure 5.8). Similarly, among the gene ontology biological process, I identified: response to stimulus, immune system process, biological adhesion and locomotion (Figure 5.9).

Data presented in Chapter 4 indicated a decrease in the frequency of $CD3^+$ T cells in CKPC compared to KPC mice (Figure 4.7). Interestingly, I observed several DE genes involved in T cell regulation and chemotaxis, among which *Gata-3, S100a4,* were downregulated*, Cxcl10* and *Cxcl12,* were upregulated. Gata-3 is a transcription factor that regulates T cell differentiation, being the master regulator of Th2 (Ho, Tai et al. 2009). Our results revealed that *Gata3* is downregulated in CKPC compared KPC tumours (Figure 5.14A). Gata-3 is necessary for $CD8^+$ T cell growth and proliferation upon activation. Lack of Gata-3 not only impairs Th2 differentiation, but also impairs $CD4^+$ (Ho, Tai et al. 2009, Wan 2014) and $CD8^+$ T cell proliferation upon TCR and cytokine stimulation (Wang, Misumi et al. 2013, Wan 2014). The lack of proliferative T cells might explain the decrease of T cells in CKPC mice.

I also observed a decrease in *S100a4*, which is a member of the S100 family of Ca^{2+}-binding proteins. S100a4 is expressed by various normal cell populations, including fibroblasts, monocytes, macrophages, granulocytes, T and endothelial cells and it is localized in the nucleus, cytoplasm, and the extracellular space (Boye and Maelandsmo 2010). Moreover, S100a4 is expressed in many human cancers, and is correlated with poor prognosis and increased metastasis formation (Fei, Qu et al. 2017). Interestingly, S100a4 plays a role not only in inducing metastasis but

also in T cells migration into the tumour (Grum-Schwensen, Klingelhofer et al. 2010, Klingelhofer, Grum-Schwensen et al. 2012). They found that the lack of S100a4 impaired the migration of $CD3^+$ T cells into the tumour (Grum-Schwensen, Klingelhofer et al. 2010). They also found that, *in vitro*, S100a4 promotes $CD3^+$ T cell migration which is blocked by the treatment with an anti-S100a4 antibody (Grum-Schwensen, Klingelhofer et al. 2010). I*n vivo* the anti-S100a4 treatment blocked the recruitment of T cells into the tumour (Klingelhofer, Grum-Schwensen et al. 2012). These data propose the role of S100a4 as an attractant of $CD3^+$ T cells into the tumour, which could explain the decrease in $CD3^+$ T cells I observed in KPC mice.

CXCL12 is expressed constitutively by various cell populations, such as fibroblasts and endothelial cells, and tissues, among which bone marrow and cardiac tissue. It binds to two different receptors, CXCR4 and CXCR7, which mediate different functions (Karin 2010). CXCR4 is expressed on most hematopoietic cell types, including macrophages, monocytes, T and B lymphocytes, neutrophils and DCs, regulating their trafficking in and out peripheral tissues. The role of the CXCL12-CXCR4 axis in tumour progression has been studied and has been associated with enhanced tumour cell survival, proliferation, and metastasis, as well as with immune cell chemotaxis. (Sun, Cheng et al. 2010). Of interest is the role of CXCL12 in regulating the $CD3^+$ T cell infiltrates into the TME. In fact, a study by Feig et al. showed that in pancreatic tumours the binding of CXCL12 to cancer cells inhibited the migration of T cells into tumour area of the TME (Feig, Jones et al. 2013). Moreover, the administration of a CXCR4 inhibitor induced the accumulation of T cells into the tumours and reduced cancer cells (Feig, Jones et al. 2013, Guo, Wang et al. 2016). Therefore, the increase in *Cxcl12* expression (Figure 5.13B) could represent another possible mechanism responsible for the decrease in $CD3^+$ T cells.

On the other hand, I also observed the upregulation of *Cxcl10* (Figure 5.13A). CXCL10, like CXCL12, mediates chemotaxis of T cells and other immune populations into inflamed site. CXCL10 is expressed under proinflammatory condition by neutrophils, eosinophils, monocytes, epithelial, endothelial and stromal cells. Its receptor CXCR3 is expressed on macrophages, DCs, NK cells and

activated $CD4^+$ and $CD8^+$ T lymphocytes. The CXCL10-CXCR3 axis mediates several functions, such as chemotaxis, apoptosis, cell growth and proliferation (Liu, Guo et al. 2011). Notably, CXCR3 is absent on naïve T cells, but is upregulated following DC-induced T-cell activation (Groom and Luster 2011).

N*lrp10*, member of the NLRs family of cytosolic proteins, is expressed by several immune cells, among which T cells, macrophages and DCs and is involved in regulating the immune system and inflammation (Damm, Lautz et al. 2013). Interestingly, a study by Eisenbarth et al. demonstrated that lack of Nlrp10 prevents the migration of DCs from the site of the infection to the draining lymph nodes, preventing the priming and activation naive $CD4^+$ T cells (Eisenbarth, Williams et al. 2012). I observed downregulation of *Nlrp10* in CKPC mice which could indicate that DC-mediated T cell activation is impaired. Notably, CXCR3 upregulation, the CXCL10 receptor, occurs following DC-induced T cell activation. Therefore, if $CD4^+$ cells are not activated by DC cells, they are unable to respond to the CXCL10 gradient present into the tumour.

The infiltration of each immune cell population into the TME is mediated primarily the binding of cytokines and chemokines to their receptors, and subsequent activation or inhibition of signalling pathways or transcription factors. As mentioned above, I observed a decrease in $CD3^+$ T cells into the TME of CKPC mice (Figure 4.7). The results obtained by the RNA sequencing analysis indicated some factors which could be responsible for it. The changing in the expression of *Cxcl12*, *Gata3*, *S100a4* and *Cxcl10* together with *Nlrp10*, either individually or combined, could promote changes in T lymphocytes or in the TME which prevented $CD3^+$ T cells access into the tumour.

I further observed that *Cebpb* was downregulated in CKPC mice compared KPC mice (Figure 5.14B). C/ebp-β is a transcription factor, which plays a role in the regulation of innate immunity, inflammation, metabolism and adipogenesis (Huber, Pietsch et al. 2012). In addition, C/ebp-β, has important roles in myeloid development and activation of macrophages, the most abundant cell population in PDAC. A study by Ruffell et al. showed that C/ebp-β was involved in the regulation

of M2-associated genes, such as *Arg1*, *Il10* and *Mrc1.* Notably, to promote M2-associated genes C/ebp-β has to be induced by another bZIP family transcription factor, the cAMP-responsive element-binding protein (Creb) (Ruffell, Mourkioti et al. 2009, Lawrence and Natoli 2011). However, *Creb*, as well as the M2 genes *Arg1* and *Mrc1*, were not among the DE genes. Moreover, sorted F4/80^{+} macrophages from KPC and CKPC tumours showed no difference in the amount of *Arg1* and *Il10* mRNA (Figure 4.11), suggesting that the lack of CX3CR1 does not promote a M2 phenotype in macrophages.

Ccl2, Ccr2, Csf1 and Csf1r are major regulators of macrophage survival and chemotaxis. There was no difference in expression of the genes encoding for these proteins in KPC and CKPC tumours. This result confirmed qRT-PCR data presented in Chapter 4 (Figure 4.8) whereby expression of *Ccl2*, *Csf1* and *Csf1r* again showed no difference between KPC and CKPC tumours. Furthermore, there was no difference in the frequency of tumour infiltrating F4/80^{+} cells (Figure 4.6). Together these data suggest that CX_3CR_1 deletion does not impact the recruitment of these cells in pancreatic cancer.

Almost half of DE genes belonged to the GO term that refers to metabolic processes (Figure 5.8). Interestingly, a link between CX3CR1 and metabolism has already been reported in literature (Ren, Zhao et al. 2013, Polyak, Ferenczi et al. 2014, Shah, O'Neill et al. 2015). In particular, Ren et al. found that CX3CL1/CX3CR1 axis reprograms glucose metabolism in PDAC. In their study, CX3CL1 induced glucose uptake and lactate secretion in pancreatic cancer cell lines, which was mediated by Hif-1 expression (Ren, Zhao et al. 2013). However, I did not observe a change in the expression of *Hif1* between KPC and CKPC tumours possibly because in our samples mRNA was extracted from whole tumour masses and not only from tumour cells. My results also revealed the downregulation of genes involved in glucose metabolism. For example, *Aldoart1* (AldoA retrogene 1) was the most downregulated gene in CKPC compared KPC tumours. It encodes for the fructose-bisphosphate aldolase enzyme, which is involved in glucose metabolism (Vemuganti, Bell et al. 2007). I also observed downregulation in genes involved in the electron transport chain, *Ndufa2*, *mt-Co3*, *Etfa* and *Etfb*. The latter two genes

are also involved in fatty acid oxidation. Together these results suggest that the lack of CX3CR1 in PDAC impaired the mitochondrial tricarboxylic acid cycle. PDAC metabolism is known to be highly deregulated, due to the poor vascularization, hypoxic and nutrient deprived TME. In fact, pancreatic tumours are characterized by the glycolytic switch (Warburg effect), upregulation of the hexosamine biosynthetic pathway, activation of lipid metabolism, autophagy and pinocytosis (Cohen, Neuzillet et al. 2015). Therefore, the lack of CX3CR1 seems to further deregulate metabolism in TME of pancreatic cancer.

As mentioned in the introduction to this chapter, the results described were obtained from different two RNA sequencing experiments. Although, the RNA extractions were not performed by the same person nor at the same time, the data showed in this chapter were obtained by analysing the RNA sequencing raw data following the same protocol. In fact, the same expression of tumour content markers together with the lack of expression of *Cx3cr1* in CKPC mice (Figure 5.11A), excludes the presence of batch effects. Moreover, as in Chapter 4, both female and male mice were used in this experiment to obtain the tumour samples.

5.8 Summary

- Identification of 16,388 filtered genes, among which 13,817 were protein coding genes
- 607 DE genes were identified, 368 genes were downregulated in CKPC mice while 239 genes were upregulated in KPC mice
- Identification of 212 DE protein-coding genes; genes that included receptors, signalling molecules, defense/immunity, cell adhesion and cytoskeletal organization.
- Upregulation of *Cxcl10* and *Cxcl12* chemokines in CKPC mice
- Downregulation of *S100a4*, calcium binding protein, and *Gata3* and *Cebpb,* transcription factors, in CKPC mice
- Downregulation of several genes involved in metabolic processes

5.9 Conclusion

In this chapter, I described the results of the RNA sequencing of KPC and CKPC tumours. The results obtained revealed some possible mechanisms which could explain the differences in the TME between KPC and CKPC mice.

Chapter 6 Conclusions and future work

6.1 Conclusion

Pancreatic cancer is responsible for 6% of cancer deaths and its incidence is expected to increase in the next years. Despite the improvements in the survival rate of several cancers, there has been little progress in the treatment of pancreatic malignancy. For this reason, research in PDAC has been focusing in the identification of new therapeutic targets.

In recent years, the role of the chemokine-chemokine receptor axis in cancer has been increasingly investigated (Balkwill 2004, O'Hayre, Salanga et al. 2008, Lazennec and Richmond 2010, Mantovani, Savino et al. 2010, Allavena, Germano et al. 2011, Balkwill 2012, Sarvaiya, Guo et al. 2013, Mukaida, Sasaki et al. 2014, Nagarsheth, Wicha et al. 2017). The role of this axis in tumour progression is complex; besides their role in the recruitment of immune cells, chemokines and their receptors are also involved in tumour cell survival and proliferation, angiogenesis and metastasis formation. For these reasons, chemokine receptors have been considered has potential therapeutic targets.

CX3CL1 and its receptor CX3CR1 are the only members of the CX3C chemokine family. The upregulation of CX3CR1 has been reported in many cancers, prostate (Shulby, Dolloff et al. 2004), breast (Andre, Cabioglu et al. 2006) and pancreatic (Allavena, Germano et al. 2011) (see Figure 1.6). In PDAC, CX3CR1 expression is associated with increased migration and metastasis formation to peripheral nerves, which is known as perineural invasion (PNI) (Marchesi, Piemonti et al. 2008, Marchesi, Locatelli et al. 2010).

In my study I investigated the impact of deletion of CX3CR1 in the tumour microenvironment, focusing on the amount and functions of infiltrating immune cells, inflammation, response to chemotherapy and survival. To do so I used a genetically engineered mouse model of PDAC, the CX3CR1$^{GFP/GFP}$LSL-KRAS$^{G12D/+}$LSL-Trp53$^{R172H/+}$Pdx1-Cre (CKPC) mouse. In these mice, the CX3CR1 protein is not functional and they express GFP instead.

In my study I showed that CX3CR1 has a subtle effect on the shaping of the TME in a mouse model of pancreatic cancer, the KPC model. At a cellular level there was a significant decrease in $CD3^+$ T cells (Figure 4.7) and a possible increase in $CD11b^+$ myeloid cells (Figure 4.6) in the TME. In terms of cytokines and chemokines, there was a significant increase in IL-10 and a possible non-significant increase in TNF-α, and IL-6 (Figure 4.10). Of interest in relation to these cell and protein changes, the RNA-seq analysis showed significant downregulation of *S100a4*, *Nlrp10, Gata3* and *Cebpb* (Figure 5.11 and 5.14) and significant upregulation of *Cxcl10* and *Cxcl12* (Figure 5.13).

However, even though the TME showed these differences, there was no overall survival difference between KPC and CKPC mice. In both mouse models tumours where palpable from three months of age and the mice had a median lifespan of was 119.5 days and 110.6 days (Figure 4.2). On contrast to our results, Celesti et al. found that human PDAC patients with $CX3CR1^+$ tumours had a longer survival compared to $CX3CR1^-$ tumours (Celesti, Di Caro et al. 2013). This discrepancy might be due by the mouse model I used. In fact, in the CKPC mouse model the CX3CR1 expression is altered not only in tumour cells, but in all CX3CR1-expressing cells. They also showed that CX3CR1 expression is an early event during carcinogenesis, being already upregulated in PanIN-1, and it is maintained through tumour progression. They also hypothesise that the association between the better survival and CX3CR1 tumour expression might be only the reflection of an earlier disease stage (Celesti, Di Caro et al. 2013).

The response to chemotherapy was also examined in KPC and CKPC mice. The tumour weight after two weeks of treatment with gemcitabine was comparable between KPC and CKPC mice (Figure 4.14). However, when I looked at the immune cell infiltration into the tumour I found some potential differences. $CD11b^+$ myeloid cells were slightly decreased (Figure 4.15) in CKPC mice while $CD3^+$ cells were increased (Figure 4.16), though not significantly. This might suggest that two weeks treatment was not sufficient to see a difference in tumour growth between chemotherapy-treated KPC and CKPC tumours.

Briefly, my results support that the lack of CX3CR1 is involved in the regulation of the TME in a mouse model of pancreatic cancer. These subtle changes in the TME were anyway not sufficient to alter, neither the lifespan nor response to chemotherapy treatment in mice with pancreatic tumour. These results gain importance considering that CX3CR1 targeting has been postulated for cancer treatment (Zhao, Gao et al. 2012, Ferretti, Pistoia et al. 2014). However, my study suggests that targeting CX3CR1 alone is not sufficient to improve tumour outcome, it does show that the lack of CX3CR1 altered various aspects of the tumour microenvironment, at cell, protein and RNA levels. However, in this work was used a mouse model where CX3CR1 deletion was global, whilst the use of CX3CR1 inhibitor might show different results. In fact, the compensatory mechanisms that might have been induced by the global deletion of CX3CR1 would be avoided by the transit use of an inhibitor.

6.2 Summary of results of this thesis

- KPC mice express CX3CR1 both on tumour cells and on immune cells infiltrating the tumour.
- Plasma and tumour CX3CL1 levels are increased in the absence of CX3CR1
- KPC and CKPC mice have comparable overall survival
- There was a decrease in $CD3^+$ T cells and an increase in IL-10 in tumours from CKPC compared to KPC mice
- The lack of CX3CR1 leads to differences in the transcriptome of CKPC mice compared to KPC mice
- Differentially expressed genes encode for proteins involved in metabolism, immunological processes and chemotaxis.

6.3 Future work

The findings of my thesis give rise to other questions on the role of CX3CR1 in pancreatic cancer, in particular related to the mechanisms involved in the regulation of the immune system and response to chemotherapy.

First of all, I would like to investigate the mechanisms involved in the changes in the decrease in $CD3^+$ T cells into the tumour. In particular, I would like to establish if the lack of CX3CR1 produces $CD3^+$ T cells unable to migrate into the tumour or if the lack of CX3CR1 in tumour cells impairs the recruitment of $CD3^+$ T cells. To answer to this question, I could use an orthotopic model of pancreatic cancer. I would generate malignant cell lines from KPC or CKPC tumours, inject into wild-type mice or CKPC mice and assess the immune infiltration into the tumour. The same profile of immune infiltration between the two groups would exclude the role of CX3CR1 expression on tumour cells in the recruitment of immune cells. Otherwise, differences in the immune cells infiltrated into the tumour would suggest that the lack of CX3CR1 on tumour cells impairs the recruitment of immune cells into pancreatic tumour.

The RNA sequencing results suggest some hypotheses that could explain the changes affecting the immune infiltration into the TME. The decrease in $CD3^+$ T cells in CKPC mice could be caused by upregulation of other chemokines (*Cxcl10* and *Cxcl12*), changes in transcription factor (*Gata3*) or in other intracellular proteins (*S100a4* and *Nlrp10*). I would like to validate these findings by looking at protein levels of these in the tumours. Next, I would verify *in vitro* using transwell migration assays to see if CXCL10 or CXCL12 induced or inhibited the migration of $CX3CR1^{GFP\text{-}GFP}$ $CD3^+$ T cells towards tumour cells.

Finally, I would like to assess if increasing the duration of treatment with chemotherapy in KPC and CKPC mice would alter tumour progression. For this reason, I would not only measure the tumour weight at the end of experiment, but I would like also to compare the tumour volume at the start and end of the experiment. This would be determined by ultrasound.

Bibliography

Allavena, P., G. Germano, F. Marchesi and A. Mantovani (2011). "Chemokines in cancer related inflammation." Exp Cell Res **317**(5): 664-673.

Allen, S. J., S. E. Crown and T. M. Handel (2007). "Chemokine: receptor structure, interactions, and antagonism." Annu Rev Immunol **25**: 787-820.

Anders, H. J., P. Romagnani and A. Mantovani (2014). "Pathomechanisms: homeostatic chemokines in health, tissue regeneration, and progressive diseases." Trends Mol Med **20**(3): 154-165.

Andre, F., N. Cabioglu, H. Assi, J. C. Sabourin, S. Delaloge, A. Sahin, K. Broglio, J. P. Spano, C. Combadiere, C. Bucana, J. C. Soria and M. Cristofanilli (2006). "Expression of chemokine receptors predicts the site of metastatic relapse in patients with axillary node positive primary breast cancer." Ann Oncol **17**(6): 945-951.

Apte, M. V., R. C. Pirola and J. S. Wilson (2012). "Pancreatic stellate cells: a starring role in normal and diseased pancreas." Front Physiol **3**: 344.

Auffray, C., D. Fogg, M. Garfa, G. Elain, O. Join-Lambert, S. Kayal, S. Sarnacki, A. Cumano, G. Lauvau and F. Geissmann (2007). "Monitoring of blood vessels and tissues by a population of monocytes with patrolling behavior." Science **317**(5838): 666-670.

Bachelerie, F., G. J. Graham, M. Locati, A. Mantovani, P. M. Murphy, R. Nibbs, A. Rot, S. Sozzani and M. Thelen (2014). "New nomenclature for atypical chemokine receptors." Nat Immunol **15**(3): 207-208.

Bachem, M. G., S. Zhou, K. Buck, W. Schneiderhan and M. Siech (2008). "Pancreatic stellate cells--role in pancreas cancer." Langenbecks Arch Surg **393**(6): 891-900.

Bailey, K. M., J. W. Wojtkowiak, A. I. Hashim and R. J. Gillies (2012). "Targeting the metabolic microenvironment of tumors." Adv Pharmacol **65**: 63-107.

Bailey, P., D. K. Chang, K. Nones, A. L. Johns, A. M. Patch, M. C. Gingras, D. K. Miller, A. N. Christ, T. J. Bruxner, M. C. Quinn, C. Nourse, L. C. Murtaugh, I. Harliwong, S. Idrisoglu, S. Manning, E. Nourbakhsh, S. Wani, L. Fink, O. Holmes, V. Chin, M. J. Anderson, S. Kazakoff, C. Leonard, F. Newell, N. Waddell, S. Wood, Q. Xu, P. J. Wilson, N. Cloonan, K. S. Kassahn, D. Taylor, K. Quek, A. Robertson, L. Pantano, L. Mincarelli, L. N. Sanchez, L. Evers, J. Wu, M. Pinese, M. J. Cowley, M. D. Jones, E. K. Colvin, A. M. Nagrial, E. S. Humphrey, L. A. Chantrill, A. Mawson, J. Humphris, A. Chou, M. Pajic, C. J. Scarlett, A. V. Pinho, M. Giry-Laterriere, I. Rooman, J. S. Samra, J. G. Kench, J. A. Lovell, N. D. Merrett, C. W. Toon, K. Epari, N. Q. Nguyen, A. Barbour, N. Zeps, K. Moran-Jones, N. B. Jamieson, J. S. Graham, F. Duthie, K. Oien, J. Hair, R. Grutzmann, A. Maitra, C. A. Iacobuzio-Donahue, C. L. Wolfgang, R. A. Morgan, R. T. Lawlor, V. Corbo, C. Bassi, B. Rusev, P. Capelli, R. Salvia, G. Tortora, D. Mukhopadhyay, G. M. Petersen, I. Australian Pancreatic Cancer Genome, D. M. Munzy, W. E. Fisher, S. A.

Karim, J. R. Eshleman, R. H. Hruban, C. Pilarsky, J. P. Morton, O. J. Sansom, A. Scarpa, E. A. Musgrove, U. M. Bailey, O. Hofmann, R. L. Sutherland, D. A. Wheeler, A. J. Gill, R. A. Gibbs, J. V. Pearson, N. Waddell, A. V. Biankin and S. M. Grimmond (2016). "Genomic analyses identify molecular subtypes of pancreatic cancer." Nature **531**(7592): 47-52.

Balkwill, F. (2004). "Cancer and the chemokine network." Nat Rev Cancer **4**(7): 540-550.

Balkwill, F. (2009). "Tumour necrosis factor and cancer." Nat Rev Cancer **9**(5): 361-371.

Balkwill, F. R. (2012). "The chemokine system and cancer." J Pathol **226**(2): 148-157.

Bardeesy, N. and R. A. DePinho (2002). "Pancreatic cancer biology and genetics." Nat Rev Cancer **2**(12): 897-909.

Bayne, L. J., G. L. Beatty, N. Jhala, C. E. Clark, A. D. Rhim, B. Z. Stanger and R. H. Vonderheide (2012). "Tumor-derived granulocyte-macrophage colony-stimulating factor regulates myeloid inflammation and T cell immunity in pancreatic cancer." Cancer Cell **21**(6): 822-835.

Bazan, J. F., K. B. Bacon, G. Hardiman, W. Wang, K. Soo, D. Rossi, D. R. Greaves, A. Zlotnik and T. J. Schall (1997). "A new class of membrane-bound chemokine with a CX3C motif." Nature **385**(6617): 640-644.

Bolm, L., S. Cigolla, U. A. Wittel, U. T. Hopt, T. Keck, D. Rades, P. Bronsert and U. F. Wellner (2017). "The Role of Fibroblasts in Pancreatic Cancer: Extracellular Matrix Versus Paracrine Factors." Transl Oncol **10**(4): 578-588.

Bottcher, J. P., M. Beyer, F. Meissner, Z. Abdullah, J. Sander, B. Hochst, S. Eickhoff, J. C. Rieckmann, C. Russo, T. Bauer, T. Flecken, D. Giesen, D. Engel, S. Jung, D. H. Busch, U. Protzer, R. Thimme, M. Mann, C. Kurts, J. L. Schultze, W. Kastenmuller and P. A. Knolle (2015). "Functional classification of memory CD8(+) T cells by CX3CR1 expression." Nat Commun **6**: 8306.

Boye, K. and G. M. Maelandsmo (2010). "S100A4 and metastasis: a small actor playing many roles." Am J Pathol **176**(2): 528-535.

Brouwer-Visser, J. and G. S. Huang (2015). "IGF2 signaling and regulation in cancer." Cytokine Growth Factor Rev **26**(3): 371-377.

Burns, W. R. and B. H. Edil (2012). "Neuroendocrine pancreatic tumors: guidelines for management and update." Curr Treat Options Oncol **13**(1): 24-34.

cancer-research-UK. (2014). "pancreatic cancer incidence." from http://www.cancerresearchuk.org/health-professional/cancer-statistics/statistics-by-cancer-type/pancreatic-cancer#heading-Zero.

Carr, R. M. and M. E. Fernandez-Zapico (2016). "Pancreatic cancer microenvironment, to target or not to target?" EMBO Mol Med **8**(2): 80-82.

Celesti, G., G. Di Caro, P. Bianchi, F. Grizzi, F. Marchesi, G. Basso, D. Rahal, G. Delconte, M. Catalano, P. Cappello, M. Roncalli, A. Zerbi, M. Montorsi, F. Novelli, A. Mantovani, P. Allavena, A. Malesci and L. Laghi (2013). "Early expression of the fractalkine receptor CX3CR1 in pancreatic carcinogenesis." Br J Cancer **109**(9): 2424-2433.

Chang, A. I., A. H. Schwertschkow, J. A. Nolta and J. Wu (2015). "Involvement of mesenchymal stem cells in cancer progression and metastases." Curr Cancer Drug Targets **15**(2): 88-98.

Chang, J. H., Y. Jiang and V. G. Pillarisetty (2016). "Role of immune cells in pancreatic cancer from bench to clinical application: An updated review." Medicine (Baltimore) **95**(49): e5541.

Cheng, W. and G. Chen (2014). "Chemokines and chemokine receptors in multiple sclerosis." Mediators Inflamm **2014**: 659206.

Cid-Arregui, A. and V. Juarez (2015). "Perspectives in the treatment of pancreatic adenocarcinoma." World J Gastroenterol **21**(31): 9297-9316.

Clark, C. E., S. R. Hingorani, R. Mick, C. Combs, D. A. Tuveson and R. H. Vonderheide (2007). "Dynamics of the immune reaction to pancreatic cancer from inception to invasion." Cancer Res **67**(19): 9518-9527.

Cleveland, M. H., J. M. Sawyer, S. Afelik, J. Jensen and S. D. Leach (2012). "Exocrine ontogenies: on the development of pancreatic acinar, ductal and centroacinar cells." Semin Cell Dev Biol **23**(6): 711-719.

Cohen, R., C. Neuzillet, A. Tijeras-Raballand, S. Faivre, A. de Gramont and E. Raymond (2015). "Targeting cancer cell metabolism in pancreatic adenocarcinoma." Oncotarget **6**(19): 16832-16847.

Collisson, E. A., A. Sadanandam, P. Olson, W. J. Gibb, M. Truitt, S. Gu, J. Cooc, J. Weinkle, G. E. Kim, L. Jakkula, H. S. Feiler, A. H. Ko, A. B. Olshen, K. L. Danenberg, M. A. Tempero, P. T. Spellman, D. Hanahan and J. W. Gray (2011). "Subtypes of pancreatic ductal adenocarcinoma and their differing responses to therapy." Nat Med **17**(4): 500-503.

Colotta, F., P. Allavena, A. Sica, C. Garlanda and A. Mantovani (2009). "Cancer-related inflammation, the seventh hallmark of cancer: links to genetic instability." Carcinogenesis **30**(7): 1073-1081.

Combadiere, C., C. Feumi, W. Raoul, N. Keller, M. Rodero, A. Pezard, S. Lavalette, M. Houssier, L. Jonet, E. Picard, P. Debre, M. Sirinyan, P. Deterre, T. Ferroukhi, S. Y. Cohen, D. Chauvaud, J. C. Jeanny, S. Chemtob, F. Behar-Cohen and F. Sennlaub (2007). "CX3CR1-dependent subretinal microglia cell accumulation is associated with cardinal features of age-related macular degeneration." J Clin Invest **117**(10): 2920-2928.

Conroy, T., F. Desseigne, M. Ychou, O. Bouche, R. Guimbaud, Y. Becouarn, A. Adenis, J. L. Raoul, S. Gourgou-Bourgade, C. de la Fouchardiere, J. Bennouna, J. B. Bachet, F. Khemissa-Akouz, D. Pere-Verge, C. Delbaldo, E. Assenat, B. Chauffert, P. Michel, C. Montoto-Grillot, M. Ducreux, U. Groupe Tumeurs Digestives of and P. Intergroup (2011). "FOLFIRINOX versus gemcitabine for metastatic pancreatic cancer." N Engl J Med **364**(19): 1817-1825.

Corbo, V., G. Tortora and A. Scarpa (2012). "Molecular pathology of pancreatic cancer: from bench-to-bedside translation." Curr Drug Targets **13**(6): 744-752.

Corcione, A., E. Ferretti and V. Pistoia (2012). "CX3CL1/fractalkine is a novel regulator of normal and malignant human B cell function." J Leukoc Biol **92**(1): 51-58.

Cox, A. D. and K. P. Olive (2012). "Silencing the killers: paracrine immune suppression in pancreatic cancer." Cancer Cell **21**(6): 715-716.

Crocker, P. R., J. C. Paulson and A. Varki (2007). "Siglecs and their roles in the immune system." Nat Rev Immunol **7**(4): 255-266.

Damm, A., K. Lautz and T. A. Kufer (2013). "Roles of NLRP10 in innate and adaptive immunity." Microbes Infect **15**(6-7): 516-523.

de Sousa Cavalcante, L. and G. Monteiro (2014). "Gemcitabine: metabolism and molecular mechanisms of action, sensitivity and chemoresistance in pancreatic cancer." Eur J Pharmacol **741**: 8-16.

Deshmane, S. L., S. Kremlev, S. Amini and B. E. Sawaya (2009). "Monocyte chemoattractant protein-1 (MCP-1): an overview." J Interferon Cytokine Res **29**(6): 313-326.

Durinck, S., Y. Moreau, A. Kasprzyk, S. Davis, B. De Moor, A. Brazma and W. Huber (2005). "BioMart and Bioconductor: a powerful link between biological databases and microarray data analysis." Bioinformatics **21**(16): 3439-3440.

Eales, K. L., K. E. Hollinshead and D. A. Tennant (2016). "Hypoxia and metabolic adaptation of cancer cells." Oncogenesis **5**: e190.

Eisenbarth, S. C., A. Williams, O. R. Colegio, H. Meng, T. Strowig, A. Rongvaux, J. Henao-Mejia, C. A. Thaiss, S. Joly, D. G. Gonzalez, L. Xu, L. A. Zenewicz, A. M. Haberman, E. Elinav, S. H. Kleinstein, F. S. Sutterwala and R. A. Flavell (2012). "NLRP10 is a NOD-like receptor essential to initiate adaptive immunity by dendritic cells." Nature **484**(7395): 510-513.

Erkan, M., C. Reiser-Erkan, C. W. Michalski, S. Deucker, D. Sauliunaite, S. Streit, I. Esposito, H. Friess and J. Kleeff (2009). "Cancer-stellate cell interactions perpetuate the hypoxia-fibrosis cycle in pancreatic ductal adenocarcinoma." Neoplasia **11**(5): 497-508.

Evans, A. and E. Costello (2012). "The role of inflammatory cells in fostering pancreatic cancer cell growth and invasion." Front Physiol **3**: 270.

Farrow, B. and B. M. Evers (2002). "Inflammation and the development of pancreatic cancer." Surg Oncol **10**(4): 153-169.

Fei, F., J. Qu, M. Zhang, Y. Li and S. Zhang (2017). "S100A4 in cancer progression and metastasis: A systematic review." Oncotarget.

Feig, C., A. Gopinathan, A. Neesse, D. S. Chan, N. Cook and D. A. Tuveson (2012). "The pancreas cancer microenvironment." Clin Cancer Res **18**(16): 4266-4276.

Feig, C., J. O. Jones, M. Kraman, R. J. Wells, A. Deonarine, D. S. Chan, C. M. Connell, E. W. Roberts, Q. Zhao, O. L. Caballero, S. A. Teichmann, T. Janowitz, D. I. Jodrell, D. A. Tuveson and D. T. Fearon (2013). "Targeting CXCL12 from FAP-expressing carcinoma-associated fibroblasts synergizes with anti-PD-L1 immunotherapy in pancreatic cancer." Proc Natl Acad Sci U S A **110**(50): 20212-20217.

Ferretti, E., V. Pistoia and A. Corcione (2014). "Role of fractalkine/CX3CL1 and its receptor in the pathogenesis of inflammatory and malignant diseases with emphasis on B cell malignancies." Mediators Inflamm **2014**: 480941.

Fong, A. M., L. A. Robinson, D. A. Steeber, T. F. Tedder, O. Yoshie, T. Imai and D. D. Patel (1998). "Fractalkine and CX3CR1 mediate a novel mechanism of leukocyte capture, firm adhesion, and activation under physiologic flow." J Exp Med **188**(8): 1413-1419.

Galluzzi, L., A. Buque, O. Kepp, L. Zitvogel and G. Kroemer (2015). "Immunological Effects of Conventional Chemotherapy and Targeted Anticancer Agents." Cancer Cell **28**(6): 690-714.

Galluzzi, L., L. Zitvogel and G. Kroemer (2016). "Immunological Mechanisms Underneath the Efficacy of Cancer Therapy." Cancer Immunol Res **4**(11): 895-902.

Gautier, E. L., C. Jakubzick and G. J. Randolph (2009). "Regulation of the migration and survival of monocyte subsets by chemokine receptors and its relevance to atherosclerosis." Arterioscler Thromb Vasc Biol **29**(10): 1412-1418.

Gerard, C. and B. J. Rollins (2001). "Chemokines and disease." Nat Immunol **2**(2): 108-115.

Girard, J. P., C. Moussion and R. Forster (2012). "HEVs, lymphatics and homeostatic immune cell trafficking in lymph nodes." Nat Rev Immunol **12**(11): 762-773.

Griffith, J. W., C. L. Sokol and A. D. Luster (2014). "Chemokines and chemokine receptors: positioning cells for host defense and immunity." Annu Rev Immunol **32**: 659-702.

Groom, J. R. and A. D. Luster (2011). "CXCR3 ligands: redundant, collaborative and antagonistic functions." Immunol Cell Biol **89**(2): 207-215.

Grum-Schwensen, B., J. Klingelhofer, M. Grigorian, K. Almholt, B. S. Nielsen, E. Lukanidin and N. Ambartsumian (2010). "Lung metastasis fails in MMTV-PyMT

oncomice lacking S100A4 due to a T-cell deficiency in primary tumors." Cancer Res **70**(3): 936-947.

Guerra, C. and M. Barbacid (2013). "Genetically engineered mouse models of pancreatic adenocarcinoma." Mol Oncol **7**(2): 232-247.

Guo, F., Y. Wang, J. Liu, S. C. Mok, F. Xue and W. Zhang (2016). "CXCL12/CXCR4: a symbiotic bridge linking cancer cells and their stromal neighbors in oncogenic communication networks." Oncogene **35**(7): 816-826.

Gurkan, U. A. and O. Akkus (2008). "The mechanical environment of bone marrow: a review." Ann Biomed Eng **36**(12): 1978-1991.

H Chen, J. T., LWeinberg, M Nikfarjam (2015). "Diffuse Pancreatic Mucinous Cystic Neoplasm Treated by Total Pancreatectomy." JOP. Journal of the Pancreas.

Hamilton, J. A. (2008). "Colony-stimulating factors in inflammation and autoimmunity." Nat Rev Immunol **8**(7): 533-544.

Heinemann, V., M. Reni, M. Ychou, D. J. Richel, T. Macarulla and M. Ducreux (2014). "Tumour-stroma interactions in pancreatic ductal adenocarcinoma: rationale and current evidence for new therapeutic strategies." Cancer Treat Rev **40**(1): 118-128.

Herreros-Villanueva, M., E. Hijona, A. Cosme and L. Bujanda (2012). "Mouse models of pancreatic cancer." World J Gastroenterol **18**(12): 1286-1294.

Hezel, A. F., A. C. Kimmelman, B. Z. Stanger, N. Bardeesy and R. A. Depinho (2006). "Genetics and biology of pancreatic ductal adenocarcinoma." Genes Dev **20**(10): 1218-1249.

Hingorani, S. R., L. Wang, A. S. Multani, C. Combs, T. B. Deramaudt, R. H. Hruban, A. K. Rustgi, S. Chang and D. A. Tuveson (2005). "Trp53R172H and KrasG12D cooperate to promote chromosomal instability and widely metastatic pancreatic ductal adenocarcinoma in mice." Cancer Cell **7**(5): 469-483.

Ho, I. C., T. S. Tai and S. Y. Pai (2009). "GATA3 and the T-cell lineage: essential functions before and after T-helper-2-cell differentiation." Nat Rev Immunol **9**(2): 125-135.

Hruban, R. H., A. Maitra and M. Goggins (2008). "Update on pancreatic intraepithelial neoplasia." Int J Clin Exp Pathol **1**(4): 306-316.

Hruban, R. H., R. E. Wilentz and S. E. Kern (2000). "Genetic progression in the pancreatic ducts." Am J Pathol **156**(6): 1821-1825.

Huber, R., D. Pietsch, T. Panterodt and K. Brand (2012). "Regulation of C/EBPbeta and resulting functions in cells of the monocytic lineage." Cell Signal **24**(6): 1287-1296.

Hundhausen, C., D. Misztela, T. A. Berkhout, N. Broadway, P. Saftig, K. Reiss, D. Hartmann, F. Fahrenholz, R. Postina, V. Matthews, K. J. Kallen, S. Rose-John and A. Ludwig (2003). "The disintegrin-like metalloproteinase ADAM10 is involved in constitutive cleavage of CX3CL1 (fractalkine) and regulates CX3CL1-mediated cell-cell adhesion." Blood **102**(4): 1186-1195.

Ierano, C., P. Giuliano, C. D'Alterio, M. Cioffi, V. Mettivier, L. Portella, M. Napolitano, A. Barbieri, C. Arra, G. Liguori, R. Franco, G. Palmieri, C. Rozzo, R. Pacelli, G. Castello and S. Scala (2009). "A point mutation (G574A) in the chemokine receptor CXCR4 detected in human cancer cells enhances migration." Cell Cycle **8**(8): 1228-1237.

Imai, T., K. Hieshima, C. Haskell, M. Baba, M. Nagira, M. Nishimura, M. Kakizaki, S. Takagi, H. Nomiyama, T. J. Schall and O. Yoshie (1997). "Identification and molecular characterization of fractalkine receptor CX3CR1, which mediates both leukocyte migration and adhesion." Cell **91**(4): 521-530.

Iodice, S., S. Gandini, P. Maisonneuve and A. B. Lowenfels (2008). "Tobacco and the risk of pancreatic cancer: a review and meta-analysis." Langenbecks Arch Surg **393**(4): 535-545.

Ishida, Y., J. L. Gao and P. M. Murphy (2008). "Chemokine receptor CX3CR1 mediates skin wound healing by promoting macrophage and fibroblast accumulation and function." J Immunol **180**(1): 569-579.

Jablonski, K. A., S. A. Amici, L. M. Webb, D. Ruiz-Rosado Jde, P. G. Popovich, S. Partida-Sanchez and M. Guerau-de-Arellano (2015). "Novel Markers to Delineate Murine M1 and M2 Macrophages." PLoS One **10**(12): e0145342.

Jamieson-Gladney, W. L., Y. Zhang, A. M. Fong, O. Meucci and A. Fatatis (2011). "The chemokine receptor CX(3)CR1 is directly involved in the arrest of breast cancer cells to the skeleton." Breast Cancer Res **13**(5): R91.

Jamieson, W. L., S. Shimizu, J. A. D'Ambrosio, O. Meucci and A. Fatatis (2008). "CX3CR1 is expressed by prostate epithelial cells and androgens regulate the levels of CX3CL1/fractalkine in the bone marrow: potential role in prostate cancer bone tropism." Cancer Res **68**(6): 1715-1722.

Jung, S., J. Aliberti, P. Graemmel, M. J. Sunshine, G. W. Kreutzberg, A. Sher and D. R. Littman (2000). "Analysis of fractalkine receptor CX(3)CR1 function by targeted deletion and green fluorescent protein reporter gene insertion." Mol Cell Biol **20**(11): 4106-4114.

Kamisawa, T., L. D. Wood, T. Itoi and K. Takaori (2016). "Pancreatic cancer." Lancet **388**(10039): 73-85.

Karin, N. (2010). "The multiple faces of CXCL12 (SDF-1alpha) in the regulation of immunity during health and disease." J Leukoc Biol **88**(3): 463-473.

Kasama, T., T. Odai, K. Wakabayashi, N. Yajima and Y. Miwa (2008). "Chemokines in systemic lupus erythematosus involving the central nervous system." Front Biosci **13**: 2527-2536.

Keane, M. G., L. Horsfall, G. Rait and S. P. Pereira (2014). "A case-control study comparing the incidence of early symptoms in pancreatic and biliary tract cancer." BMJ Open **4**(11): e005720.

Kim, K. W., A. Vallon-Eberhard, E. Zigmond, J. Farache, E. Shezen, G. Shakhar, A. Ludwig, S. A. Lira and S. Jung (2011). "In vivo structure/function and expression analysis of the CX3C chemokine fractalkine." Blood **118**(22): e156-167.

Kim, Y. T. (2008). "[Chemotherapy for pancreatic cancer]." Korean J Gastroenterol **51**(2): 111-118.

Klimczak, A. and U. Kozlowska (2016). "Mesenchymal Stromal Cells and Tissue-Specific Progenitor Cells: Their Role in Tissue Homeostasis." Stem Cells Int **2016**: 4285215.

Klingelhofer, J., B. Grum-Schwensen, M. K. Beck, R. S. Knudsen, M. Grigorian, E. Lukanidin and N. Ambartsumian (2012). "Anti-S100A4 antibody suppresses metastasis formation by blocking stroma cell invasion." Neoplasia **14**(12): 1260-1268.

Kosaki, K., R. Kosaki, W. J. Craigen and N. Matsuo (2000). "Isoform-specific imprinting of the human PEG1/MEST gene." Am J Hum Genet **66**(1): 309-312.

Kryczek, I., A. Lange, P. Mottram, X. Alvarez, P. Cheng, M. Hogan, L. Moons, S. Wei, L. Zou, V. Machelon, D. Emilie, M. Terrassa, A. Lackner, T. J. Curiel, P. Carmeliet and W. Zou (2005). "CXCL12 and vascular endothelial growth factor synergistically induce neoangiogenesis in human ovarian cancers." Cancer Res **65**(2): 465-472.

Kumari, N., B. S. Dwarakanath, A. Das and A. N. Bhatt (2016). "Role of interleukin-6 in cancer progression and therapeutic resistance." Tumour Biol **37**(9): 11553-11572.

Kusmartsev, S., S. Nagaraj and D. I. Gabrilovich (2005). "Tumor-associated CD8+ T cell tolerance induced by bone marrow-derived immature myeloid cells." J Immunol **175**(7): 4583-4592.

La Rosa, S., F. Sessa and C. Capella (2015). "Acinar Cell Carcinoma of the Pancreas: Overview of Clinicopathologic Features and Insights into the Molecular Pathology." Front Med (Lausanne) **2**: 41.

Landsman, L., L. Bar-On, A. Zernecke, K. W. Kim, R. Krauthgamer, E. Shagdarsuren, S. A. Lira, I. L. Weissman, C. Weber and S. Jung (2009). "CX3CR1 is required for monocyte homeostasis and atherogenesis by promoting cell survival." Blood **113**(4): 963-972.

Lawrence, T. and G. Natoli (2011). "Transcriptional regulation of macrophage polarization: enabling diversity with identity." Nat Rev Immunol **11**(11): 750-761.

Lazennec, G. and A. Richmond (2010). "Chemokines and chemokine receptors: new insights into cancer-related inflammation." Trends Mol Med **16**(3): 133-144.

Lee, S. J., S. Namkoong, Y. M. Kim, C. K. Kim, H. Lee, K. S. Ha, H. T. Chung, Y. G. Kwon and Y. M. Kim (2006). "Fractalkine stimulates angiogenesis by activating the Raf-1/MEK/ERK- and PI3K/Akt/eNOS-dependent signal pathways." Am J Physiol Heart Circ Physiol **291**(6): H2836-2846.

Lesina, M., M. U. Kurkowski, K. Ludes, S. Rose-John, M. Treiber, G. Kloppel, A. Yoshimura, W. Reindl, B. Sipos, S. Akira, R. M. Schmid and H. Algul (2011). "Stat3/Socs3 activation by IL-6 transsignaling promotes progression of pancreatic intraepithelial neoplasia and development of pancreatic cancer." Cancer Cell **19**(4): 456-469.

Lewis, A. M., S. Varghese, H. Xu and H. R. Alexander (2006). "Interleukin-1 and cancer progression: the emerging role of interleukin-1 receptor antagonist as a novel therapeutic agent in cancer treatment." J Transl Med **4**: 48.

Liu, M., S. Guo, J. M. Hibbert, V. Jain, N. Singh, N. O. Wilson and J. K. Stiles (2011). "CXCL10/IP-10 in infectious diseases pathogenesis and potential therapeutic implications." Cytokine Growth Factor Rev **22**(3): 121-130.

Liu, M., S. Guo and J. K. Stiles (2011). "The emerging role of CXCL10 in cancer (Review)." Oncol Lett **2**(4): 583-589.

Liu, P., Y. R. Yu, J. A. Spencer, A. E. Johnson, C. T. Vallanat, A. M. Fong, C. Patterson and D. D. Patel (2008). "CX3CR1 deficiency impairs dendritic cell accumulation in arterial intima and reduces atherosclerotic burden." Arterioscler Thromb Vasc Biol **28**(2): 243-250.

Liu, W., L. Jiang, C. Bian, Y. Liang, R. Xing, M. Yishakea and J. Dong (2016). "Role of CX3CL1 in Diseases." Arch Immunol Ther Exp (Warsz) **64**(5): 371-383.

Longley, D. B., D. P. Harkin and P. G. Johnston (2003). "5-fluorouracil: mechanisms of action and clinical strategies." Nat Rev Cancer **3**(5): 330-338.

Longo, V., O. Brunetti, A. Gnoni, S. Cascinu, G. Gasparini, V. Lorusso, D. Ribatti and N. Silvestris (2016). "Angiogenesis in pancreatic ductal adenocarcinoma: A controversial issue." Oncotarget **7**(36): 58649-58658.

Lunardi, S., R. J. Muschel and T. B. Brunner (2014). "The stromal compartments in pancreatic cancer: are there any therapeutic targets?" Cancer Lett **343**(2): 147-155.

Ma, X., K. Norsworthy, N. Kundu, W. H. Rodgers, P. A. Gimotty, O. Goloubeva, M. Lipsky, Y. Li, D. Holt and A. Fulton (2009). "CXCR3 expression is associated with poor survival in breast cancer and promotes metastasis in a murine model." Mol Cancer Ther **8**(3): 490-498.

Macri, C., C. Dumont, A. P. Johnston and J. D. Mintern (2016). "Targeting dendritic cells: a promising strategy to improve vaccine effectiveness." Clin Transl Immunology **5**(3): e66.

Madalli, S., M. Beyrau, J. Whiteford, J. Duchene, I. Singh Nandhra, N. S. Patel, M. P. Motwani, D. W. Gilroy, C. Thiemermann, S. Nourshargh and R. S. Scotland (2015). "Sex-specific regulation of chemokine Cxcl5/6 controls neutrophil recruitment and tissue injury in acute inflammatory states." Biol Sex Differ **6**: 27.

Mahadevan, D. and D. D. Von Hoff (2007). "Tumor-stroma interactions in pancreatic ductal adenocarcinoma." Mol Cancer Ther **6**(4): 1186-1197.

Mannino, M. H., Z. Zhu, H. Xiao, Q. Bai, M. R. Wakefield and Y. Fang (2015). "The paradoxical role of IL-10 in immunity and cancer." Cancer Lett **367**(2): 103-107.

Mantovani, A., B. Savino, M. Locati, L. Zammataro, P. Allavena and R. Bonecchi (2010). "The chemokine system in cancer biology and therapy." Cytokine Growth Factor Rev **21**(1): 27-39.

Marchesi, F., M. Locatelli, G. Solinas, M. Erreni, P. Allavena and A. Mantovani (2010). "Role of CX3CR1/CX3CL1 axis in primary and secondary involvement of the nervous system by cancer." J Neuroimmunol **224**(1-2): 39-44.

Marchesi, F., L. Piemonti, G. Fedele, A. Destro, M. Roncalli, L. Albarello, C. Doglioni, A. Anselmo, A. Doni, P. Bianchi, L. Laghi, A. Malesci, L. Cervo, M. Malosio, M. Reni, A. Zerbi, V. Di Carlo, A. Mantovani and P. Allavena (2008). "The chemokine receptor CX3CR1 is involved in the neural tropism and malignant behavior of pancreatic ductal adenocarcinoma." Cancer Res **68**(21): 9060-9069.

Marsh Rde, W., M. S. Talamonti, M. H. Katz and J. M. Herman (2015). "Pancreatic cancer and FOLFIRINOX: a new era and new questions." Cancer Med **4**(6): 853-863.

Mastracci, T. L. and L. Sussel (2012). "The Endocrine Pancreas: insights into development, differentiation and diabetes." Wiley Interdiscip Rev Membr Transp Signal **1**(5): 609-628.

Maxwell, P. J., R. Gallagher, A. Seaton, C. Wilson, P. Scullin, J. Pettigrew, I. J. Stratford, K. J. Williams, P. G. Johnston and D. J. Waugh (2007). "HIF-1 and NF-kappaB-mediated upregulation of CXCR1 and CXCR2 expression promotes cell survival in hypoxic prostate cancer cells." Oncogene **26**(52): 7333-7345.

McCarthy, D. J., Y. Chen and G. K. Smyth (2012). "Differential expression analysis of multifactor RNA-Seq experiments with respect to biological variation." Nucleic Acids Res **40**(10): 4288-4297.

McKenna, L. R. and B. H. Edil (2014). "Update on pancreatic neuroendocrine tumors." Gland Surg **3**(4): 258-275.

Mebius, R. E. and G. Kraal (2005). "Structure and function of the spleen." Nat Rev Immunol **5**(8): 606-616.

Mehrad, B., M. P. Keane and R. M. Strieter (2007). "Chemokines as mediators of angiogenesis." Thromb Haemost **97**(5): 755-762.

Menghini, R., L. Fiorentino, V. Casagrande, R. Lauro and M. Federici (2013). "The role of ADAM17 in metabolic inflammation." Atherosclerosis **228**(1): 12-17.

Mestdagt, M., M. Polette, G. Buttice, A. Noel, A. Ueda, J. M. Foidart and C. Gilles (2006). "Transactivation of MCP-1/CCL2 by beta-catenin/TCF-4 in human breast cancer cells." Int J Cancer **118**(1): 35-42.

Mi, H., A. Muruganujan and P. D. Thomas (2013). "PANTHER in 2013: modeling the evolution of gene function, and other gene attributes, in the context of phylogenetic trees." Nucleic Acids Res **41**(Database issue): D377-386.

Mielgo, A. and M. C. Schmid (2013). "Impact of tumour associated macrophages in pancreatic cancer." BMB Rep **46**(3): 131-138.

Mukaida, N., S. Sasaki and T. Baba (2014). "Chemokines in cancer development and progression and their potential as targeting molecules for cancer treatment." Mediators Inflamm **2014**: 170381.

Mukherjee, D. and J. Zhao (2013). "The Role of chemokine receptor CXCR4 in breast cancer metastasis." Am J Cancer Res **3**(1): 46-57.

Muller, A., B. Homey, H. Soto, N. Ge, D. Catron, M. E. Buchanan, T. McClanahan, E. Murphy, W. Yuan, S. N. Wagner, J. L. Barrera, A. Mohar, E. Verastegui and A. Zlotnik (2001). "Involvement of chemokine receptors in breast cancer metastasis." Nature **410**(6824): 50-56.

Murphy, P. M., M. Baggiolini, I. F. Charo, C. A. Hebert, R. Horuk, K. Matsushima, L. H. Miller, J. J. Oppenheim and C. A. Power (2000). "International union of pharmacology. XXII. Nomenclature for chemokine receptors." Pharmacol Rev **52**(1): 145-176.

Nagarsheth, N., M. S. Wicha and W. Zou (2017). "Chemokines in the cancer microenvironment and their relevance in cancer immunotherapy." Nat Rev Immunol.

Neesse, A., P. Michl, K. K. Frese, C. Feig, N. Cook, M. A. Jacobetz, M. P. Lolkema, M. Buchholz, K. P. Olive, T. M. Gress and D. A. Tuveson (2011). "Stromal biology and therapy in pancreatic cancer." Gut **60**(6): 861-868.

Nibbs, R. J. and G. J. Graham (2013). "Immune regulation by atypical chemokine receptors." Nat Rev Immunol **13**(11): 815-829.

Nishimura, M., H. Umehara, T. Nakayama, O. Yoneda, K. Hieshima, M. Kakizaki, N. Dohmae, O. Yoshie and T. Imai (2002). "Dual functions of fractalkine/CX3C ligand 1 in trafficking of perforin+/granzyme B+ cytotoxic effector lymphocytes that are defined by CX3CR1 expression." J Immunol **168**(12): 6173-6180.

Noble, S. and K. L. Goa (1997). "Gemcitabine. A review of its pharmacology and clinical potential in non-small cell lung cancer and pancreatic cancer." Drugs **54**(3): 447-472.

Nomiyama, H., N. Osada and O. Yoshie (2011). "A family tree of vertebrate chemokine receptors for a unified nomenclature." Dev Comp Immunol **35**(7): 705-715.

O'Boyle, G. (2012). "The yin and yang of chemokine receptor activation." Br J Pharmacol 166(3): 895-897.

O'Hayre, M., C. L. Salanga, T. M. Handel and S. J. Allen (2008). "Chemokines and cancer: migration, intracellular signalling and intercellular communication in the microenvironment." Biochem J **409**(3): 635-649.

Ocana, A., C. Nieto-Jimenez, A. Pandiella and A. J. Templeton (2017). "Neutrophils in cancer: prognostic role and therapeutic strategies." Mol Cancer **16**(1): 137.

Ottenhof, N. A., R. F. de Wilde, A. Maitra, R. H. Hruban and G. J. Offerhaus (2011). "Molecular characteristics of pancreatic ductal adenocarcinoma." Patholog Res Int **2011**: 620601.

Ozdemir, B. C., T. Pentcheva-Hoang, J. L. Carstens, X. Zheng, C. C. Wu, T. R. Simpson, H. Laklai, H. Sugimoto, C. Kahlert, S. V. Novitskiy, A. De Jesus-Acosta, P. Sharma, P. Heidari, U. Mahmood, L. Chin, H. L. Moses, V. M. Weaver, A. Maitra, J. P. Allison, V. S. LeBleu and R. Kalluri (2014). "Depletion of carcinoma-associated fibroblasts and fibrosis induces immunosuppression and accelerates pancreas cancer with reduced survival." Cancer Cell **25**(6): 719-734.

Pancreatic-Cancer-UK. (2016). "Types of pancreatic cancer." from https://www.pancreaticcancer.org.uk/types.

Pandol, S., M. Edderkaoui, I. Gukovsky, A. Lugea and A. Gukovskaya (2009). "Desmoplasia of pancreatic ductal adenocarcinoma." Clin Gastroenterol Hepatol **7**(11 Suppl): S44-47.

Patel, J., K. M. Channon and E. McNeill (2013). "The downstream regulation of chemokine receptor signalling: implications for atherosclerosis." Mediators Inflamm **2013**: 459520.

Payne, A. S. and L. A. Cornelius (2002). "The role of chemokines in melanoma tumor growth and metastasis." J Invest Dermatol **118**(6): 915-922.

Pei, Q., J. Pan, H. Zhu, X. Ding, W. Liu, Y. Lv, X. Zou and H. Luo (2014). "Gemcitabine-treated pancreatic cancer cell medium induces the specific CTL antitumor activity by stimulating the maturation of dendritic cells." Int Immunopharmacol **19**(1): 10-16.

Phillips, P. (2012). Pancreatic stellate cells and fibrosis. Pancreatic Cancer and Tumor Microenvironment. P. J. Grippo and H. G. Munshi. Trivandrum (India).

Pollard, J. W. (2004). "Tumour-educated macrophages promote tumour progression and metastasis." Nat Rev Cancer **4**(1): 71-78.

Polyak, A., S. Ferenczi, A. Denes, Z. Winkler, R. Kriszt, B. Pinter-Kubler and K. J. Kovacs (2014). "The fractalkine/Cx3CR1 system is implicated in the development of metabolic visceral adipose tissue inflammation in obesity." Brain Behav Immun **38**: 25-35.

Provenzano, P. P., C. Cuevas, A. E. Chang, V. K. Goel, D. D. Von Hoff and S. R. Hingorani (2012). "Enzymatic targeting of the stroma ablates physical barriers to treatment of pancreatic ductal adenocarcinoma." Cancer Cell **21**(3): 418-429.

Quail, D. F. and J. A. Joyce (2013). "Microenvironmental regulation of tumor progression and metastasis." Nat Med **19**(11): 1423-1437.

Raman, D., T. Sobolik-Delmaire and A. Richmond (2011). "Chemokines in health and disease." Exp Cell Res **317**(5): 575-589.

Rasheed, Z. A., W. Matsui and A. Maitra (2012). Pathology of pancreatic stroma in PDAC. Pancreatic Cancer and Tumor Microenvironment. P. J. Grippo and H. G. Munshi. Trivandrum (India).

Ren, H., T. Zhao, J. Sun, X. Wang, J. Liu, S. Gao, M. Yu and J. Hao (2013). "The CX3CL1/CX3CR1 reprograms glucose metabolism through HIF-1 pathway in pancreatic adenocarcinoma." J Cell Biochem **114**(11): 2603-2611.

Reznik, R., A. E. Hendifar and R. Tuli (2014). "Genetic determinants and potential therapeutic targets for pancreatic adenocarcinoma." Front Physiol **5**: 87.

Richmond, A. (2002). "Nf-kappa B, chemokine gene transcription and tumour growth." Nat Rev Immunol **2**(9): 664-674.

Robinson, M. D., D. J. McCarthy and G. K. Smyth (2010). "edgeR: a Bioconductor package for differential expression analysis of digital gene expression data." Bioinformatics **26**(1): 139-140.

Roy, I., D. B. Evans and M. B. Dwinell (2014). "Chemokines and chemokine receptors: update on utility and challenges for the clinician." Surgery **155**(6): 961-973.

Ruffell, B., N. I. Affara and L. M. Coussens (2012). "Differential macrophage programming in the tumor microenvironment." Trends Immunol **33**(3): 119-126.

Ruffell, D., F. Mourkioti, A. Gambardella, P. Kirstetter, R. G. Lopez, N. Rosenthal and C. Nerlov (2009). "A CREB-C/EBPbeta cascade induces M2 macrophage-specific gene expression and promotes muscle injury repair." Proc Natl Acad Sci U S A **106**(41): 17475-17480.

Ryan, D. P., T. S. Hong and N. Bardeesy (2014). "Pancreatic adenocarcinoma." N Engl J Med **371**(11): 1039-1049.

Saederup, N., L. Chan, S. A. Lira and I. F. Charo (2008). "Fractalkine deficiency markedly reduces macrophage accumulation and atherosclerotic lesion formation

in CCR2-/- mice: evidence for independent chemokine functions in atherogenesis." Circulation **117**(13): 1642-1648.

Sanjurjo, L., G. Aran, N. Roher, A. F. Valledor and M. R. Sarrias (2015). "AIM/CD5L: a key protein in the control of immune homeostasis and inflammatory disease." J Leukoc Biol **98**(2): 173-184.

Santoni, M., S. Bracarda, M. Nabissi, F. Massari, A. Conti, E. Bria, G. Tortora, G. Santoni and S. Cascinu (2014). "CXC and CC chemokines as angiogenic modulators in nonhaematological tumors." Biomed Res Int **2014**: 768758.

Sarvaiya, P. J., D. Guo, I. Ulasov, P. Gabikian and M. S. Lesniak (2013). "Chemokines in tumor progression and metastasis." Oncotarget **4**(12): 2171-2185.

Schett, G., J. M. Dayer and B. Manger (2016). "Interleukin-1 function and role in rheumatic disease." Nat Rev Rheumatol **12**(1): 14-24.

Schmall, A., H. M. Al-Tamari, S. Herold, M. Kampschulte, A. Weigert, A. Wietelmann, N. Vipotnik, F. Grimminger, W. Seeger, S. S. Pullamsetti and R. Savai (2015). "Macrophage and cancer cell cross-talk via CCR2 and CX3CR1 is a fundamental mechanism driving lung cancer." Am J Respir Crit Care Med **191**(4): 437-447.

Schober, M., R. Jesenofsky, R. Faissner, C. Weidenauer, W. Hagmann, P. Michl, R. L. Heuchel, S. L. Haas and J. M. Lohr (2014). "Desmoplasia and chemoresistance in pancreatic cancer." Cancers (Basel) **6**(4): 2137-2154.

Schulz, C., A. Schafer, M. Stolla, S. Kerstan, M. Lorenz, M. L. von Bruhl, M. Schiemann, J. Bauersachs, T. Gloe, D. H. Busch, M. Gawaz and S. Massberg (2007). "Chemokine fractalkine mediates leukocyte recruitment to inflammatory endothelial cells in flowing whole blood: a critical role for P-selectin expressed on activated platelets." Circulation **116**(7): 764-773.

Shah, R., S. M. O'Neill, C. Hinkle, J. Caughey, S. Stephan, E. Lynch, K. Bermingham, G. Lynch, R. S. Ahima and M. P. Reilly (2015). "Metabolic Effects of CX3CR1 Deficiency in Diet-Induced Obese Mice." PLoS One **10**(9): e0138317.

Shulby, S. A., N. G. Dolloff, M. E. Stearns, O. Meucci and A. Fatatis (2004). "CX3CR1-fractalkine expression regulates cellular mechanisms involved in adhesion, migration, and survival of human prostate cancer cells." Cancer Res **64**(14): 4693-4698.

Sica, A. and A. Mantovani (2012). "Macrophage plasticity and polarization: in vivo veritas." J Clin Invest **122**(3): 787-795.

Sideras, K., H. Braat, J. Kwekkeboom, C. H. van Eijck, M. P. Peppelenbosch, S. Sleijfer and M. Bruno (2014). "Role of the immune system in pancreatic cancer progression and immune modulating treatment strategies." Cancer Treat Rev **40**(4): 513-522.

Sionov, R. V., Z. G. Fridlender and Z. Granot (2015). "The Multifaceted Roles Neutrophils Play in the Tumor Microenvironment." Cancer Microenviron **8**(3): 125-158.

Smyth, M. J., E. Cretney, M. H. Kershaw and Y. Hayakawa (2004). "Cytokines in cancer immunity and immunotherapy." Immunol Rev **202**: 275-293.

Snady, H., H. Bruckner, A. Cooperman, J. Paradiso and L. Kiefer (2000). "Survival advantage of combined chemoradiotherapy compared with resection as the initial treatment of patients with regional pancreatic carcinoma. An outcomes trial." Cancer **89**(2): 314-327.

Soeda, A., Y. Morita-Hoshi, H. Makiyama, C. Morizane, H. Ueno, M. Ikeda, T. Okusaka, S. Yamagata, N. Takahashi, I. Hyodo, Y. Takaue and Y. Heike (2009). "Regular dose of gemcitabine induces an increase in CD14+ monocytes and CD11c+ dendritic cells in patients with advanced pancreatic cancer." Jpn J Clin Oncol **39**(12): 797-806.

Stanley, E. R. and V. Chitu (2014). "CSF-1 receptor signaling in myeloid cells." Cold Spring Harb Perspect Biol **6**(6).

Steele, C. W., N. B. Jamieson, T. R. Evans, C. J. McKay, O. J. Sansom, J. P. Morton and C. R. Carter (2013). "Exploiting inflammation for therapeutic gain in pancreatic cancer." Br J Cancer **108**(5): 997-1003.

Sun, X., G. Cheng, M. Hao, J. Zheng, X. Zhou, J. Zhang, R. S. Taichman, K. J. Pienta and J. Wang (2010). "CXCL12 / CXCR4 / CXCR7 chemokine axis and cancer progression." Cancer Metastasis Rev **29**(4): 709-722.

Suresh, P. and A. Wanchu (2006). "Chemokines and chemokine receptors in HIV infection: role in pathogenesis and therapeutics." J Postgrad Med **52**(3): 210-217.

Szekanecz, Z., A. Vegvari, Z. Szabo and A. E. Koch (2010). "Chemokines and chemokine receptors in arthritis." Front Biosci (Schol Ed) **2**: 153-167.

Tan, M. C., P. S. Goedegebuure, B. A. Belt, B. Flaherty, N. Sankpal, W. E. Gillanders, T. J. Eberlein, C. S. Hsieh and D. C. Linehan (2009). "Disruption of CCR5-dependent homing of regulatory T cells inhibits tumor growth in a murine model of pancreatic cancer." J Immunol **182**(3): 1746-1755.

Tao, L., G. Huang, H. Song, Y. Chen and L. Chen (2017). "Cancer associated fibroblasts: An essential role in the tumor microenvironment." Oncol Lett **14**(3): 2611-2620.

Teague, A., K. H. Lim and A. Wang-Gillam (2015). "Advanced pancreatic adenocarcinoma: a review of current treatment strategies and developing therapies." Ther Adv Med Oncol **7**(2): 68-84.

Thurber, R. V., M. Haynes, M. Breitbart, L. Wegley and F. Rohwer (2009). "Laboratory procedures to generate viral metagenomes." Nat Protoc **4**(4): 470-483.

Tsuchikawa, T., S. Takeuchi, T. Nakamura, T. Shichinohe and S. Hirano (2016). "Clinical impact of chemotherapy to improve tumor microenvironment of pancreatic cancer." World J Gastrointest Oncol **8**(11): 786-792.

Turley, S. J., V. Cremasco and J. L. Astarita (2015). "Immunological hallmarks of stromal cells in the tumour microenvironment." Nat Rev Immunol **15**(11): 669-682.

Turner, M. D., B. Nedjai, T. Hurst and D. J. Pennington (2014). "Cytokines and chemokines: At the crossroads of cell signalling and inflammatory disease." Biochim Biophys Acta **1843**(11): 2563-2582.

Ulvmar, M. H., E. Hub and A. Rot (2011). "Atypical chemokine receptors." Exp Cell Res **317**(5): 556-568.

Vela, M., M. Aris, M. Llorente, J. A. Garcia-Sanz and L. Kremer (2015). "Chemokine receptor-specific antibodies in cancer immunotherapy: achievements and challenges." Front Immunol **6**: 12.

Vemuganti, S. A., T. A. Bell, C. O. Scarlett, C. E. Parker, F. P. de Villena and D. A. O'Brien (2007). "Three male germline-specific aldolase A isozymes are generated by alternative splicing and retrotransposition." Dev Biol **309**(1): 18-31.

Viehl, C. T., T. T. Moore, U. K. Liyanage, D. M. Frey, J. P. Ehlers, T. J. Eberlein, P. S. Goedegebuure and D. C. Linehan (2006). "Depletion of CD4+CD25+ regulatory T cells promotes a tumor-specific immune response in pancreas cancer-bearing mice." Ann Surg Oncol **13**(9): 1252-1258.

Vincent, A., J. Herman, R. Schulick, R. H. Hruban and M. Goggins (2011). "Pancreatic cancer." Lancet **378**(9791): 607-620.

Von Hoff, D. D., T. Ervin, F. P. Arena, E. G. Chiorean, J. Infante, M. Moore, T. Seay, S. A. Tjulandin, W. W. Ma, M. N. Saleh, M. Harris, M. Reni, S. Dowden, D. Laheru, N. Bahary, R. K. Ramanathan, J. Tabernero, M. Hidalgo, D. Goldstein, E. Van Cutsem, X. Wei, J. Iglesias and M. F. Renschler (2013). "Increased survival in pancreatic cancer with nab-paclitaxel plus gemcitabine." N Engl J Med **369**(18): 1691-1703.

Vonlaufen, A., S. Joshi, C. Qu, P. A. Phillips, Z. Xu, N. R. Parker, C. S. Toi, R. C. Pirola, J. S. Wilson, D. Goldstein and M. V. Apte (2008). "Pancreatic stellate cells: partners in crime with pancreatic cancer cells." Cancer Res **68**(7): 2085-2093.

Vonlaufen, A., P. A. Phillips, Z. Xu, D. Goldstein, R. C. Pirola, J. S. Wilson and M. V. Apte (2008). "Pancreatic stellate cells and pancreatic cancer cells: an unholy alliance." Cancer Res **68**(19): 7707-7710.

Wachsmann, M. B., L. M. Pop and E. S. Vitetta (2012). "Pancreatic ductal adenocarcinoma: a review of immunologic aspects." J Investig Med **60**(4): 643-663.

Waddell, N., M. Pajic, A. M. Patch, D. K. Chang, K. S. Kassahn, P. Bailey, A. L. Johns, D. Miller, K. Nones, K. Quek, M. C. Quinn, A. J. Robertson, M. Z. Fadlullah, T. J. Bruxner, A. N. Christ, I. Harliwong, S. Idrisoglu, S. Manning, C. Nourse, E. Nourbakhsh, S. Wani, P. J. Wilson, E. Markham, N. Cloonan, M. J. Anderson, J. L. Fink, O. Holmes, S. H. Kazakoff, C. Leonard, F. Newell, B. Poudel, S. Song, D. Taylor, N. Waddell, S. Wood, Q. Xu, J. Wu, M. Pinese, M. J. Cowley, H. C. Lee, M. D. Jones, A. M. Nagrial, J. Humphris, L. A. Chantrill, V. Chin, A. M. Steinmann, A. Mawson, E. S. Humphrey, E. K. Colvin, A.

Chou, C. J. Scarlett, A. V. Pinho, M. Giry-Laterriere, I. Rooman, J. S. Samra, J. G. Kench, J. A. Pettitt, N. D. Merrett, C. Toon, K. Epari, N. Q. Nguyen, A. Barbour, N. Zeps, N. B. Jamieson, J. S. Graham, S. P. Niclou, R. Bjerkvig, R. Grutzmann, D. Aust, R. H. Hruban, A. Maitra, C. A. Iacobuzio-Donahue, C. L. Wolfgang, R. A. Morgan, R. T. Lawlor, V. Corbo, C. Bassi, M. Falconi, G. Zamboni, G. Tortora, M. A. Tempero, I. Australian Pancreatic Cancer Genome, A. J. Gill, J. R. Eshleman, C. Pilarsky, A. Scarpa, E. A. Musgrove, J. V. Pearson, A. V. Biankin and S. M. Grimmond (2015). "Whole genomes redefine the mutational landscape of pancreatic cancer." Nature **518**(7540): 495-501.

Wan, Y. Y. (2014). "GATA3: a master of many trades in immune regulation." Trends Immunol **35**(6): 233-242.

Wang, X. and Y. Lin (2008). "Tumor necrosis factor and cancer, buddies or foes?" Acta Pharmacol Sin **29**(11): 1275-1288.

Wang, Y., I. Misumi, A. D. Gu, T. A. Curtis, L. Su, J. K. Whitmire and Y. Y. Wan (2013). "GATA-3 controls the maintenance and proliferation of T cells downstream of TCR and cytokine signaling." Nat Immunol **14**(7): 714-722.

Weber, C. (2008). "Chemokines in atherosclerosis, thrombosis, and vascular biology." Arterioscler Thromb Vasc Biol **28**(11): 1896.

Westphalen, C. B. and K. P. Olive (2012). "Genetically engineered mouse models of pancreatic cancer." Cancer J **18**(6): 502-510.

Whatcott, C. J., R. G. Posner, D. D. Von Hoff and H. Han (2012). Desmoplasia and chemoresistance in pancreatic cancer. Pancreatic Cancer and Tumor Microenvironment. P. J. Grippo and H. G. Munshi. Trivandrum (India).

Whipple, C. and M. Korc (2008). "Targeting angiogenesis in pancreatic cancer: rationale and pitfalls." Langenbecks Arch Surg **393**(6): 901-910.

White, G. E., A. J. Iqbal and D. R. Greaves (2013). "CC chemokine receptors and chronic inflammation--therapeutic opportunities and pharmacological challenges." Pharmacol Rev **65**(1): 47-89.

Wickham, H. (2009). ggplot2, Springer-Verlag New York.

Wood, L. D. and R. H. Hruban (2012). "Pathology and molecular genetics of pancreatic neoplasms." Cancer J **18**(6): 492-501.

Wood, L. D. and R. H. Hruban (2015). "Genomic landscapes of pancreatic neoplasia." J Pathol Transl Med **49**(1): 13-22.

Wormann, S. M., K. N. Diakopoulos, M. Lesina and H. Algul (2014). "The immune network in pancreatic cancer development and progression." Oncogene **33**(23): 2956-2967.

Wu, Y., X. Zhu, N. Li, T. Chen, M. Yang, M. Yao, X. Liu, B. Jin, X. Wang and X. Cao (2011). "CMRF-35-like molecule 3 preferentially promotes TLR9-triggered

proinflammatory cytokine production in macrophages by enhancing TNF receptor-associated factor 6 ubiquitination." J Immunol **187**(9): 4881-4889.

Yuen, A. and B. Diaz (2014). "The impact of hypoxia in pancreatic cancer invasion and metastasis." Hypoxia (Auckl) **2**: 91-106.

Zhao, T., S. Gao, X. Wang, J. Liu, Y. Duan, Z. Yuan, J. Sheng, S. Li, F. Wang, M. Yu, H. Ren and J. Hao (2012). "Hypoxia-inducible factor-1alpha regulates chemotactic migration of pancreatic ductal adenocarcinoma cells through directly transactivating the CX3CR1 gene." PLoS One **7**(8): e43399.

Zhao, X., W. Fan, Z. Xu, H. Chen, Y. He, G. Yang, G. Yang, H. Hu, S. Tang, P. Wang, Z. Zhang, P. Xu and M. Yu (2016). "Inhibiting tumor necrosis factor-alpha diminishes desmoplasia and inflammation to overcome chemoresistance in pancreatic ductal adenocarcinoma." Oncotarget **7**(49): 81110-81122.

Zheng, J., M. Yang, J. Shao, Y. Miao, J. Han and J. Du (2013). "Chemokine receptor CX3CR1 contributes to macrophage survival in tumor metastasis." Mol Cancer **12**(1): 141.

Zhou, C., J. Zhang, Y. Zheng and Z. Zhu (2012). "Pancreatic neuroendocrine tumors: a comprehensive review." Int J Cancer **131**(5): 1013-1022.

Zlotnik, A. and O. Yoshie (2000). "Chemokines: a new classification system and their role in immunity." Immunity **12**(2): 121-127.

Zlotnik, A. and O. Yoshie (2012). "The chemokine superfamily revisited." Immunity **36**(5): 705-716.

Zweemer, A. J., J. Toraskar, L. H. Heitman and I. J. AP (2014). "Bias in chemokine receptor signalling." Trends Immunol **35**(6): 243-252.